

**THE ROLE OF ENERGY METABOLISM IN THE PATHOGENESIS  
OF ALZHEIMER'S DISEASE**

by

**RICHARD R. CLOUGH**

**A Thesis Submitted to the Faculty of Graduate Studies in Partial  
Fulfilment of the Requirements for the Degree of**

**MASTER OF SCIENCE**

**Department of Biochemistry and Molecular Biology**

**Faculty of Medicine**

**University of Manitoba, Winnipeg, Manitoba, Canada**

**© August, 1999**



National Library  
of Canada

Acquisitions and  
Bibliographic Services

395 Wellington Street  
Ottawa ON K1A 0N4  
Canada

Bibliothèque nationale  
du Canada

Acquisitions et  
services bibliographiques

395, rue Wellington  
Ottawa ON K1A 0N4  
Canada

*Your file* *Votre référence*

*Our file* *Notre référence*

The author has granted a non-exclusive licence allowing the National Library of Canada to reproduce, loan, distribute or sell copies of this thesis in microform, paper or electronic formats.

The author retains ownership of the copyright in this thesis. Neither the thesis nor substantial extracts from it may be printed or otherwise reproduced without the author's permission.

L'auteur a accordé une licence non exclusive permettant à la Bibliothèque nationale du Canada de reproduire, prêter, distribuer ou vendre des copies de cette thèse sous la forme de microfiche/film, de reproduction sur papier ou sur format électronique.

L'auteur conserve la propriété du droit d'auteur qui protège cette thèse. Ni la thèse ni des extraits substantiels de celle-ci ne doivent être imprimés ou autrement reproduits sans son autorisation.

0-612-45034-1

**Canada**

**THE UNIVERSITY OF MANITOBA  
FACULTY OF GRADUATE STUDIES  
\*\*\*\*\*  
COPYRIGHT PERMISSION PAGE**

**The Role of Energy Metabolism in the Pathogenesis of Alzheimer's Disease**

**BY**

**Richard R. Clough**

**A Practicum submitted to the Faculty of Graduate Studies of The University  
of Manitoba in partial fulfillment of the requirements of the degree**

**of**

**MASTER OF SCIENCE**

**RICHARD R. CLOUGH©1999**

**Permission has been granted to the Library of The University of Manitoba to lend or sell copies of this thesis/practicum, to the National Library of Canada to microfilm this thesis and to lend or sell copies of the film, and to Dissertations Abstracts International to publish an abstract of this thesis/practicum.**

**The author reserves other publication rights, and neither this thesis/practicum nor extensive extracts from it may be printed or otherwise reproduced without the author's written permission.**

## **ACKNOWLEDGMENTS**

I would like to thank my supervisor, Dr. Francis Amara, for allowing me to participate in such an exciting field of research, and for creating an environment that demanded independent thought and action.

Thanks also to my thesis advisors, Dr. G. Arthur and Dr. I. Dixon, for their expert guidance on academic and personal matters.

My appreciation to fellow student Binhua Liang for his support and encouragement over the last two years.

I extend special thanks to my wife, Kathleen, for her invaluable expertise in the preparation of this document, and for her support and advice during the last three years.

To my daughters, Céline and Rebecca: Thank you for being my fan club.

## TABLE OF CONTENTS

ABSTRACT .....	v
LIST OF FIGURES .....	vii
LIST OF TABLES .....	viii
LIST OF ABBREVIATIONS .....	ix
1.0 REVIEW OF LITERATURE .....	1
1.1 Histopathology of Alzheimer's Disease .....	1
1.2 Genetic Factors .....	3
1.3.0 Amyloid Precursor Protein .....	5
1.3.1 Suspected functions of APP .....	5
1.3.2 Processing of APP .....	6
1.4.0 Pathophysiology of APP and $\beta$ AP .....	8
1.4.1 Evidence supporting $\beta$ AP pathogenicity .....	9
1.4.2 Pathogenic mechanisms of $\beta$ AP .....	10
1.5 Bioenergetic Defects .....	13
1.6 COX Deficit .....	15
1.7 Overexpression of APP .....	21
1.8 Oxidative Stress .....	22
1.9 Apoptosis .....	26
2.0 AIM AND HYPOTHESIS .....	31
3.0 MATERIALS AND METHODS .....	32

3.1.0	Preparation of Plasmid/APP DNA Constructs .....	32
3.1.1	pAS2-1/APP <sub>770/2583</sub> construct .....	32
3.1.2.	pAS2-1/APP <sub>770/N-T2020</sub> construct .....	40
3.1.3	pAS2-1/APP <sub>770/N-T1554</sub> and pAS2-1/APP <sub>770/N-T208</sub> constructs ..	43
3.1.4	pCMV/myc/mito/APP <sub>770/2583</sub> construct .....	44
3.1.5	pEGFP-N1/APP <sub>695/N-T1795</sub> construct .....	48
3.1.6	pEGFP-N1/APP <sub>695/N-T208</sub> construct .....	51
3.1.7	pCMV/myc/mitoGFP plasmid .....	52
3.2.0	Yeast Two-Hybrid System .....	53
3.2.1	Library-scale yeast two-hybrid assay .....	53
3.2.2	Small-scale yeast two-hybrid assay .....	56
3.3.0	Assays of APP Stably-transfected Neuroblastoma Cell Line .....	58
3.3.1	Neuroblastoma cell culture .....	58
3.3.2	Transfection of neuroblastoma cell line .....	58
3.3.3	Isolation of mitochondria from the neuroblastoma cell line .	59
3.3.4	COX activity assay in APP-transfected neuroblastoma cell line. .....	59
3.3.5	Complex I activity assay in APP-transfected neuroblastoma cell line .....	60
3.3.6	Detection of apoptosis in APP-transfected neuroblastoma cell line .....	61
3.3.7	Assay for ROS levels in APP-transfected neuroblastoma cell	

	line .....	61
3.3.8	Assay of glutathione peroxidase activity in APP-transfected neuroblastoma cell line .....	62
3.3.9	Assay of superoxide dismutase activity in APP-transfected neuroblastoma cell line .....	62
3.4.0	Classic <i>In Vitro</i> Mitochondrial Import Assay .....	63
3.4.1	TnT <i>in vitro</i> transcription-translation system .....	63
3.4.2	Isolation of rat mitochondria .....	64
3.4.3	<i>In vitro</i> mitochondrial import assay .....	65
3.5	Treatment of Neuroblastoma Cells with MitoTracker Probes .....	66
3.6.0	Immunoelectron Microscopy .....	67
3.6.1	Immunoelectron microscopy to detect APP in mammalian tissue .....	67
3.6.2	Immunoelectron microscopy to detect APP and $\beta$ AP in human brain .....	68
4.0	RESULTS .....	69
4.1	Yeast Two-Hybrid Technology .....	71
4.2	Analysis of Positive Clones .....	73
4.3	Verification of specificity of APP/COX I interaction .....	77
4.4	Yeast Two-hybrid Assay With APP Deletion Constructs .....	82
4.5.0	APP and Mitochondria .....	83
4.5.1	Mitochondrial targeting signal .....	83

<b>4.6.0</b>	<b>Assays on Neuroblastoma Cells Overexpressing APP</b>	<b>84</b>
4.6.1	Assays of COX and Complex I enzymatic activities	85
4.6.3	APP overexpression and apoptosis in neuroblastoma cell line	88
4.6.4	APP overexpression and ROS production in neuroblastoma cell line	88
4.6.5	APP overexpression and the formation of lipid peroxidation	90
4.6.6	Anti-oxidant enzyme assays	90
<b>4.7.0</b>	<b>Evidence for the Physiological Location of APP in Mitochondria</b>	<b>93</b>
4.7.1	Classic <i>in vitro</i> mitochondrial import assay	93
4.7.2	Dual color <i>in vivo</i> fluorescence microscopy of neuroblastoma cell line	96
4.7.3	Immunoelectron microscopy to detect endogenous APP and $\beta$ AP in mammalian tissue	103
4.7.4	Immunoelectron microscopy to detect endogenous APP and $\beta$ AP in AD and control brains	105
<b>5.0</b>	<b>DISCUSSION</b>	<b>108</b>
<b>6.0</b>	<b>REFERENCES</b>	<b>117</b>



## **ABSTRACT**

**In Alzheimer's disease, neuronal degeneration due to apoptosis has been linked to overexpression and aberrant amyloidogenic processing of the amyloid precursor protein (APP), as well as to bioenergetic defects characterized by deficits in the electron transport chain's cytochrome c oxidase (COX) which leads to the generation of radical oxygen species. Several cellular mechanisms underlying the bioenergetic defects have been proposed. Inhibition of oxidative energy metabolism increased the amyloidogenic processing of APP, which led to neurotoxicity. Overexpression of APP in cultured normal human muscle fibres caused a specific decrease in COX activity, followed by ultrastructural abnormalities of mitochondria. Thus, it appears that energy metabolism and APP processing are closely linked. However, the mechanisms underlying this relationship are unclear. We have demonstrated, using the yeast two-hybrid system, that APP interacts with COX subunit 1 (COX I), and that this interaction involves the extracellular domain of APP. This suggests a direct interaction between the two proteins, and that APP may be localized to mitochondria. We demonstrated that APP caused specific deficits in COX activity, induced the production of radical oxygen species and lipid peroxidation, and enhanced neuronal apoptosis. However, anti-oxidant enzyme activity was variable, and probably represented a compensatory reaction to elevated oxygen radicals. To directly interact with COX, APP must be targeted to, and localized in, mitochondria. This possibility was tested with an *in vitro* mitochondrial import assay which showed that APP is transported to mitochondria in an energy-dependent manner. Furthermore, dual fluorescence microscopy with chimeric APP-green fluorescent protein,**

**and immunoelectron microscopy, demonstrated the presence of endogenous APP and  $\beta$ -amyloid peptide (the neurotoxic cleavage product of APP) in mitochondria of post-mortem human brain tissue, with increased levels of  $\beta$ -amyloid peptide in AD brains compared to non-AD brains. Cumulatively, the data supports a model of the direct involvement of APP and its potentially amyloidogenic derivatives in the generalized bioenergetic deficit. This then leads to the generation of increased radical oxygen species and subsequently, neuronal apoptosis, in a self perpetuating cycle of mitochondrial and cellular degeneration involved in the pathophysiology of Alzheimer's disease.**

## LIST OF FIGURES

Figure 1	Schematic representation of the human $\beta$ -amyloid precursor protein(APP) ..... 2	2
Figure 2	Schematic of pGEM9zf restriction map and MCS ..... 33	33
Figure 3	Schematic of pGEM5zf restriction map and MCS ..... 35	35
Figure 4	Schematic of pAS2-1 restriction map and MCS ..... 39	39
Figure 5	Schematic of human APP <sub>770/2583</sub> construct ..... 41	41
Figure 6	Schematic diagram of the MATCHMAKER GAL4-based two-hybrid systems ..... 72	72
Figure 7	Screening an AD fusion library for proteins that interact with a bait protein ..... 74	74
Figure 8	Matchmaker two-hybrid screen ..... 75	75
Figure 9	Sequence of clone A-14; the partial COX I-tRNA <sup>Ser</sup> gene ..... 76	76
Figure 10	Restriction enzyme digestion of pAS2-1/APP <sub>770/2583</sub> with EcoR 1 ... 80	80
Figure 11	Sac 1 restriction enzyme digestion of pAS2-1/APP <sub>770/N-T2020</sub> construct . 81	81
Figure 12	Hind III restriction of constructs pAS2-1/APP <sub>770/N-T208</sub> & pAS2- 1/APP <sub>770/NT1554</sub> ..... 83a	83a
Figure 13	Targeting APP into mitochondria potentiates apoptosis ..... 89	89
Figure 14	Induction of ROS and lipid peroxidation in SK-N-SH cells ..... 91	91
Figure 15	Comparison of the free radical scavenging enzyme activities ..... 94	94
Figure 16	Mitochondrial import <i>in vitro</i> ..... 97	97
Figure 17	EcoR 1 and BamH 1 restriction of pEGFP-N1/APP <sub>695/N-T1795</sub> ligation	

	<b>constructs</b> .....	<b>100</b>
<b>Figure 18</b>	<b>EcoR 1 restriction of pEGFP-N1 and pEGFP-N1/APP<sub>695/N-T208</sub></b> .....	<b>101</b>
<b>Figure 19</b>	<b>Pst 1 restriction of pCMV/myc/mito/GFP</b> .....	<b>102</b>
<b>Figure 20</b>	<b>SK-N-SH neuroblastoma cell mitochondrial labelling</b> .....	<b>104</b>
<b>Figure 21</b>	<b>Localization of APP by immunoelectron microscopy in mammalian brain and kidney.</b> .....	<b>106</b>
<b>Figure 22</b>	<b>Localization of APP and <math>\beta</math>AP by immunoelectron microscopy in human AD and non-AD brain.</b> .....	<b>107</b>

#### **LIST OF TABLES**

<b>Table 1</b>	<b>Interaction of APP and COX I in yeast</b> .....	<b>78</b>
<b>Table 2</b>	<b>Complex I and complex IV enzyme activities in neuroblastoma cells overexpressing APP</b> .....	<b>87</b>

## LIST OF ABBREVIATIONS

8OHdG	8-hydroxy-2'-deoxyguanosine
AA	arachidonic acid
ActD	activation domain
ADDL	beta-amyloid peptide-derived diffusible ligand
AGEP	advanced glycation end product
AIF	apoptosis inducing factor
amp	ampicillin
apo-E	apolipoprotein E
BD	binding domain
CAA	cerebral amyloid angiopathy
cfu	colony forming units
Ci	curie
CIAP	calf intestinal alkaline phosphatase
CMR(glc)	cortical and cerebellar glucose metabolic rate
CoQ	coenzyme Q
CPA	<i>cis</i> -parinaric acid
cyh	cycloheximide
DCF	dichlorofluoroscين
DCF-DA	dichlorofluoroscein diacetate
$\Delta\psi$	electrochemical gradient, or proton motive force
ER	endoplasmic reticulum

<b>FAD</b>	<b>familial Alzheimer's disease</b>
<b>GSase</b>	<b>glutamine synthase</b>
<b>GT</b>	<b>glutamate transporter</b>
<b>HNE</b>	<b>4-hydroxynonenol</b>
<b>kan</b>	<b>kanamycin</b>
<b>LTP</b>	<b>long term potentiation</b>
<b>MFO</b>	<b>mixed function oxidation</b>
<b>NFT</b>	<b>neurofibrillary tangles</b>
<b>NMDA</b>	<b><i>N</i>-methyl-<i>D</i>-aspartate</b>
<b>NP</b>	<b>neuritic (or senile) plaque</b>
<b><math>\rho^0</math></b>	<b>mitochondria-deficient</b>
<b>PCIAA</b>	<b>phenol/chloroform/isoamyl alcohol</b>
<b>PHF</b>	<b>paired helical filaments</b>
<b>PS</b>	<b>presenilin protein</b>
<b>PTP</b>	<b>permeability transition pore</b>
<b>RAGE</b>	<b>receptor for advanced glycation end products</b>
<b>RE</b>	<b>restriction endonuclease</b>
<b>ROI</b>	<b>reactive oxygen intermediate</b>
<b>sAPP</b>	<b>secretory (or soluble) APP</b>
<b>SR</b>	<b>scavenger receptor</b>
<b>TMD</b>	<b>transmembrane domain</b>

## **1.0 REVIEW OF LITERATURE**

### **1.1 Histopathology of Alzheimer's Disease**

Alzheimer's disease (AD) is a cerebral degenerative disorder characterized by gradual loss of memory, reasoning, orientation and judgment affecting 1% of the population of the western world (Katzman, 1986), and 5-10% of all people over 65 years of age (Hurtley, 1998). Symptoms are correlated with the appearance of amyloid deposits mainly in the hippocampus and association cortex of the brain (Roth *et al.*, 1966; Goedert, 1993; Haas and Selkoe, 1993; Kosik, 1994; Trowjanowski and Lee, 1994). The brains of AD patients contain many extracellular, amyloid neuritic plaques (NP), which are dense, heterogeneous, extracellular deposits, largely composed of the 39-43 amino acid beta-amyloid peptides ( $\beta$ AP), the cytotoxic cleavage products of the beta-amyloid precursor protein (APP) (Figure 1). AD brains also contain neurofibrillary tangles (NFT; intracellular accumulation of abnormally phosphorylated microtubule-associated protein tau, arranged into paired helical filaments [PHF]), dystrophic neurites (enlarged neuronal processes filled with PHFs), and show profound synaptic loss and gliosis (activated microglia and reactive astrocytes) (Glennner and Wong, 1984 a and b; Masters *et al.*, 1985 a and b; Masters and Bayreuther, 1988; Games *et al.*, 1995; Lamb, 1997).

The classic NP consists of a central  $\beta$ AP-immunoreactive amyloid core surrounded by dystrophic neurites (Cummings *et al.*, 1998). Amyloid is deposited in cerebral blood vessels (cerebral amyloid angiopathy [CAA]) as well as in diffuse and

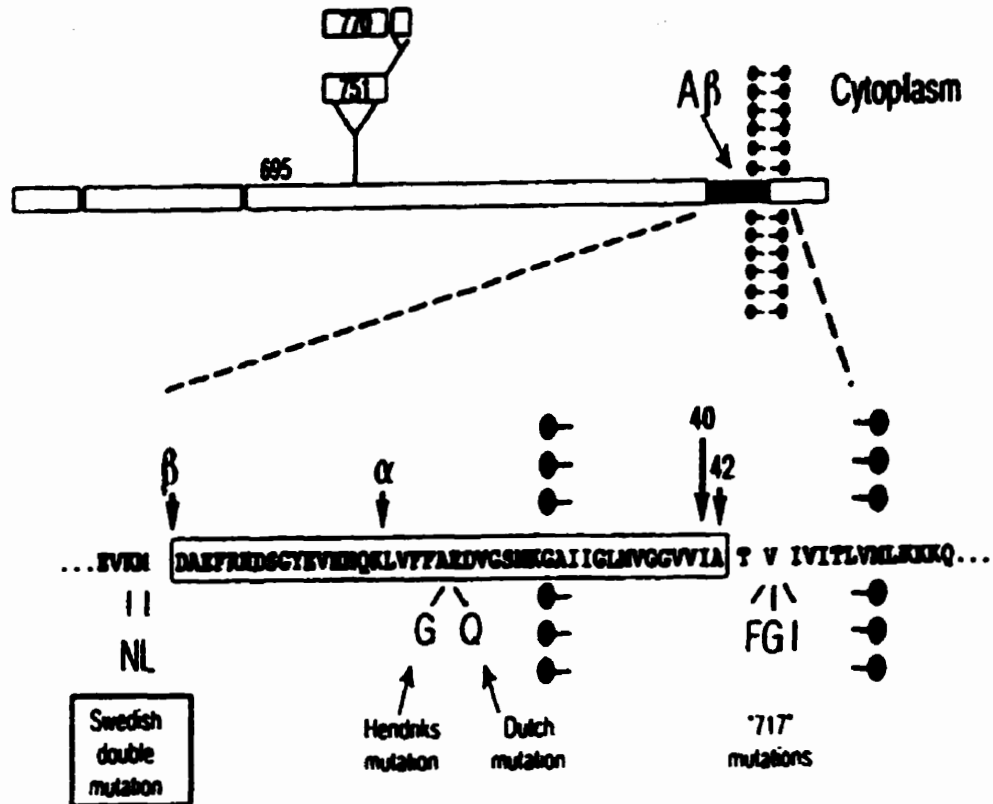


Figure 1 Schematic representation of the human  $\beta$ -amyloid precursor protein (APP). Various isoforms of APP are produced by alternative splicing of pre-mRNAs to exclude the OX-2 antigen domain (amino acids 345-364 of APP<sub>770</sub>) to produce APP<sub>751</sub>, the Kunitz-type protease-inhibitor domain (amino acids 389-344 of APP<sub>770</sub>) to produce APP<sub>714</sub>, or both domains to produce APP<sub>695</sub>.  $\alpha$ -secretase-mediated cleavage of a proportion of cellular APP molecules at Lys<sup>687</sup>-Leu<sup>688</sup> of APP<sub>770</sub> ( $\beta$ AP Lys<sup>16</sup>-Leu<sup>17</sup>) precludes the formation of  $\beta$ AP. Intracellular processing of APP by  $\beta$ - and  $\gamma$ -secretases, however, yields intact  $\beta$ AP, consisting of 28 amino acids derived from the extracellular domain and 12-14 amino acids from the transmembrane domain. A number of point mutations in the APP molecule have been identified in the vicinity of the  $\beta$ AP sequence. These mutations co-segregate with family pedigrees predisposed to early onset FAD, and are characterized by alterations in the formation and deposition of  $\beta$ AP. (Price *et al.*, 1998).



neuritic plaques (Olichney *et al.*, 1995; Vinters *et al.*, 1996). Nerve cell loss, particularly affecting the larger neurons of the superficial cortex, is a consistent feature of AD (McGeer *et al.*, 1994; Morris, 1995; Terry, 1997; Gomez-Isla *et al.*, 1997). Presynaptic terminal density is decreased by an average of 45% at the time of autopsy (McGeer *et al.*, 1994), and synapses are greatly reduced in the region of NPs (Terry *et al.*, 1991). Extraneuronal ghost tangles may be seen in the entorhinal cortex and represent the insoluble residue of neurons that have died (Morris, 1995).

## 1.2 Genetic Factors

AD occurs in two forms: (i) the rare, early onset familial AD (FAD), an autosomal dominant disorder caused by mutations in the genes encoding three integral membrane proteins, APP, presenilin1 (PS1) and presenilin 2 (PS2), whose precise functions are unknown (Goate *et al.*, 1991; Chartier-Harlin *et al.*, 1991; Murrell, 1991; Hendricks *et al.*, 1992; Mullan *et al.*, 1992; Levy-Lahard, 1995; Rogaev *et al.*, 1995; Sherrington *et al.* 1995; Hardy, 1997; Price and Sisodia, 1998), and (ii) the common sporadic, non-familial AD, in which the non-mutated forms of all three proteins are probably involved (Dewji and Singer, 1997).

Down Syndrome (DS) patients over the age of 30 almost universally have AD-type pathology in the brain, and the prevalence of dementia increases with age (Wisniewski *et al.*, 1985). Patients with DS have three copies of chromosome 21, which bears the gene for APP, and have increased production of  $\beta$ AP (Govoni *et al.*, 1996;

Hardy, 1997).

Several missense mutations of the APP gene have been described in a limited number of early-onset AD families. The mutations occur near the beginning and the end of the  $\beta$ AP sequence within the APP gene. They affect APP processing in different ways, but all increase the production of  $\beta$ AP (Goate *et al.*, 1991; Chartier-Harlin *et al.*, 1991; Hardy, 1997), particularly the form with 42 amino acids ( $\beta$ AP<sub>42</sub>), which has the greatest association with neurotoxicity (Mann *et al.*, 1996; Lendon *et al.*, 1997; Hardy, 1997; Cummings *et al.*, 1998).

Several missense mutations of the PS1 gene on chromosome 14 account for most cases of FAD. These mutations also increase the production of  $\beta$ AP<sub>42</sub> (Sherrington *et al.*, 1995; Mann *et al.*, 1996; Hardy, 1997). A small number of families have mutations of the PS2 gene on chromosome 1 (Rogaev *et al.*, 1995; Levy-Lahard *et al.*, 1995 a and b), which also increases production of  $\beta$ AP<sub>42</sub> (Mann *et al.*, 1997).

A major genetic risk factor for late-onset sporadic AD is possession of the apoE  $\epsilon$ 4 allele (apoE-4) (Corder *et al.*, 1993), which is associated with increased deposition of  $\beta$ AP (primarily  $\beta$ AP<sub>40</sub>), an apparent facilitated configurational change from diffuse to aggregated amyloid in a beta-pleated sheet configuration (Gomez-Isla *et al.*, 1996), and an increased frequency of NPs and CAA (Gomez-Isla *et al.*, 1996; Olichney *et al.*, 1996). A mutation in the gene encoding  $\alpha_2$ -macroglobulin ( $\alpha_2$ M) also increases the susceptibility to develop AD, possibly by allowing  $\beta$ AP to accumulate to abnormally high levels (Marx, 1998).

There is an increased risk for AD in offspring of AD affected women, suggesting

one risk factor for AD is maternal inheritance. This could be related to inheritance of mitochondrial DNA (mtDNA) (Edland *et al.*, 1996), as it is known mitochondrial function is impaired in AD.

### **1.3.0 Amyloid Precursor Protein**

APPs are synthesized as *N*- and *O*-glycosylated integral transmembrane proteins which span the lipid bilayer once. There is a large amino (NH<sub>2</sub>)-terminal extracellular domain, a transmembrane domain (TMD) and a short 47 residue long cytoplasmic domain (Dyrks *et al.*, 1988; Weidemann *et al.*, 1989) (Figure 1). Different transcripts of APP arise from alternative splicing of APP mRNA, the major transcripts having 695 residues (APP<sub>695</sub>), 751 residues (APP<sub>751</sub>), and 770 residues (APP<sub>770</sub>) (Kang *et al.*, 1987; Tanzi *et al.*, 1988; Kitaguchi *et al.*, 1988; Ponte *et al.*, 1988; Oltersdorf *et al.*, 1989; Van Nostrand *et al.*, 1989). The boxes above the APP schematic in Figure 1 (containing numbers 770 and 751) represent the amino acid sequences missing from APP<sub>695</sub>, that when spliced into APP, generate the isoforms, APP<sub>770</sub> and APP<sub>751</sub> (Price *et al.*, 1998).

#### **1.3.1 Suspected functions of APP**

One problem in understanding the pathophysiology of AD is that the biological functions of APP are unknown. Suspected functions of membrane-bound APP include inhibition of extracellular serine proteases (Oltersdorf *et al.*, 1989), inhibition of platelet coagulation factor XIa (Smith *et al.*, 1990), involvement in cell adhesion (Schubert *et al.*,

1989; Breen *et al.*, 1991; Small *et al.*, 1992; Jin *et al.*, 1994), neurite outgrowth and extension (LeBlanc *et al.*, 1992; Milward *et al.*, 1992; Koo *et al.*, 1993; Small *et al.*, 1994; Jin *et al.*, 1994; Qiu *et al.*, 1995), synaptic plasticity (Mattson *et al.*, 1993 a), and synaptotrophic effects (Mattson *et al.*, 1993 a; Mucke *et al.*, 1994). The secreted form of APP (sAPP), the large NH<sub>2</sub>-terminal fragment produced by normal, non-amyloidogenic proteolytic cleavage within the βAP sequence region by α-secretase (Figure 1), stabilizes intracellular free Ca<sup>2+</sup> ([Ca<sup>2+</sup>]<sub>i</sub>) and protects neurons against excitotoxic insults (Mattson, 1994). This suggests sAPPs are important for modulating activity-dependent processes throughout the brain. It was shown that sAPP activated high conductance potassium (K<sup>+</sup>) channels that caused a decrease in [Ca<sup>2+</sup>]<sub>i</sub> (Furukawa *et al.*, 1996), thereby suppressing [Ca<sup>2+</sup>]<sub>i</sub> responses to the excitatory neurotransmitter, glutamate (Glu), and modulating the effects of Glu on neurite outgrowth and cell survival (Mattson *et al.*, 1993 a; Mattson, 1994). This may explain the effects of APP on synaptogenesis (Roch *et al.*, 1994) and synaptic plasticity (Huber *et al.*, 1993).

APP may function as a cell surface receptor, connected to various intracellular pathways via its cytoplasmic domain interacting with intracellular effector molecules. Its structure is similar to that of the extracellular matrix protein receptors, the integrins, and its carboxy (COOH)-terminal region bound an intracellular protein, APP-BP1, which may be involved in the cellular ubiquitination pathway (Chow *et al.*, 1996).

### **1.3.2 Processing of APP**

A fundamental event in the pathogenesis of AD is the enhanced, aberrant,

amyloidogenic processing of APP, which causes excessive production of neurotoxic  $\beta$ AP species. A constitutive, non-amyloidogenic, proteolytic cleavage of APP, by an uncharacterized  $\alpha$ -secretase, occurs in the *trans*-Golgi network or other end-stage compartments of the protein secretory pathway (Sambamurti *et al.*, 1992; De Strooper *et al.*, 1993; Kuentzel *et al.*, 1993), including caveolae (Ikezu *et al.*, 1998), or at the cell surface (Sisodia, 1992). The  $\alpha$ -secretase generates the soluble 90-110 kDa sAPP (the ectodomain of APP) and a membrane-bound 9 kDa COOH-terminal derivative. The sAPP COOH-terminal site of cleavage is at amino acid 16 of the  $\beta$ AP sequence, which means the NH<sub>2</sub> terminus of  $\beta$ AP is not produced by normal non-amyloidogenic proteolytic cleavage (Wiedemann *et al.*, 1989; Sisodia *et al.*, 1990; Esch *et al.*, 1990; Anderson *et al.*, 1991; Sisodia, 1992; Haas and Selkoe, 1993).

$\beta$ APs are generated by endoproteolytic cleavage of APP (amyloidogenic processing) by uncharacterized endopeptidases called  $\beta$ - and  $\gamma$ -secretases, at the amino and carboxy termini, respectively, of the  $\beta$ AP sequence of APP (Haas and Selkoe, 1993). The initial step in the abnormal processing of APP in AD occurs at the NH<sub>2</sub>-terminus of the  $\beta$ AP sequence, generating a potentially amyloidogenic COOH-terminal fragment containing the  $\beta$ AP sequence, the transmembrane, and cytoplasmic domains of APP (Estus *et al.*, 1992) (Figure 1). It is believed this cleavage occurs in the *medial*-golgi network and endosomal/lysosomal pathways (Shoji *et al.*, 1992; Caporaso *et al.*, 1992; Estus *et al.*, 1992; Golde *et al.*, 1992; Haas *et al.*, 1992; Knops *et al.*, 1992; Perez *et al.*, 1996; Thinakaran *et al.*, 1996), or in the secretory pathway proximal to the cell membrane (Busciglio *et al.*, 1993; Haass *et al.*, 1993; Seubert *et al.*, 1993). The  $\beta$ -

secretase cleavage is thus the first step in Alzheimer's-type amyloidogenesis, and sets the stage for the next cleavage by  $\gamma$ -secretase. The latter cleaves between residues 40 and 41, or residues 42 and 43 (cleavage between residues 43 and 44 can also occur) of the COOH-terminal fragment (Kosik, 1999). The  $\gamma$ -secretase cleavage site requires exposure by membrane damage, such as induced by lipid peroxidation (Dyrks *et al.*, 1992). Cleavage of the COOH-terminal amyloid fragments by  $\gamma$ -secretases to release the 39-43 amino acid  $\beta$ AP species probably occurs in the endosome/lysosome pathway (Busciglio *et al.*, 1993), although it appears that the endoplasmic reticulum (ER) may be the site of generation of  $\beta$ AP<sub>42</sub> but not  $\beta$ AP<sub>40</sub> in neurons (Hartmann *et al.*, 1997).

#### **1.4.0 Pathophysiology of APP and $\beta$ AP**

The formation and slow accumulation of the cytotoxic  $\beta$ AP in NPs in the hippocampus and adjoining areas of the brain, altered metabolism of APP, overexpression of APP, reduced glucose uptake into brain cells, impaired oxidative phosphorylation (OXPHOS) due to mitochondrial dysfunction, oxidative damage to cellular proteins, lipids and nucleic acids, neuronal excitotoxic mechanisms, and apoptosis have all been implicated in the neurodegenerative process of AD (Mattson, 1993[a] and 1994; Mark *et al.*, 1995; Dewji and Singer, 1996; Keller *et al.*, 1997; Shoulson, 1998).

There are numerous  $\beta$ AP species with extensive NH<sub>2</sub>- and COOH-terminal heterogeneity (Murphy *et al.*, 1999). About 90% of secreted  $\beta$ APs are the soluble forty

amino acid long  $\beta$ AP<sub>40</sub>, and 10% are the 42 and 43 residue  $\beta$ AP<sub>42</sub> and  $\beta$ AP<sub>43</sub>, which are highly fibrillogenic, readily aggregated, and neurotoxic (Jarrett and Lansbury, 1993; Yankner, 1996 ; Mann *et al.*, 1996 & 1997; Lansbury, 1997; Mattson, 1997). The major  $\beta$ AP species in cell culture media and cerebrospinal fluid (CSF) were found to be  $\beta$ AP<sub>40</sub> (50-70%), although some  $\beta$ AP<sub>42</sub> (5-20%) was also present, as well as lesser amounts of other peptides, including  $\beta$ AP<sub>39</sub> (Murphy *et al.*, 1999). Self-association occurs faster for the longer, more hydrophobic form of  $\beta$ AP ( $\beta$ AP<sub>42</sub> versus  $\beta$ AP<sub>40</sub>) (Jarrett *et al.*, 1993; Snyder *et al.*, 1994), it assembles more rapidly into filaments *in vitro* (Jarrett *et al.*, 1993), and is prone to aggregate into amyloid fibrils. The amyloid fibril is the neurotoxic form of  $\beta$ AP, with the soluble and non-fibrillar aggregates mostly being non-toxic (Pike *et al.*, 1993; Lorenzo and Yankner, 1994).  $\beta$ AP<sub>42</sub> and  $\beta$ AP<sub>43</sub> peptides are deposited early and selectively in plaques (Roher *et al.*, 1986; Iwatsubo *et al.*, 1994; Lemere *et al.*, 1996), and are deposited earlier in the disease process than  $\beta$ AP<sub>40</sub> (Saido *et al.*, 1995).

#### **1.4.1 Evidence supporting $\beta$ AP pathogenicity**

The production and accumulation of  $\beta$ AP is accepted as being the primary event involved in the pathogenesis of AD (Cordell, 1994; Selkoe, 1994 a), and the abnormal accumulation of  $\beta$ AP is thought to be due partially to increased generation of APP and to abnormal processing of it (Selkoe, 1994b and c). A primary pathogenic role for APP and  $\beta$ AP is suggested by the findings that aggregated  $\beta$ AP is directly toxic to cultured nerve cells and clonal cell lines (Yankner *et al.*, 1989 and 1990; Koh *et al.*, 1990; Pike *et al.*, 1991 and 1993; Mattson *et al.*, 1992; Loo *et al.*, 1993; Behl *et al.*, 1992 and 1994),

increased accumulation of  $\beta\text{AP}_{42}$  in the brain causes amyloid neurotoxicity leading to dementia (Yankner *et al.*, 1990),  $\beta\text{AP}_{42}$  is more abundant in AD brain tissue than in age-matched controls (Selkoe, 1994 d), and all FAD mutations influence APP processing in a manner that results in elevated production of the highly amyloidogenic  $\beta\text{AP}_{42}$  and  $\beta\text{AP}_{43}$  peptides (Price *et al.*, 1998). All mutations causing FAD must alter the proteolytic processing of APP, such as by altering  $\gamma$ -secretase activity (Scheuner *et al.*, 1996; Murphy *et al.*, 1999). This may result in decreased production of the neuroprotective sAPP (Mattson *et al.*, 1993).

#### **1.4.2 Pathogenic mechanisms of $\beta\text{AP}$**

In relation to the pathophysiology of AD, it is known that  $\beta\text{AP}$  and  $\beta$ -amyloid fibrils disturb the integrity of cell membranes, generate reactive oxygen intermediates (ROI) and the accompanying cytotoxic cellular oxidant stress, increase susceptibility to Glu-induced excitotoxic stress, promote microglial activation and cytokine release, and eventually cause neuronal cytotoxicity and cell death (Yankner *et al.*, 1990; Davis *et al.*, 1992; Araujo and Cotman, 1992; 1993; Koo *et al.*, 1993; Pike *et al.*, 1993; Haass and Selkoe, 1993; Kosik, 1994; Trowjanowski and Lee, 1994; Hensley *et al.*, 1994; Behl *et al.*, 1994; Klegeris *et al.*, 1994; Lorenzo and Yankner, 1994; Meda *et al.*, 1995; Benzi and Moretti, 1995; Cotman and Anderson, 1995; Busciglio and Yankner, 1995).

$\beta\text{AP}$ 's induction of plasma membrane lipid peroxidation, impairment of ion-motive ATPases and Glu uptake, uncoupling of G-protein-linked receptors, and generation of reactive oxygen species (ROS), all contribute to loss of  $[\text{Ca}^{2+}]_i$  homeostasis



that contributes to cell death (Mark *et al.*, 1996).

One way  $\beta$ AP adversely affects neuronal function and survival is by its reported stimulation of the production of hydrogen peroxide ( $H_2O_2$ ), which led to oxidative damage and cell death (Behl *et al.*, 1992 and 1994). Oxygen radicals produce injury to neuronal membranes and to mtDNA (Mecocci *et al.*, 1994), make neurons more vulnerable to dysfunction produced by Glu (Beal, 1992), and contribute to aggregation and deposition of  $\beta$ AP (Beal, 1995).  $\beta$ AP also induces activation of microglia leading to secretion of toxic free radicals and cytokines, which may further damage neurons (Meda *et al.*, 1995).

Proposed mechanisms for  $\beta$ AP's deleterious effects include direct neurotoxicity (Yankner *et al.*, 1989 and 1990), and induction of  $Ca^{2+}$  metabolism derangements leading to enhanced excitotoxicity (Mattson *et al.*, 1992 and 1993 b; Mattson, 1994 a), membrane permeability enhancement (Simmons and Schneider, 1993), and formation of  $Ca^{2+}$  channels that lead to abnormally high cytosolic  $Ca^{2+}$  concentration and subsequent cell death (Arispe *et al.*, 1993).  $\beta$ AP forms free radical peptides and aggregates that destabilize  $[Ca^{2+}]_i$  and make neurons vulnerable to metabolic insults (Mattson, 1994 a). The disturbed  $Ca^{2+}$  homeostasis and increased intraneuronal  $Ca^{2+}$  concentration induced by  $\beta$ AP may activate intracellular proteases, lipases, and other enzymes, leading to cell death (Mattson *et al.*, 1993 b; Hardy and Higgins, 1992; Khachaturian, 1994).

Senile plaques (NPs) contain a high concentration of microglia that express class A scavenger receptors (SR) (Wisniewski *et al.*, 1989; Christie *et al.*, 1996), and glycated matrix proteins that are ligands for class A SRs are present in Alzheimer lesions (Smith

*et al.*, 1994; Vitek *et al.*, 1994). It is postulated that deposition of  $\beta$ -amyloid fibrils induces microglia to adhere to  $\beta$ -amyloid fibrils via their class A SRs, probably in an attempt to clear them from the extracellular milieu. The high density of SR ligands in these  $\beta$ AP deposits causes immobilization of microglia that come into contact with them, and induces these microglia to secrete cytokines, ROS and nitrogen species that injure neighbouring neurons (El Khoury *et al.*, 1996). It has previously been shown that SRs participate in the production of ROS (Hartung *et al.*, 1986).

Advanced glycation end products (AGEP) could play an important role in the etiology of AD. AGEPs produce modified structures that form protein cross-links, and are known to generate ROIs (Vitek *et al.*, 1994; Yan *et al.*, 1994; Ledesma *et al.*, 1994). Protein cross-linking inhibits the physiological function of many proteins, and AGEPs may contribute to the transformation of the soluble form of  $\beta$ AP into its insoluble version. Their induction of oxidative stress may also contribute to their suspected role in the pathogenicity in AD (Thome *et al.*, 1996).

The receptor for advanced glycation end products (RAGE) is one receptor postulated to mediate the interaction of  $\beta$ AP with endothelial cells and neurons, resulting in cellular oxidant stress, and with microglia, resulting in cellular activation (cytokine production, chemotaxis, haptotaxis). Interaction of  $\beta$ AP with neurons and vascular cells caused oxidant stress and subsequent deleterious effects on cellular function and organic homeostasis (Yan *et al.*, 1996).

$\beta$ AP aggregates and amyloid fibrils have also been found inside cells (Knauer *et al.*, 1992; Fuller *et al.*, 1995; Yang *et al.*, 1995; Turner *et al.*, 1996; Wild-Bode *et al.*,

1997; Xia *et al.*, 1997; Xu *et al.*, 1997; Tierari *et al.*, 1997; La Ferla *et al.*, 1997), and  $\beta$ AP can be generated in the ER (Wild-Bode *et al.*, 1997; Tienari *et al.*, 1997) and be taken up by endocytosis (Knauer *et al.*, 1992; Yang *et al.*, 1995; La Ferla *et al.*, 1997; Urmoneit *et al.*, 1997). Therefore,  $\beta$ AP may target intracellular molecules (e.g. ERAB), mediating cellular stress and ultimately apoptosis, due to increased amounts of  $\beta$ AP (Yan *et al.*, 1997).

### **1.5 Bioenergetic Defects**

It has been known for some time that there are specific bioenergetic defects in multiple tissues in AD patients (Swerdlow *et al.*, 1997), and that a bioenergetic mechanism may be a primary event in the pathogenesis of AD (Blass *et al.*, 1988; Blass and Gibson, 1991; Beal, 1992; Hoyer, 1993; Mutisya *et al.*, 1993; Swerdlow *et al.*, 1994). Defects in glucose utilization and citric acid cycle metabolism have been described in AD (Parker and Parks, 1995).

Abundant evidence indicates that abnormalities of cerebral metabolism are a major factor underlying the pathogenesis of AD. Many reports have shown that reductions in AD brain occur in the pyruvate dehydrogenase complex (the link of glycolysis to the Krebs's cycle), the alpha-ketoglutarate dehydrogenase complex (the link of Krebs's cycle to glutamate metabolism) and COX of the mitochondrial ETC (the link of the Krebs's cycle to oxygen utilization). Additional results indicate that the reductions can also be secondary to other causes including oxidative stress. A variety of data suggest

that the mitochondrial insufficiencies contribute significantly to the pathophysiology of AD (Gibson *et al.*, 1998).

A key process in AD is decreased glucose turnover and a subsequently decreased oxidative phosphorylation, linked directly to secondary amyloid formation and nerve cell atrophy (i.e. disturbances of OXPHOS and glucose turnover induce  $\beta$ AP production) (Roberts *et al.*, 1991; Meier-Ruge and Bertoni-Freddari, 1997). The reduced OXPHOS causes the generation of  $\beta$ AP and the loss of neuronal synapses, because APP is not inserted into neuronal membranes in the absence of sufficient ATP. This leads to the generation of  $\beta$ AP and to amyloidosis (Meier-Ruge and Bertoni-Freddari, 1997).

Blood glucose levels are abnormally low in Alzheimer's dementia, and it was found that the fasting plasma glucose level was significantly reduced (about 20%) in patients with Alzheimer's dementia compared to those without the disease (Itagaki *et al.*, 1996). *In vivo* imaging of AD patients using positron emission tomography (PET) showed progressive reduction in brain glucose metabolism and blood flow in relation to dementia severity. The reductions reflect physiological down-regulation of gene expression for glucose delivery, OXPHOS, and energy consumption in brain (Chandrasekaran *et al.*, 1996). In a study (using PET) measuring the cerebellar and cerebral metabolic rate for glucose (CMR<sub>glc</sub>) in AD and age-matched normal control subjects, it was found that, in severe AD, both cerebellar and cerebral glucose metabolism were significantly reduced (Ishii *et al.*, 1997). Plasma protein glycation specifically derived from glucose was evaluated in moderate and severe AD patients and compared with an age-matched control group. The results suggested an eventual

impairment in glucose peripheral use or an increase in protein glycation rate associated with AD (Riviere *et al.*, 1998).

Deficits in energy metabolism are a major cause of amyloidogenic processing of APP. Inhibition of cytochrome c oxidase (COX, Complex IV) of the electron transport chain (ETC) caused amyloidogenic processing of APP (Gabuzda *et al.*, 1993; Iverfeldt *et al.*, 1993). ATP depletion markedly induced the production of a potentially amyloidogenic 11.5 kDa COOH-terminal derivative of APP in the secretory pathway (Gabuzda *et al.*, 1994). In COS cells, metabolic stress due to glucose deprivation caused a 26% decrease in soluble APP (sAPP) secretion. Sodium azide, an inhibitor of COX, decreased sAPP release in a concentration dependent manner (maximum -75%). These results suggest that the inhibition of energy metabolism can influence APP processing leading to a decreased secretion of non-amyloidogenic fragments of APP (Gasparini *et al.*, 1997), and an increased generation of potentially amyloidogenic fragments (Gabuzda *et al.*, 1994).

## 1.6 COX Deficit

The mitochondrial ETC's cytochrome c oxidase (Complex IV, COX) is a thirteen subunit multimeric enzyme, located in the inner mitochondrial membrane. Only three of its subunits (COX I, COX II, COX III) are encoded by mtDNA (Edland *et al.*, 1996). COX is involved in the mitochondria generation of ATP by the process of oxidative phosphorylation (Wallace, 1999).

COX was shown to be catalytically depressed and kinetically abnormal in AD cerebral cortex, fibroblasts and platelets, suggesting the enzyme may be structurally altered. It was, however, expressed at normal levels (Parker *et al.*, 1990; Kish *et al.*, 1992; Mutisya *et al.*, 1993 and 1994; Parker *et al.*, 1994 a and b; Beal, 1995; Parker and Parks, 1995).

The COX and other ETC activities were assayed in platelet mitochondria isolated from patients with AD. Five of 6 patients had striking 50% reductions of platelet activity. Other ETC catalytic activities were not significantly different than control values. It was postulated that AD may be a systemic illness, a primary defect in COX may be pathogenically important in its production, and the mitochondrial genes encoding COX subunits may be important in producing the defect (Parker *et al.*, 1990; Parker, 1991). In another assay, mean platelet COX activity in AD patients was significantly less (~18%) than in controls. Complex III (ubiquinol:cytochrome c oxidoreductase), complex II (succinic dehydrogenase), and citrate synthase were all assayed as internal controls and were not significantly different in controls and Alzheimer patients. This points to a relatively specific loss of platelet COX activity in Alzheimer disease patients (Parker *et al.*, 1994 a).

Fibroblasts from AD patients have also displayed decreased COX activity. The results from determining the basal oxygen consumption rate ( $QO_2$ ) supported the hypothesis that subtle dysfunctions of oxidative energy-producing processes are present in fibroblasts from sporadic AD patients. In tissues, such as the brain, that rely heavily on oxidative metabolism for their function, similar alterations may trigger molecular

mechanisms leading to cell damage (Curti *et al.*, 1997). The ETC activities in mitochondria isolated from autopsied brain samples from AD patients and from controls with and without known neurologic disease demonstrated a generalized depression of activity of all ETC complexes, being most marked in COX activity. These findings agree with the proposition that the ETC is defective in AD brain, and the defect centers about COX (Parker *et al.*, 1994 b ). The activity of COX in homogenates of autopsied brain regions of patients with AD and controls showed that mean COX activity in AD brain was reduced in frontal (-26%), temporal (-17%), and parietal (-16%, though not significant) cortices. The reduction of COX activity, which is tightly coupled to neuronal metabolic activity, was proposed to be explained by hypofunction of neurons, neuronal or mitochondrial loss, or possibly by a more primary, but region-specific, defect in the enzyme itself. It was concluded that the absence of a COX activity reduction in all of the examined brain areas does not support the notion of a generalized brain COX abnormality. Although the functional significance of a 16-26% cerebral cortical COX deficit in human brain is not known, a deficiency of this key energy-metabolizing enzyme could reduce energy stores and thereby contribute to the brain dysfunction and neurodegenerative processes in AD (Kish *et al.*, 1995). Parker and Parks (1995) showed that purified AD brain COX displayed anomalous kinetic behavior compared with control brain COX, in that the low Km binding site was kinetically unidentifiable. For purposes of comparison, COX was also purified from a standard beef heart preparation and was found to display normal kinetic behavior. It was thus proposed that AD brain COX may be structurally abnormal and may, in agreement with other findings, make an

important contribution to the bioenergetic defect seen in AD (Parker and Parks, 1995). Mutisya *et al.* (1994) measured the activities of Complexes I-IV in frontal, temporal, parietal, and occipital cortices of AD brains. Complexes I-III showed a small decrease in activity in the occipital cortex only. The most consistent change was a 25-30% reduction of COX in four cortical regions examined. Reichmann *et al.* (1993) demonstrated a marked decrease in COX, and lesser deficits in Complex II and III activities, in homogenate and purified mitochondrial fractions from AD patients compared with controls. Another study that evaluated the level of COX in various brain regions of post-mortem AD and control patients, found that there was reduced COX levels and activity in all cortical areas examined, suggesting a generalized suppression of oxidative metabolism throughout the cortex (Wong-Riley *et al.*, 1997).

Alteration in mitochondrial COX gene expression might underlie the reduction in COX activity in AD. There was found to be a selective reduction in mRNA levels for the mitochondrial-encoded COX II subunit, both in regions with NFTs, senile NPs, and neuronal loss and regions relatively spared from these neuropathological changes. The data suggested that the reduction in COX activity in brain regions from individuals with AD may be a result of an alteration in mitochondrial COX gene expression that extends beyond neurons directly affected by structural pathology (Simonian and Hyman, 1994). Supporting the above findings, brains from five patients with AD showed a 50%-65% decrease in mRNA levels of COX subunits I and III in the middle temporal association neocortex, but not in the primary motor cortex, as compared to five control brains (Chandrasekaran *et al.*, 1994). There was also found to be a 50% decrease in mRNA



levels of mtDNA-encoded COX I and III in post-mortem AD brains, in an association neocortical region (midtemporal cortex), but not in the primary motor cortex unaffected in AD. There were 50-60% decreases in mRNA levels of nuclear DNA (nDNA)-encoded COX IV and the beta-subunit of the F<sub>0</sub>F<sub>1</sub>-ATP synthase in midtemporal cortex, but not in the primary motor cortices of the AD brains (Chandrasekaran *et al.*, 1997). Follow up work demonstrated that COX II mRNA from post-mortem brain tissue was markedly reduced in the entorhinal cortex and the hippocampal formation compared with control brains. In the hippocampus, reductions were in regions severely affected by AD pathology as well as in regions that were relatively spared (Chandrasakaran *et al.*, 1998). These data suggest that the decrease in COX I, II and III subunits mRNA in affected brain regions may contribute to reduced brain oxidative metabolism in AD (COX is a marker for oxidative metabolism) (Chandrasakaran *et al.*, 1994). As well, it appears reduced neuronal activity and downregulation of OXPHOS machinery cause coordinated decreases in expression of mitochondrial and nuclear genes in the association cortex of AD brains (Chandrasekaran *et al.*, 1997), and reduced mitochondrial energy metabolism reflects loss of neuronal connections (Chandrasekaran *et al.*, 1998).

Cybrids have been used to study OXPHOS. Cybrids are formed by the transferring of mitochondria from living patients to mitochondria-deficient cells ( $\rho^0$  cells). The resulting cybrids enable one to determine whether any observed defects in OXPHOS in a patient's tissues are attributable to alterations in a patient's mtDNA, as the patient's mitochondria now function in the presence of a different nuclear genome (Beal, 1997). Neuroblastoma AD cybrids demonstrated a 52% decrease in COX activity, an

elevation of ROS levels, increased basal cytosolic  $[Ca^{2+}]$  and an enhanced sensitivity to inositol-1,4,5-triphosphate-mediated release. It was suggested that the subtle alterations in  $Ca^{2+}$  homeostasis and ROS generation might lead to increased susceptibility to cell death under circumstances not ordinarily toxic (Sheehan *et al.*, 1997). AD cybrids were shown to have increased levels of ROS in the presence of increased, compensatory free radical scavenging enzymes. It was postulated a primary biochemical defect (COX dysfunction) creates a secondary biochemical defect (increased ROS generation), both being relevant to neurodegeneration (Swerdlow *et al.*, 1997; Beal, 1997).

COX may also play a critical role in specific groups of neurons involved in learning and memory (Parker *et al.*, 1994 b). Inhibition of COX in rats resulted in their cognitive impairment and abnormal hippocampal LTP (Bennett *et al.*, 1992). And there is some correspondence between the expression of mRNA of COX I, COX II and COX III and cell groups involved in AD, which may allow for a widespread modest depression of COX activity to produce focal CNS disease (Chandrasakaran *et al.*, 1992 a and b). It is known COX failure would cause depression of ATP synthesis and bioenergetic impairment, and such impairment resulting from primary ETC dysfunction has been shown to cause late onset and focal CNS disease (Wallace *et al.*, 1988; Parker *et al.*, 1989 a and b, and 1990 b; Gato *et al.*, 1990; Shapira *et al.*, 1990; Shoffner *et al.*, 1990 and 1991; Howell *et al.*, 1991). COX abnormalities have also been linked to other disorders characterized by cortical degeneration (Prick *et al.*, 1983; Danks, 1983).

## 1.7 Overexpression of APP

In AD, the abnormal accumulation of  $\beta$ AP is thought to be due partially to increased generation of APP and to abnormal processing of it (Selkoe, 1994 b and c). The pathogenic mechanisms of plaque formation include alterations in APP gene expression. There is augmented expression of APP gene transcripts in Down's Syndrome and in specific areas of the brain in AD (Higgans *et al.*, 1988; Cohen *et al.*, 1988; Neve *et al.*, 1988; Johnson *et al.*, 1990). Duplication of the APP gene on chromosome 21 is sufficient for amyloid deposition and subsequent development of Alzheimer-type neuropathology (Hyman, 1992). Post-mitotic neurons overexpressing full-length APP showed degeneration *in vitro* (Yoshikawa *et al.*, 1992).

Marked increase in APP gene expression accompany environmental risk factors for AD, such as brain trauma, temporary ischemia and heat shock. The process is potentiated by an ischemic Glu release that opens cellular  $Ca^{2+}$  channels, inhibiting glucose turnover and ATP production, and which is accompanied by the generation of  $\beta$ AP (Roberts *et al.*, 1991; Meier-Ruge and Bertoni-Freddari, 1997). It has been postulated that increased expression of the APP gene may alter the processing of the protein, producing more insoluble  $\beta$ AP (Nalbantoglu *et al.*, 1997).

There is a relationship between APP overexpression and abnormalities of COX and mitochondrial structure (Shigenaga *et al.*, 1994). The overexpression of APP via an adenovirus vector in cultured normal human muscle fibres caused decreased COX activity and structural abnormalities of mitochondria, in a dose- and duration-dependent

manner. Decreased COX activity preceded the mitochondrial structural changes (Askanas *et al.*, 1996).

## **1.8 Oxidative Stress**

Oxidative stress is an important factor in the development of AD, as an etiopathogenic oxidative stress hypothesis has been supported by several experimental findings (Olanow and Arendash, 1994; Beal, 1995; Harman, 1995; Benzi and Moretti, 1995). Oxidative stress refers to the cytotoxic consequences of oxygen radicals - superoxide anion ( $O_2^-$ ), hydroxy radical ( $OH$ ), and hydrogen peroxide ( $H_2O_2$ ) - which are generated as byproducts of normal and aberrant metabolic processes that utilize molecular oxygen (Coyle and Puttfarcken, 1993). The brain consumes a disproportionate amount of the body's oxygen, deriving its energy almost exclusively from oxidative metabolism of the mitochondrial respiratory chain (Halliwell and Gutteridge, 1989). ROS are continuously produced by mitochondria, and if the cell's anti-oxidant defense mechanisms are overwhelmed, oxidative stress occurs (Mecocci *et al.*, 1998). Many processes and enzymes in the brain also increase the levels of ROS and radical nitrogen species, by producing them as by-products of their reactions (Coyle and Puttfarcken, 1993). Oxidative stress damages lipids, proteins and DNA, resulting in necrosis or apoptosis (Simonian and Coyle, 1996).

Direct evidence supporting increased oxidative stress in AD include (i) increased brain iron, aluminum and mercury in AD capable of stimulating free radical generation,

(ii) increased lipid peroxidation and decreased polyunsaturated fatty acids (PUFA) in AD brain, and increased 4-hydroxynonenal (HNE), an aldehyde product of lipid peroxidation in AD ventricular fluid, (iii) increased protein and DNA oxidation in AD brain, (iv) diminished energy metabolism and decreased COX in brain in AD, (v) AGEP, malondialdehyde, carbonyls, peroxynitrite, heme-oxygenase-1 and superoxide dismutase 1 (SOD-1) in NFTs, and AGEP, heme oxygenase-1 and SOD-1 in senile plaques, (vi) plus the fact that  $\beta$ AP can generate ROS. Indirect evidence comes from many *in vitro* studies showing that free radicals are capable of mediating neuron degeneration and death, whether or not they are a primary or secondary (e.g. to tissue damage) event (Markesbery, 1997). It has been demonstrated that AD COX does act as a ROS generator (Partridge *et al.*, 1994; Lakis *et al.*, 1995; Parker and Parks, 1995), which would account for the increased levels of lipid peroxidation in AD brain and other indicators of free radical involvement (Subbaro *et al.*, 1990; Volicer and Crino, 1990). There is a relationship between the redox state of the cell and the degeneration in AD (Smith *et al.*, 1991; Behl *et al.*, 1994 a). When the ETC is inhibited, electrons accumulate in the early stages of the ETC (complex I and CoQ), where they can be donated directly to molecular oxygen to give superoxide anion. This is detoxified by mitochondrial manganese SOD (MnSOD) and glutathione peroxidase. Chronic ROS exposure leads to oxidative damage to mitochondrial and cellular proteins, lipids, and nucleic acids, and acute ROS exposure can inactivate the iron-sulphur centres of ETC complexes I, II, and III, and aconitase of the Krebb's cycle, resulting in shutdown of mitochondrial energy production (Wallace 1997 and 1999). It is known  $\beta$ AP causes plasma membrane lipid peroxidation and

generation of ROS that contribute to cell death (Mark *et al.*, 1996). The neurotoxic actions of  $\beta$ AP could be blocked by antioxidants (Behl *et al.*, 1992), and relied on the presence of reactive oxygen intermediates (Behl *et al.*, 1994).

It has been shown that  $\beta$ AP caused oxyradical-mediated impairment of glucose transport, Glu transport, and mitochondrial function in rat neocortical synaptosomes. Several antioxidants prevented the  $\beta$ AP-induced impairment of glucose transport, indicating that lipid peroxidation was causally linked to the adverse action of  $\beta$ AP. It is suggested that oxidative stress occurring at synapses may contribute to the reduced glucose uptake and synaptic degeneration that occurs in AD patients (Keller *et al.*, 1997).

One mechanism of oxidative stress is the nitration of tyrosine residues in proteins, mediated by peroxynitrite breakdown. The latter is a reaction product of NO and superoxide radicals. Oxidative stress is linked to NFT formation, and NO excitotoxicity and expression is linked to the pathogenesis of AD (Good *et al.*, 1996).

Brain, and specifically neurons, are particularly vulnerable to impairments of oxidative metabolism because of their tight dependence on continuous oxidation of glucose to maintain their structure and function. Several studies have shown the brain areas of greatest vulnerability in AD include those particularly sensitive to oxidative impairments (Blass and Gibson, 1991). As well, brain cells are at great risk from damage caused by free radicals. The brain has an extremely high rate of oxygen consumption, and CNS neuronal membranes are high in PUFAs that are very vulnerable to lipid peroxidation (Behl *et al.*, 1994 a). The free radical attack on PUFAs causes lipid peroxidation and organic peroxy radicals to build up in a self-perpetuating cycle. As well,

the abstracted lipid hydrogen atoms combine with the peroxy radicals to form lipid hydroperoxides which, in the presence of ferrous ions, decompose to alkoxy radicals and aldehydes. Thus, the end result is the generation of numerous toxic reactants that rigidify membranes by cross-linking, disrupt membrane integrity, and damage membrane proteins (Coyle and Puttfarcken, 1993).

A critical reason why oxidative stress is important in AD, is that the aggregation of  $\beta$ AP and other amyloidogenic APP-derived peptides depends on radical generation systems (metal catalyzed oxidation systems) which transform soluble peptides into insoluble aggregating molecules. This involves radical-induced cross-linking of tyrosyl hydroxyl groups of the  $\beta$ -amyloidogenic peptides, the primary event leading to amyloid formation (Dyrks *et al.*, 1992). The aggregation of PHFs, like  $\beta$ AP fibrils, is also linked to increased oxidation. The findings support the notion that the increase in redox potential and an excess protein oxidation found in aging brain provide a link for the aggregation of  $\beta$ AP fibres and PHFs (Schweers *et al.*, 1995).

Of relevance to AD, is that energy failure due to anoxia or hypoglycemia caused a marked efflux of Glu to achieve concentrations in the extracellular space compatible with neurotoxic effects (Benveniste *et al.*, 1984; Katchman and Hershkowitz, 1993). Activation of glutamate-gated cation channels is the most important source of oxidative stress in the brain. These two mechanisms can act in concert to produce neurodegeneration (Coyle and Puttfarcken, 1993). In turn, active glutamate receptors (NMDA and  $\alpha$ -amino-3-hydroxy-5-methyl-4-isoxazolepropionate-kainate) cause a depletion of ATP and the induction of lactic acidemia (Retz and Coyle, 1982). The acidic

conditions favor the liberation of cellular  $Fe^{2+}$  which promotes the Fenton reaction and the liberation of  $H_2O_2$  (Halliwell and Gutteridge, 1989). Related to this, it is known NMDA receptor stimulation produces marked elevations in  $\cdot O_2^-$  and  $\cdot OH$  (Lafon-Cazal *et al.*, 1995). As well, NMDA receptor-mediated stimulation of phospholipase  $A_2$  and the subsequent release of arachidonic acid (AA) leads to the generation of oxygen radicals (Dumuis *et al.*, 1988; Lazararewicz *et al.*, 1988). Added to this, AA and oxygen radicals enhance the release of Glu and inhibits its uptake inactivation by neuronal and glial transporter processes, promoting a self perpetuating cycle (Pellegrini-Giampietro *et al.*, 1988; Williams *et al.*, 1989).

## 1.9 Apoptosis

Accumulating evidence links apoptotic pathways to neurodegeneration in AD. Histochemical studies report apoptosis to be a pathological feature of AD (Su *et al.*, 1994; Cotman and Anderson, 1995; Lassmann *et al.*, 1995; Smale *et al.*, 1995). The loss of hippocampal neurons by apoptotic cell death is a prominent feature of AD (Smale *et al.*, 1995; Cotman and Su, 1996; Li *et al.*, 1997; Su *et al.*, 1997). One potential factor contributing to the susceptibility of these cells to premature death arises from the cytotoxic effects of  $\beta AP$  deposition at or near sites of neuronal degeneration. Cultured human cells, including neurons, undergo apoptosis when treated with  $\beta AP$ s (Loo *et al.*, 1993; LaFeria *et al.*, 1995; Forloni *et al.*, 1996), and neurons undergoing apoptosis generate elevated levels of cytotoxic  $\beta AP$  species (LeBlanc, 1995; Gervais *et al.*, 1999).



This agrees with the proposition that the elevated  $\beta$ AP that occurs due to genetic predisposition or other physiological factors, provokes partial activation of apoptosis in susceptible neurons. These sensitized cells then produce more  $\beta$ AP, leading to a self-perpetuating cycle which culminates in the progressive neuronal loss seen in AD (Gervais *et al.*, 1999)

As well, caspases, the primary mediators of apoptosis, have been shown to be involved in proteolytic cleavage of APP and in the biogenesis of amyloidogenic  $\beta$ AP species. Caspase-3 was found to be elevated in dying neurons of human AD brain. It was demonstrated that caspase-mediated proteolysis occurred in hippocampal neurons *in vivo* during acute brain injury (cell death). The caspase-cleaved APP also co-localized with senile plaques and increased the rate of  $\beta$ AP formation in neuronal cells (Gervais *et al.*, 1999). It was also shown that there was enhanced  $\beta$ AP formation in cells harboring the Swedish mutation of APP, and that this was dependent on caspase proteolysis at the  $\beta$ -secretase site (Gervais *et al.*, 1999).

It is proposed that cleavage of APP at endogenous caspase consensus sites corrupts the normal, non-amyloidogenic intracellular processing of APP. The following steps may then lead to a self-perpetuating cycle: caspase-3-mediated truncation of APP at the COOH terminus, adulteration of normal APP processing with shunting of the residual polypeptide toward an amyloidogenic pathway, generation of elevated levels of  $\beta$ AP resulting in  $\beta$ AP-induced neuronal stress, progressive upregulation and/or activation of caspases, and exacerbated APP proteolysis (Gervais *et al.*, 1999). Thus, APP is a target for certain caspases and is involved in apoptotic pathways (Gervais *et al.*, 1999;

Weidemann *et al.*, 1999). Elevated APP levels have been reported in dying neurons (Barnes *et al.*, 1998), which could potentially feed more APP into the cycle (Weidemann *et al.*, 1999).

It has recently been shown that mitochondria contain a caspase-like enzymatic activity in addition to three biological activities previously suggested to participate in the apoptotic process: (a) cytochrome c; (b) an apoptosis-inducing factor (AIF) which causes isolated nuclei to undergo apoptosis *in vitro*; and (c) a DNase activity. All of these factors are released upon opening of the PTP. Experimental data suggest that caspase-2 and -9 zymogens are essentially localized in mitochondria and that the disruption of the outer mitochondrial membrane occurring early during apoptosis may be critical for their sub-cellular redistribution and activation (Susin *et al.*, 1999). Loss of mitochondrial barrier function during neuronal damage from ischemia or other insults (e.g. AD pathology) therefore may play an important role in making certain caspases available to participate in apoptosis (Krajewski *et al.*, 1999). In support of caspases and apoptosis being involved in AD, the protein levels of both caspase-2 and -3 were significantly increased in AD brains (Shimohama *et al.*, 1999).

Of consequence to AD, neurons are particularly vulnerable to degeneration by apoptosis. Inducers of apoptosis (e.g.  $\beta$ AP, oxidative damage, low energy metabolism) are also present in AD brains. Some neurons in vulnerable regions of AD brain show evidence of DNA damage, nuclear apoptotic bodies, chromatin condensation, and the induction of select genes characteristic of apoptosis in cell culture and animal models (Cotman and Su, 1996). Evidence supporting the involvement of apoptotic processes in

neurodegeneration *in vivo* include the finding that apoptotic mediator proteins like Par-4 are increased in neurons of AD brains (Guo *et al.*, 1998). Expression of mutant APP carrying FAD mutations have induced apoptosis, indicating that apoptosis may contribute to neuronal loss in FAD (Yamatsuji *et al.*, 1996 a and b; Zhao *et al.*, 1997). This has been shown to be dependent on a short stretch within the cytosolic domain of APP, and is a site where caspase cleavage occurs (Wiedemann *et al.*, 1999). Caspases may thus play an important role in the generation of  $\beta$ AP as well as in the ultimate death of neurons by apoptosis in AD (Gervais *et al.*, 1999).

Mitochondrial dysfunction appears to occur in AD (Beal, 1992), and mitochondria provide a major switch in the initiation of apoptosis. A decrease in mitochondrial membrane potential ( $\Delta\Psi$ ) causes opening of the mitochondrial inner membrane channel, the PTP, which has been implicated as a critical effector of apoptosis in a variety of non-neural cells (Zoratti and Szabo, 1995; Petit *et al.*, 1996; Green and Reed, 1998; Tatton and Chalmers-Redman, 1998). Opening of the MTP causes collapse of the proton motive force ( $\Delta\Psi$ ), swelling of the mitochondrial inner membrane, and release of death-promoting factors, such as cytochrome c, AIF, and latent forms of caspases (Wallace, 1999). Opening of the PTP and the accompanying death of the cell can be initiated by the mitochondrion's excessive uptake of  $\text{Ca}^{2+}$ , increased exposure to ROS, or decline in energetic capacity (Zoratti and Szabo, 1995; Liu *et al.*, 1996; Brustovetsky and Klingenberg, 1996; Green and Reed, 1998; Marzo *et al.*, 1998; Susin *et al.*, 1999; Earnshaw *et al.*, 1999). Thus, a marked reduction in mitochondrial energy production and a chronic increase in oxidative stress, as known to occur in AD, could

theoretically activate the PTP and initiate apoptosis.(Wallace, 1999).

Oxidative stress and apoptosis are closely linked. It is known that  $H_2O_2$  induces apoptosis in different cells, including rat neurons (Whittemore *et al.*, 1994), and human neuroblastoma cells (Zhang *et al.*, 1997).  $\beta$ AP can induce both necrotic (Behl *et al.*, 1994 b) and apoptotic cell death, which can also be caused by oxidative damage (Loo *et al.*, 1993; Hockenbery *et al.*, 1993; Forloni *et al.*, 1993; Watt *et al.*, 1994; Whittemore *et al.*, 1994; Anderson *et al.*, 1995; La Ferla *et al.*, 1995).  $\beta$ AP-induced neurotoxicity correlates with elevated  $H_2O_2$ . A large number of antioxidants and free radical scavengers protected from  $\beta$ AP toxicity and inhibited peroxide accumulation.  $\beta$ AP increased lipid peroxidation that could be inhibited by antioxidants (Behl *et al.*, 1992 and 1994 a). Zhang *et al* (1997) demonstrated that  $H_2O_2$ -induced apoptosis altered APP processing, producing an apoptosis-associated 5.5 kDa APP COOH-terminal fragment, suggesting  $\beta$ AP is a mediator of apoptosis. The generation of  $H_2O_2$  by  $\beta$ AP reduces the flow of electrons through the ETC. As well,  $H_2O_2$  is converted to the  $\cdot OH$ , which interferes with the ETC directly and via lipid peroxidation of the mitochondrial membrane (Behl *et al.*, 1994 a). The increased generation of ROS has also been directly linked to neuronal apoptosis in fetal neurons of Down's syndrome (Busciglio and Yankner, 1995). Zhang *et al.* (1997) postulate that a cycle may exist between  $H_2O_2$ ,  $\beta$ AP and apoptosis.  $\beta$ AP induces increased  $H_2O_2$  levels, which enhances the amyloidogenic, and inhibits the normal  $\alpha$ -secretase, processing of APP, producing more  $\beta$ AP. As well, increased  $H_2O_2$  and  $\beta$ AP levels induce apoptosis, which stimulates more  $\beta$ AP production.

## **2.0 AIM AND HYPOTHESIS**

To date, deficits in energy metabolism and COX activity, oxidative stress and lipid peroxidation of biological membranes, overexpression of APP, amyloidogenic processing of APP and the accompanying excessive production of  $\beta$ AP species, as well as neuronal degeneration and apoptosis, have all been implicated in the pathogenesis of AD. However, the exact mechanisms underlying the pathophysiology of AD have yet to be elucidated. Our initial aim was to identify APP effector binding proteins in order to deduce a mechanism whereby APP and its amyloidogenic derivatives may be involved in the pathogenesis of AD. Through the use of a yeast two-hybrid system, it was discovered that APP interacted with COX I, a catalytic subunit of Complex IV of the mitochondrial ETC. This finding may, therefore, link APP (and perhaps its amyloidogenic derivatives), to the deficits in energy metabolism (and specifically reduced COX activity), that have been well documented in AD. From this finding, our hypothesis was that APP is targeted to, and resides in, mitochondria, where, under some circumstances (e.g. overexpression of APP), the direct and aberrant involvement of APP and its potentially amyloidogenic derivatives with COX I causes (i) deficits in COX activity (bioenergetic defect), (ii) generation of ROS and its accompanying lipid peroxidation, (iii) aberrant amyloidogenic processing of APP, and (IV) subsequent neuronal apoptosis. The pathogenic postulates (i) to (iv) have already been demonstrated to occur in AD. However, we have tried to tie these aspects together into a working model, as our hypothesis states.

To substantiate our hypothesis, we wished to carry out the following experiments:

1. Determine what regions of APP are involved in the interaction, by restriction enzyme (RE)-based deletions.
2. Demonstrate that overexpression of APP in neuroblastoma cells causes a selective deficit in COX activity, increased generation of ROS and lipid peroxidation, and increased apoptosis.
3. Show that APP is targeted to, and localized in, mitochondria.
4. Demonstrate that  $\beta$ AP also resides in mitochondria, suggesting APP is processed in this organelle.

### **3.0 MATERIALS AND METHODS**

#### **3.1.0 Preparation of Plasmid/APP DNA Constructs**

##### **3.1.1 pAS2-1/APP<sub>770/2583</sub> construct**

APP<sub>770</sub> cDNA containing 3432 base pairs (bps) plus 15 bps of the 5' untranslated region (UTR) was received inserted into the pGEM9zf plasmid (Promega) (Figure 2). To amplify the pGEM9zf/APP<sub>770/3432</sub> construct, 100  $\mu$ l *E. coli* XL1-Blue supercompetent cells (Stratagene) were transformed with 1  $\mu$ g pGEM9zf/APP<sub>770/3432</sub>, following the standard protocol as per Promega. That is, the bacteria/DNA mixture was cold shocked on ice 0.5 hour (hr), followed by heat shock for 1 minute (min.) at 42°C, and then put on ice for another 2 min. Next, 1 millilitre (ml) Luria-Bertani (LB) broth was added and the

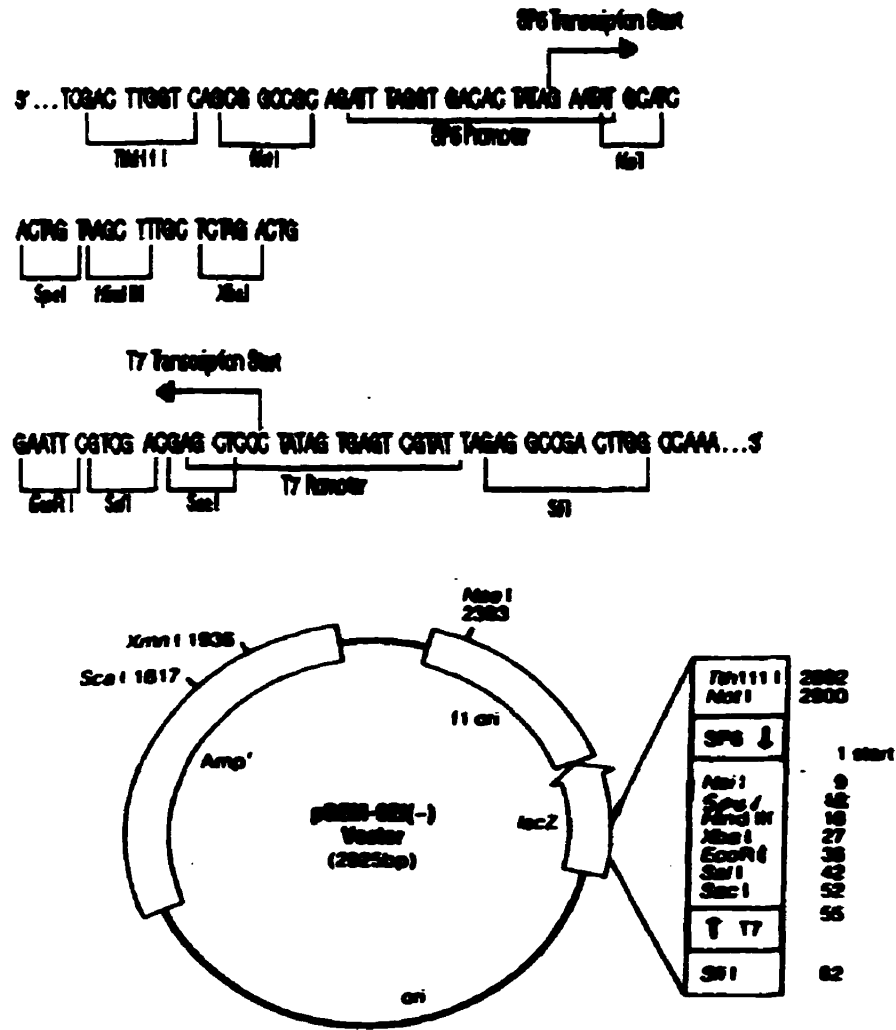


Figure 2 Schematic of pGEM9zf restriction map and MCS. The APP<sub>770/3432</sub> cDNA was inserted between the EcoR 1 and Sal 1 RE sites in the MCS of the pGEM9zf vector. The sequence shown corresponds to RNA synthesized by SP6 RNA polymerase and is complementary to RNA synthesized by T7 RNA polymerase. Some sequence reference points: SP6 RNA polymerase transcription initiation site, (1); T7 RNA polymerase transcription initiation site, (55); SP6 RNA polymerase promoter, (2909-6); T7 RNA polymerase promoter, (50-72); multiple cloning sites, (5-54), *lacZ* start codon, (107); beta-lactamase (*Amp<sup>r</sup>*) coding region, (1264-2124). (Adapted from Promega).

mixture incubated for 1 hr at 37°C on a rotating incubator (250 revolutions per minute [rpm]). Ampicillin (amp) (100 µg/ml - this is the concentration used in all future references to ampicillin, unless otherwise specified) was added and the *E. coli*/pGEM9zf/APP<sub>770/3578</sub>/amp mixture was incubated overnight at 37°C and 250 rpm. About 300 µl of the incubate was added to 1 litre (L) LB/amp broth, and the mixture incubated overnight at 37°C and 250 rpm. A plasmid maxiprep (QIAGEN's *Plasmid Maxi Kit*) was performed to purify and extract the pGEM9zf/APP<sub>770/3432</sub> DNA, whose concentration was determined photometrically from the equation:

$$[\text{DNA}] \mu\text{g}/\mu\text{l} = \text{A} \times 50 \text{ (for double stranded DNA)} \times (1000 [\mu\text{l} \text{ water in cuvette}] + \mu\text{l sample DNA}) / (1000 \times \mu\text{l sample DNA}).$$

To verify the DNA isolated by the plasmid prep was the correct plasmid construct, the DNA was restricted with Bgl II. Reaction mixture: 20 µl distilled, deionized water (ddwater), 2 µl buffer, 2 µg pGEM9zf/APP<sub>770/3432</sub>, 2 µl Bgl II. This was incubated in a water bath for 3 hr at 37°C, following which, a 0.8% agarose gel electrophoresis (AGE) of the Bgl II-restricted pGEM9zf/APP<sub>770/3432</sub> was performed.

To prepare the APP<sub>770</sub> fragment for insert into pGEM5zf plasmid (Promega) (Figure 3), the pGEM9zf/APP<sub>770/3432</sub> construct was restricted with Spe I. Reaction mixture: In each of five tubes, 40 µl ddwater, 5 µl buffer, 5 µg pGEM9zf/APP<sub>770/3432</sub>, 2 µl Spe I. The mixtures were incubated for 3 hr at 37°C, followed by a 0.8% AGE. The appropriate APP<sub>770/2583</sub> DNA was cut from the gel, and the DNA isolated and purified via QIAGEN's *QIAEX II Gel Extraction Kit*.

To prepare the pGEM5zf plasmid to receive the APP<sub>770/2583</sub> insert, the plasmid





was first amplified by transforming 100  $\mu$ l *E. coli* XL1-Blue supercompetent cells with 1  $\mu$ g pGEM5zf DNA, protocol as above. A plasmid maxiprep (QIAGEN's *Plasmid Maxi Kit*) was performed and the plasmid construct verified by RE analysis. The pGEM5zf plasmid was then restricted with Spe 1 to prepare it to accept the Spe 1-restricted APP<sub>770/3432</sub> fragment. Reaction mixture: In five separate tubes, 70  $\mu$ l ddwater, 10  $\mu$ l buffer, 10  $\mu$ g pGEM5zf, 3  $\mu$ l Spe I. The mixtures were incubated overnight at 37°C, and then subjected to 0.8% AGE. The Spe 1-restricted pGEM5zf band was cut from the gel, isolated and purified via QIAGEN's *QIAEX II Gel Extraction Kit*, and its concentration determined photometrically.

To prevent the plasmid from self-ligating before accepting the insert, the Spe 1-restricted pGEM5zf was de-phosphorylated, as per Promega, as follows. First, the amount of picomole (pmol) of ends of linear double stranded DNA was calculated, according to the formula: ( $\mu$ g DNA/Kb size of DNA) X 3.04 = pmol of ends. Reaction mixture: 10  $\mu$ l calf intestinal alkaline phosphatase (CIAP) 10X reaction buffer, 0.03 u CIAP/pmol of ends of DNA (i.e. 0.3 u CIAP per 10  $\mu$ g of pGEM5zf), 20  $\mu$ g pGEM5zf, ddwater to make a final volume of 100  $\mu$ l. The reaction mixture was incubated at 37°C for 30 min, after which, an equal volume of CIAP was added and the mixture incubated for another 30 min at 37°C. The reaction was then stopped by adding 2.0  $\mu$ l of 0.5 M EDTA and heated at 65°C for 20 min. The de-phosphorylated, Spe 1-restricted pGEM5zf was precipitated and purified with phenol/chloroform/isoamyl alcohol (PCIAA) and ethanol, as per Promega, as follows: An equal volume PCIAA was added to the DNA mixture, vortexed for 1 min., and centrifuged at 12,000 rpm for 5 min. The upper

aqueous layer was transferred to a new tube, to which was added 0.1% 3 M sodium acetate (pH 5.2) and two volumes of 100% ethanol, followed by storage at -20°C for 30 min, and then centrifugation at 12,000 rpm for 30 min. The supernatant was discarded and 200 µl 70% ethanol added. This was centrifuged for 15 min at 12,000 rpm. The supernatant was discarded and the pellet allowed to dry, after which it was re-suspended in 50 µl ddwater.

The APP<sub>770/2583</sub> fragment was ligated into the de-phosphorylated, Spe I-restricted pGEM5zf, using Clontech's *Ligation Express Kit*, to create the construct, pGEM5zf/APP<sub>770/2583</sub>. Next, 100 µl *E. coli* XL1-Blue supercompetent cells were transformed with the whole ligation mixture, as per Promega. Following this, 100 µl of re-suspended transformed cells were spread onto an LB/amp/isopropylthiogalactoside [IPTG]/Xgal agar plate (as per Sambrook *et al.*, 1989), and incubated overnight at 37°C. If the APP DNA was inserted into the plasmid, it would disrupt the *LacZ* gene, resulting in white colonies. To determine the correct orientation of the insert, ten white colonies were selected and each colony was added to separate tubes of 3 ml LB/amp. These were incubated overnight at 37°C and 250 rpm. After 2 ml of each incubate were pelleted (5000 rpm for 10 min), a plasmid miniprep (QIAGEN's *Plasmid Mini Kit*) was performed. Each plasmid prep DNA was restricted separately with Sac I and Pst I. Reaction mixture: 20 µl ddwater, 3 µl buffer, 1 µg DNA, 1 µl Sac I or Pst I. The reaction mixtures were incubated for 2 hr at 37°C, after which, a 0.8% AGE was performed. The contents of the tube from which the correctly oriented *E. coli*/pGEM5zf/APP<sub>770/2583</sub> construct originated were added to 1 L LB/amp and incubated

overnight at 37°C and 250 rpm. This was followed by a plasmid maxiprep (QIAGEN's *Plasmid Maxi Kit*) to isolate and purify the pGEM5zf/APP<sub>770/2583</sub> construct.

To prepare the APP<sub>770/2583</sub> insert and the GAL-4 binding domain (BD) plasmid, pAS2-1 (Figure 4), to receive the insert, both the pGEM5zf/APP<sub>770/2583</sub> construct and pAS2-1, which had been previously amplified and purified as above, were simultaneously restricted with Nco I and Sal I. **Reaction mixture:** Five separate tubes of 50 µl ddwater, 10 µl buffer, 10 µg DNA, 3 µl Nco I and 3 µl Sal I. The reaction was incubated overnight at 37°C followed by 0.8% AGE.

The appropriate DNA bands were cut from the gel and the DNA eluted into TAE buffer by standard membrane electrophoresis procedures. The DNA was purified and precipitated from the resulting TAE/DNA mixture by PCIAA and ethanol, as per Promega. The APP<sub>770/2583</sub> was then ligated into the Nco I/Sal I-restricted pAS2-1, using Clontech's "Ligation Express Kit". Following this, the whole ligation mixture was added to 100 µl *E. coli* DH5α cells, and the cells transformed as per Promega. The *E. coli*/pAS2-1/APP<sub>770/2583</sub> pellet was re-suspended in 100 µl LB broth, spread on to an LB/amp plate and incubated overnight at 37°C. Ten colonies were added to separate tubes of 5 ml LB/amp and incubated overnight at 37°C and 250 rpm. A plasmid miniprep (QIAGEN's *Plasmid Mini Kit*) was performed on each incubate.

To verify the correct construct was present, the pAS2-1/APP<sub>770/2583</sub> was restricted in separate tubes with Pst I, Bgl II or Hind III. **Reaction mixture:** 25 µl ddwater, 4 µl buffer, 2 µg DNA, 2 µl RE. The mixtures were incubated for 2 hr at 37°C, and then subjected to 0.8% AGE.

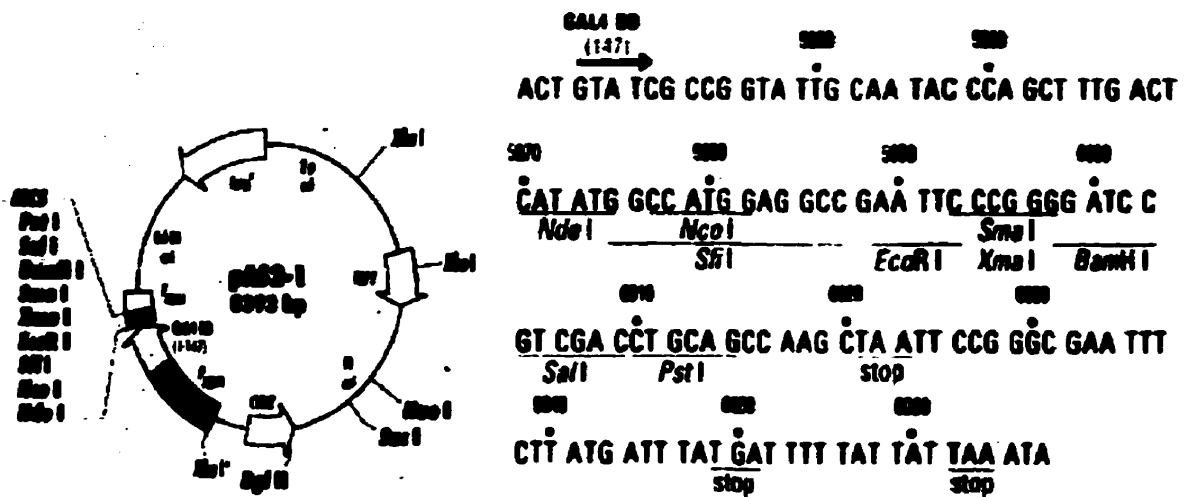


Figure 4 Schematic of pAS2-1 restriction map and MCS. (Unique restriction sites are in bold). Location of Features: 2μ origin of replication, (1-1348); TRP1 coding sequences; Start codon (ATG), (1884-1886); Stop codon, (2256-2258); CYH2 gene, (3765-4627); Promoter; Fragment from *Saccharomyces cerevisiae* containing the ADH1 promoter, (4767-5474); GAL4 binding domain polypeptide; Start codon (ATG), (5502-5504); GAL4 codons 1-147, (5502-5944); MCS, (5970-6015); Transcription termination signal; Fragment carrying the *S. cerevisiae* ADH1 terminator, (6031-6223); Translation stop codon, (6063-6056); Ampicillin resistance gene, (7403-8263). (Adapted from Clontech).

The contents of correct incubates were added to 1 L LB/amp broth and incubated overnight at 37°C and 250 rpm. A plasmid maxiprep (QIAGEN's *Plasmid Maxi Kit*) was performed to isolate and purify the pAS2-1/APP<sub>770/2583</sub> construct. Figure 5 shows a schematic of the APP<sub>770/2583</sub> insert.

### 3.1.2. pAS2-1/APP<sub>770/N-T2020</sub> construct

To isolate the APP<sub>770/N-T2020</sub> fragment, pAS2-1- APP<sub>770/2583</sub> was restricted with EcoR 1 and subjected to 0.8% AGE. Reaction mix: Five separate tubes of 40 µl ddwater, 5 µl buffer, 10 µg pAS2-1, 3 µl EcoR 1. The mixtures were incubated overnight at 37°C. The pAS2-1 and APP<sub>770/N-T2020</sub> bands were cut out of the gel, and the DNA extracted with QIAGEN's *QIEX II Gel Extraction Kit*. To verify the APP<sub>770/N-T2020</sub> fragment was present, an additional 0.8% AGE was performed on the fragment alone (data not shown).

To prepare pAS2-1 to accept the APP<sub>770/N-T2020</sub> fragment, previously amplified and verified pAS2-1 plasmid was restricted with EcoR 1. Reaction mixture: Five separate tubes of 40 µl ddwater, 5 µl buffer, 8 µg pAS2-1, 2 µl EcoR 1. Mixtures were incubated overnight at 37°C, followed by 0.8% AGE and extraction of the DNA from the gel with QIAGEN's *QIEX II Gel Extraction Kit*.

To prevent self-ligation, the EcoR 1-restricted pAS2-1 plasmid was de-phosphorylated according to Promega, except that five tubes were used, each with about 25 µg EcoR 1-restricted pAS2-1, 0.1 u CIAP, 30 µl CIAP Buffer, 270 µl ddwater. The de-phosphorylated, EcoR 1-restricted pAS2-1 was purified and precipitated with PCIAA and ethanol, as per Promega, and the concentration of the de-phosphorylated DNA was

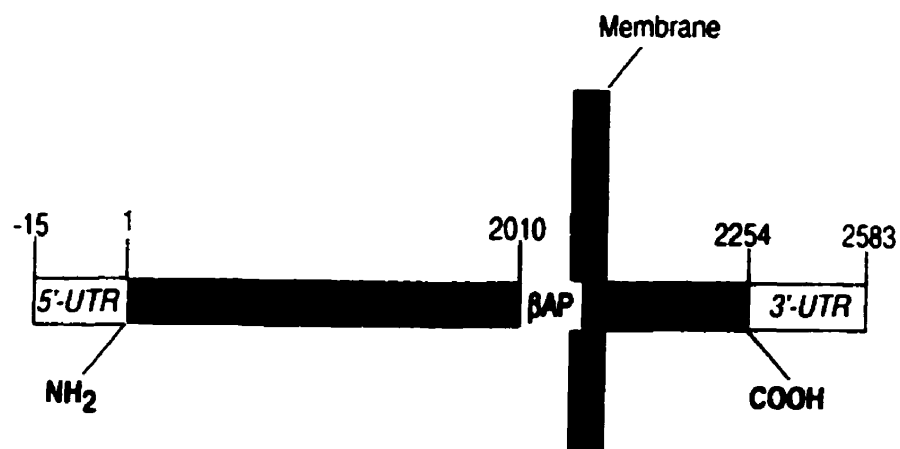


Figure 5 Schematic of human APP<sub>770/2583</sub> construct. The APP<sub>770/2583</sub> construct consisted of nucleotides 1-2254, plus a 15 base pair 5' UTR and a 329 base pair 3' UTR. The construct included most of the coding region of APP<sub>770</sub>.

photometrically determined.

The APP<sub>770/N-T2020</sub> fragment insert was ligated into the EcoR 1-restricted and dephosphorylated pAS2-1, using Boehringer-Mannheim's *Rapid DNA Ligation Kit*, with following modifications: 50 ng pAS2-1, 500 ng APP<sub>770/N-T2020</sub>, 30 µl dilution buffer, 30 µl ligase buffer, 3 µl T4 DNA ligase, and the ligation reaction was incubated at room temperature for 30 min. Next, 100 µl *E. coli* DH5α cells were transformed with the whole ligation mixture following Promega's protocol, except that the *E. coli*/plasmid mix was incubated overnight at 37°C. The overnight incubate was then spread onto four LB/amp plates which were incubated overnight at 37°C.

To check for correct ligation, five colonies were selected and each put into separate tubes of 3 ml LB/amp broth. They were incubated for 48 hr at 37°C and 250 rpm. A plasmid miniprep as per Promega's *Wizard Plasmid MiniPrep Kit* was performed on the pAS2-1/APP<sub>770/N-T2020</sub> incubates, and the concentration determined photometrically. To verify correct ligation and orientation, the pAS2-1/APP<sub>770/N-T2020</sub> DNA from each colony was restricted with Sac 1. Reaction mixture: 35 µl ddwater, 3 µl buffer, 1 µg DNA, 1 µl Sac 1. The reaction was incubated overnight at 37°C, and then subjected to 0.8% AGE.

An appropriate vial containing the correctly oriented APP insert was transferred to 1 L LB/amp broth and incubated overnight at 37°C & 250 rpm. A plasmid maxiprep (Promega *Wizard Plasmid Maxi Prep*) of the amplified pAS2-1/APP<sub>770/N-T2020</sub> construct was performed. To re-verify the correct construct, the pAS2-1/APP<sub>770/N-T2020</sub> preparation was restricted with Sac 1. Reaction mix: 35 µl ddwater, 3 µl buffer, 1 µg DNA, 1 µl Sac



1. The reaction was incubated for 2.5 hr at 37°C, after which a 0.8% AGE was performed.

### 3.1.3 pAS2-1/APP<sub>770/N-T1554</sub> and pAS2-1/APP<sub>770/N-T208</sub> constructs

To create further deletions of APP, the following REs were used:

(i) Bam H1. Reaction mixture: Five separate tubes of 40 µl ddwater, 6 µl buffer, 8 µg DNA, 4 µl BamH 1, incubated overnight at 37°C. (ii) Pst 1. Reaction mixture: Five tubes of 45 µl ddwater, 5 µl buffer, 10 µg DNA, 3 µl Pst 1, incubated for 3 hr at 37°C. A 0.8% AGE of BamH 1- and Pst 1-restricted pAS2-1/APP<sub>770/N-T208</sub> was performed.

The appropriate gel slices containing the pAS2-1/APP<sub>770/N-T1554</sub> and pAS2-1/APP<sub>770/N-T208</sub> DNA were cut from the gel, and the DNA extracted by membrane electrophoresis. The pAS2-1/APP<sub>770/N-T1554</sub> and pAS2-1/APP<sub>770/N-T208</sub> fragments were purified and precipitated by PCIAA and ethanol, as per Promega, and the concentration determined photometrically. This was followed by ligation of the EcoR 1-restricted pAS2-1/APP<sub>770/N-T2020</sub>, BamH 1-restricted pAS2-1/APP<sub>770/N-T1554</sub> and Pst 1-restricted pAS2-1/APP<sub>770/N-T208</sub> constructs with Boehringer-Mannheim's *Rapid DNA Ligation Kit*, with the following modifications: 30 µl DNA dilution buffer, 700 ng DNA, 30 µl ligase buffer, 3 µl T4 DNA ligase, and the reaction mixtures were incubated for 1 hr at room temperature. Next, three tubes of 100 µl *E. coli* DH5α cells were transformed with the whole ligation mixtures, using the protocol as per Promega, except for the following modifications: After adding the DNA to cells, they were stored on ice for 30 min., subjected to 42°C for 1 min., and put back on ice for 2 min. The cells were then transferred to 3 ml LB broth and incubated for 2 hr at 37°C and 225 rpm. 2 ml of the

incubates were removed and pelleted (centrifuged at 5000 g for 5 min), followed by resuspension in 100 µl LB broth. This was spread on LB/amp plates and incubated overnight at 37°C. Two colonies from each of the three LB/amp plates (transformed with ligated pAS2-1/APP<sub>770/N-T2020</sub>, pAS2-1/APP<sub>770/N-T1554</sub> and pAS2-1/APP<sub>770/N-T208</sub>) were selected and put in six separate vials of 5 ml LB broth. The tubes were incubated for 1 hr at 30°C and 250 rpm and then had 10 µl ampicillin added. They were incubated overnight at 30°C and 250 rpm, after which the incubates were added to 200 ml LB/amp and incubated overnight at 37°C & 250 rpm. A plasmid maxiprep (Promega's *Wizard MaxiPrep DNA Purification System*) was performed on the incubates and the concentration of the purified DNA calculated photometrically.

The pAS2-1/APP<sub>770/N-T208</sub> and pAS2-1/APP<sub>770/N-T1554</sub> constructs were verified using Hind III. Reaction mixture: 22 µl ddwater, 3 µl buffer, 1 µg DNA, 1 µl Hind III. The reactions were incubated overnight at 37°C, followed by 0.8% AGE.

#### **3.1.4 pCMV/myc/mito/APP<sub>770/2583</sub> construct**

First, the pCMV/myc/mito plasmid and the pGEM5zf/APP<sub>770/2583</sub> construct were amplified and verified to be correct. To amplify pCMV/myc/mito plasmid, 50 µl of *E. coli* DH5α (GibcoBRL) cells were transformed with 1 µg pCMV/myc/mito plasmid (Invitrogen). Protocol as per GibcoBRL, as follows: 1 µg pCMV/myc/mito plasmid was added to 50 µl DH5α competent cells, gently tapping the tube to mix. The cells were incubated on ice for 30 min, then heat shocked at 37°C for 20 sec, and finally placed on ice for 2 min. Next, 1 ml of room temperature LB was added and the mixture then

incubated for 1 hr at 37°C & 250 rpm. After 1 hr, the incubate was centrifuged at 14,000 rpm for 10 sec to pellet the cells. The pellet was re-suspended in 100 µl LB broth, and spread on to an LB/amp plate. Three colonies of *E. coli*/pCMV/myc/mito and four colonies of *E. coli*/pGEM5zf/APP<sub>770/2583</sub> were selected to be added to separate tubes of 5 ml LB broth. These were incubated for 1 hr at 37°C and 250 rpm, at which time 10 µl ampicillin (50 mg/ml) was added, and the incubates were then incubated overnight at 37°C and 250 rpm. 3 ml each of the *E. coli*/pCMV/myc/mito and *E. coli*/pGEM5zf/APP<sub>770/2583</sub> incubates were transferred to 200 ml LB/amp (100 µg/ml) broth, and incubated overnight at 37°C and 250 rpm. This was followed by plasmid maxipreps of the incubates (Promega's *Wizard Plus Maxiprep DNA Purification System*), with the concentration of the DNA being determined photometrically. To verify plasmids, (i) pGEM5zf/APP<sub>770/2583</sub> was restricted with Sac I, and (ii) pCMV/myc/mito was restricted with Sal I. In both constructs, expected bands were seen on 0.8% AGE (data not shown).

To isolate the APP<sub>770/2583</sub> insert, the pGEM5zf/APP<sub>770/2583</sub> construct was restricted with Spe I.. Reaction mixture: Two separate tubes of 50 µl ddwater, 8 µl buffer, 10 µg DNA, 4 µl Spe I. The reactions were incubated for 3 hr at 37°C, followed by 0.8% AGE. The 2.62 Kb APP<sub>770/2583</sub> band was cut from the gel, and the DNA extracted and purified with BioRad's *Prep-A-Gene DNA Purification System*. The DNA concentration was determined photometrically. The pBluescript II SK plasmid was then amplified by transforming 50 µl *E. coli* DH5α cells with 1 µg pBluescript II SK plasmid, protocol as per GibcoBRL. After the transformed cells had been incubating for 1 hr at 37°C, 10 µl

ampicillin (50 mg/ml) were added and cells incubated overnight at 37°C. The 5 ml incubate of *E. coli*/pBluescript II SK was added to 500 ml LB/amp broth, and incubated overnight at 37°C and 250 rpm. This was followed by a plasmid maxiprep of the *E. coli*/pBluescript II SK incubate, using Promega's *Wizard plus MaxiPreps DNA Purification System*, after which, the DNA concentration was determined photometrically.

The pBluescript II SK was next restricted with Spe I to allow it to accept the Spe I-restricted APP<sub>770/2583</sub> fragment. Reaction mixture: Two tubes of 50 µl ddwater, 8 µl buffer, 10 µg DNA, 4 µl Spe I. The reaction was incubated overnight at 37°C, followed by 0.8% AGE of the Spe I-restricted pBluescript II SK DNA. The Spe I-restricted pBluescript II SK DNA band was excised from the gel, and the DNA isolated and purified via BioRad's *Prep-A-Gene DNA Purification System*. The DNA concentration was determined photometrically.

To prevent the pBluescript II SK vector from self-ligating during the subsequent ligation reaction, 14 µg Spe I-restricted pBluescript II SK was de-phosphorylated, as per Promega. This amount was calculated to contain 14.18 pmol ends, which at 0.03 u CIAP/pmol end required a total of 0.43 u CIAP ( 0.5u CIAP was used). The de-phosphorylated, Spe I-restricted pBluescript II SK was purified using BioRad's *Prep-A-Gene DNA Purification Kit*.

Next, to create the pBluescript II SK/APP<sub>770/2583</sub> construct, 4 µg Spe I-restricted APP<sub>770/2583</sub> was ligated into 1 µg de-phosphorylated, Spe I-restricted pBluescript II SK, using B-M's *Rapid DNA Ligation Kit*. Protocol as in kit, except the reaction was

incubated for 15 min at room temperature. The whole ligation mixture was then added to 100  $\mu$ l *E. coli* DH5 $\alpha$  cells, and the transformation protocol as per GibcoBRL was followed. The protocol is identical to that described for transformation of 50  $\mu$ l *E. coli* DH5 $\alpha$  cells, except the cells are heat shocked for 45 secs. At the end of the procedure, 100  $\mu$ l of re-suspended cells was spread onto LB/amp plates and incubated overnight at 37°C. This was followed by a plasmid miniprep to verify the correct orientation of the insert, and subsequently a large plasmid prep of the appropriate pBluescript II SK/APP<sub>770/2583</sub> construct (data not shown).

To prepare the pCMV/myc/mito plasmid to accept the APP<sub>770/2583</sub> insert, it was simultaneously restricted with Sal I & Not I REs. Reaction mixture: Two tubes of 50  $\mu$ l ddwater, 10  $\mu$ l buffer, 10  $\mu$ g DNA, 3  $\mu$ l each enzyme. The reactions were incubated overnight at 37°C, after which a 0.8% AGE was performed. The 4.9 Kb Sal I/Not I-restricted pCMV/myc/mito band was cut from the gel, and the DNA isolated and purified with BioRad's *Prep-A-Gene DNA Purification System*. The DNA concentration was determined photometrically.

The next step involved removal of the APP<sub>770/2583</sub> fragment from the pBluescript II SK/APP<sub>770/2583</sub> transcript, to allow the fragment to be ligated into the pCMV/myc/mito plasmid. To achieve this, the pBluescript II SK/APP<sub>770/2583</sub> construct was restricted simultaneously with Sal I and Not I, the APP<sub>770/2583</sub> DNA was isolated and purified from an agarose gel, and subsequently ligated into Sal I/Not I-restricted pCMV/myc/mito, using Boehringer-Mannheim's *Rapid DNA Ligation Kit*. The whole ligation mixture was added to 100  $\mu$ l *E. coli* DH5 $\alpha$  cells, and the transformation protocol as per GibcoBRL

was followed. At the end of the transformation procedure, 100 µl of re-suspended cells were spread onto LB/amp plates and incubated overnight at 37°C . This was followed by a plasmid miniprep and RE analysis to verify the correct construct, and a plasmid maxiprep of appropriate preparation to isolate and purify the pCMV/myc/mito/APP<sub>770/2583</sub> construct (data not shown).

### 3.1.5 pEGFP-N1/APP<sub>695/N-T1795</sub> construct

In summary, this involved cutting the APP<sub>695/1795</sub> insert out of a pGEM9zf/APP<sub>695/3207</sub> construct with EcoR 1, and ligating it into an EcoR 1-restricted pEGFP-N 1 plasmid. The APP<sub>695/3207</sub> cDNA was received identically inserted into pGEM9zf as was APP<sub>770/3432</sub>.

To prepare the APP<sub>695/N-T1795</sub> fragment (APP<sub>695</sub>, bases 1-1795), pGEM9zf/APP<sub>695/3207</sub> was restricted with EcoR 1. Reaction mixture: Two tubes of 40 µl ddwater, 5 µ buffer, 12 µg DNA, 3 µl EcoR 1. The reaction was incubated overnight at 37°C, and was followed by 0.8% AGE.. The 1.8 Kb band (APP<sub>695/N-T1795</sub>) was cut from the gel and the DNA extracted via membrane electrophoresis. The APP<sub>695/N-T1795</sub> DNA fragment was purified via PCIAA and ethanol as per Promega, and the concentration determined photometrically.

pEGFP-N1 was amplified by transforming 100 µl *E coli* DH5α cells with 1 µg pEGFP-N1 plasmid, and following the transformation protocol as per Gibco BRL. After the transformation procedure, 50 µl of the 100 µl re-suspended cell pellet was spread on LB/kanamycin (50 µg/ml) [kanamycin (kan) concentration used in all procedures was 50

$\mu\text{g/ml}$ ] plates and incubated overnight at 37°C. Several colonies were selected and all added to 1 ml LB/kan broth, which was incubated overnight at 37°C and 225 rpm. The incubate was transferred to 500 ml LB/kan and incubated overnight at 37°C and 225 rpm. A plasmid maxiprep (QIAGEN's *Plasmid Maxi Kit*) was performed and the concentration determined photometrically. To verify that it was pEGFP-N1 isolated, the plasmid prep was restricted with EcoR 1. Reaction mixture: 20  $\mu\text{l}$  ddwater, 2  $\mu\text{l}$  buffer, 1  $\mu\text{g}$  DNA, 1  $\mu\text{l}$  EcoR 1. The reaction was incubated for 1.5 hr at 37°C, after which it was subjected to a small 0.8% AGE. To re-verify pEGFP-N1, two more restrictions of pEGFP-N1 with EcoR 1 were carried out, followed by 0.8% AGE. The last restriction showed only the 4.7 Kb band (data not shown). Confident that the correct plasmid was present, the 4.7 Kb pEGFP-N1 band was cut from the gel and the DNA extracted via membrane electrophoresis. The isolated DNA was then purified via PCIAA and ethanol, as per Promega, following which the concentration was determined photometrically.

To prevent the EcoR 1-restricted pEGFP-N1 DNA from self ligating in the subsequent ligation steps, it was de-phosphorylated, as per Promega. It was calculated (Promega) that 15  $\mu\text{g}$  EcoR 1-restricted pEGFP-N1 contained 10 pmol ends. At 0.03 u CIAP per pmol ends of DNA, 0.3 u CIAP was used in the ligation reaction. Reaction mixture: Four tubes of 15  $\mu\text{g}$  EcoR 1-restricted pEGFP-N1, 13  $\mu\text{l}$  ddwater, 5  $\mu\text{l}$  10X CIAP buffer, 0.3 u CIAP. The reaction protocol as per Promega was followed. The de-phosphorylated, EcoR 1-restricted pEGFP-N1 was precipitated and purified via PCIAA and ethanol as per Promega, with the concentration being determined photometrically.

The next step involved ligation of APP<sub>695/N-T1795</sub> into the de-phosphorylated, EcoR

1-restricted pEGFP-N1. As calculated (Promega), a 1:3 ratio of vector to insert was equivalent to 1 µg pEGFP-N1 and 1.1 µg APP<sub>695/N-T1795</sub>. For the ligation, Boehringer-Mannheim's *Rapid DNA Ligation Kit* was used. The kit protocol was followed, except for the following parameters: 1.12 µg APP<sub>695/N-T1795</sub>, 1.08 µg pEGFP-N1, 3 µl 1X dilution buffer, 13 µl ligase buffer, 1.4 µl T4 DNA ligase, and the reaction was incubated at room temperature for 1.5 hr.

To amplify the construct, 100 µl *E. coli* DH5α cells were transformed with the whole ligation mixture, and then the protocol as per Gibco BRL was followed. The transformed cells were pelleted (14,000 rpm for 20 sec) and re-suspended in 100 µl LB broth, which was subsequently spread on an LB/kan plate and incubated overnight at 37°C.

To verify that the ligation was successful, ten colonies were selected and added to ten separate tubes of 4 ml LB/kan broth. These were incubated overnight at 37°C and 225 rpm, following which, a plasmid miniprep (QIAGEN's *Plasmid Mini Kit*) was performed on each incubate. Having calculated the concentration of the DNA photometrically, 3 µg DNA from each tube was restricted with EcoR 1. Reaction mixture: 40 µl ddwater, 6 µl buffer, 3 µg DNA, 3 µl EcoR 1. The reactions were incubated for 4 hr at 37°C, followed by 0.8% AGE.

To verify that the insert was correctly oriented, the remaining contents of the tube with the ligated pEGFP-N1/APP<sub>695/N-T1795</sub> constructs were added to 300 ml LB/kan broth and incubated overnight at 37°C and 225 rpm. A large plasmid prep of each of the incubates (QIAGEN's *Plasmid Maxi Kit*) was then carried out, followed by restriction



of 2 µg of each pEGFP-N1/APP<sub>695/N-T1795</sub> construct with BamH 1. Reaction mixture: 60 µl water, 8 µl buffer, 2 µg DNA, 2 µl EcoR 1. The reactions were incubated for 2 hr at 37°C, following which, a 0.8% AGE was performed. To re-verify the constructs, ten more colonies were selected from the pEGFP-N1/APP<sub>695/N-T1795</sub> ligation plate and added to 5 ml LB/kan (50 µg/ml). These were incubated overnight at 37°C and 250 rpm shake. A plasmid miniprep (QIAGEN's *Plasmid Mini Kit*) was performed on the incubates and the DNA restricted separately with EcoR 1 and BamH 1. Reaction mixture: 6 µl ddwater, 3 µl buffer, 1.6 µg (20 µl) DNA, 1 µl EcoR 1 or BamH 1. The reactions were incubated for 4 hr at 37°C. A 0.8% AGE showed similar overlapping supercoils. Therefore, in order to get a better separation of the DNA bands, the small AGE was repeated with 1.6% agarose.

### 3.1.6 pEGFP-N1/APP<sub>695/N-T208</sub> construct

To produce the shorter pEGFP-N1/APP<sub>695/N-T208</sub> construct (APP<sub>695</sub>, bases 1-208), the pEGFP-N1/APP<sub>695/N-T1795</sub> construct was restricted with Pst 1. This produced linearized pEGFP-N1/APP<sub>695/N-T208</sub>, which was then sealed by ligation. Reaction mixture: Four tubes of 150 µl ddwater, 20 µl buffer, 50 µg pEGFP-N1/APP<sub>695/N-T1795</sub>, 10 µl Pst 1. The reactions were incubated overnight at 37°C, following which, a 0.8% AGE was performed (data not shown). The 4.9 Kb pEGFP-N1/APP<sub>695/N-T208</sub> band was cut from the gel, and the DNA extracted by membrane electrophoresis. The DNA was precipitated and purified via PCIAA and ethanol, as per Promega, and 1.5 µg of the pEGFP-N1/APP<sub>695/N-T208</sub> construct was ligated using Boehringer-Mannheim's *Rapid DNA Ligation Kit*. The

protocol followed was as per kit, except that the ligation mixture was incubated for 1 hr at room temperature.

To verify the constructs, pEGFP-N1/APP<sub>695/N-T208</sub> and pEGFP-N1 were restricted with EcoR 1. Reaction mixture: 25 µl ddwater, 3 µl buffer, 1.7 µg DNA, 1 µl EcoR 1. The reactions were incubated overnight at 37°C, followed by 0.8% AGEs.

### **3.1.7 pCMV/myc/mitoGFP plasmid**

To amplify the pCMV/myc/mito/GFP plasmid, 100 µl *E coli* DH5α cells were transformed with 1 µg pCMV/myc/mito/GFP plasmid, protocol as per Gibco BRL. After the transformation procedure, the cells were re-suspended in 100 µl LB broth, and 50 µl of this spread on an LB/amp plate and incubated overnight at 37°C. Three colonies of the *E coli*/pCMV/myc/mito/GFP were selected and added to separate vials of 7 ml LB/amp broth. These were incubated for 5 hr at 37°C and 225 rpm. The contents of one vial were added to 500 ml LB/amp broth and incubated overnight at 37°C and 225 rpm. A plasmid maxiprep ( QIAGEN's *Plasmid Maxi Kit*) was performed on the incubate, and the DNA concentration determined photometrically.

To verify the plasmid, the preparation was restricted with Pst 1. Reaction mixture: 24 µl water, 3 µl buffer, 1.2 µg pCMV/myc/mito/GFP, 1 µl Pst 1. The reaction was incubated for 1 hr at 37°C, followed by a 0.8% AGE.

## **3.2.0 Yeast Two-Hybrid System**

### **3.2.1 Library-scale yeast two-hybrid assay**

#### **Amplification of the pACT2/human brain cDNA plasmid expression library**

The pACT2 library contained  $5 \times 10^6$  independent clones (or  $10^8$  colony forming units) per ml library. It consisted of normal human brain cDNAs inserted into the GAL-4 activation domain plasmid, pACT2 (Clontech). Initially, 4  $\mu$ l (40,000 cfu) of the pACT2 library were spread onto each of two hundred 150 mm LB/amp plates, and the plates incubated at 30°C for 48 hr. On to each plate were spread 5 ml LB/glycerol (25% v/v glycerol), and the cells scraped into the liquid. All the liquid was pooled and plasmid maxipreps (QIAGEN's *Plasmid Maxi Kit*) performed to isolate the library pACT2/brain cDNA.

#### **Preparation of competent yeast cells**

To prepare sufficient yeast cells for the experiment, 200  $\mu$ l of yeast strain Y190 was spread on to a YPD complete yeast medium plate and incubated for 4 days at 30°C. YPD medium is composed of 20 g/L peptone, 10 g/L yeast extract, 20 g/L agar and 2% dextrose, pH 5.8, following Clontech's *Matchmaker Gal4 Two-Hybrid User Manual*. Several of the yeast colonies were scraped into 1 ml YPD medium. After vortexing, cells were transferred to 150 ml YPD liquid medium (same composition as YPD agar, except no agar added) and incubated overnight at 30°C and 250 rpm. The incubate was transferred to 1 L YPD liquid medium and incubated for 3 hr at 30°C and 250 rpm. The cells were divided into 50 ml tubes and centrifuged at 1,000 x g for 5 min. The super-

natant was discarded and the cells re-suspended in 500 ml ddwater. The cells were pelleted (1,000 x g for 5 min), the supernatant discarded, and cells re-suspended in 8 ml 1 X TE/lithium acetate (TE/LiAc). The TE/LiAc was made from stock solutions 10X TE buffer (0.1 M Tris-HCl, 10 mM EDTA, pH 7.5) and 10X LiAc (1 M lithium acetate, adjusted to pH 7.5 with acetic acid [Sigma]).

#### Transformation of yeast cells

To a tube were added and mixed 1 mg pAS2-1/APP<sub>770/2583</sub>, 0.5 mg pACT2/brain cDNA, and 1 mg herring testes carrier DNA (Clontech). The herring testis DNA was first denatured by placing it in a boiling water bath for 20 min and then immediately cooling on ice. To the DNA mixture was added the 8 ml of yeast Y190 competent cells, and the contents mixed by vortexing. Next, 60 ml of polyethylene glycol/LiAc (PEG/LiAc) solution was added and mixed by vortexing. Each 10 ml PEG/LiAc solution was composed of 8 ml of 50% polyethylene glycol (Sigma), 1 ml of 10X TE buffer, and 1 ml 10X LiAc. The transformation solution was incubated for 30 min at 30°C and 200 rpm, following which 7 ml dimethyl sulfoxide (DMSO) (Sigma) was added and gently mixed. The solution was heat-shocked for 15 min at 42°C, followed by chilling on ice for 2 min. Next, the cells were centrifuged for 5 min at 1,000 x g, and re-suspended in 10 ml 1X TE buffer. The transformed cells (200 µl) were spread on to each of fifty 150 mm SD/-His/-Leu/-Trp/+ 45 mM 3-AT plates (i.e., a selection and phenotype-testing drop-out minimal medium lacking amino acids histidine [expressed by Y190], leucine [expressed by pAS2-1] and tryptophan [expressed by pACT2], and with added 3-aminotriazole [3-AT] to suppress a leaky His promoter), plus essential nutrients such as a yeast nitrogen base,

dextrose, and a specific mixture of amino acids and nucleotides. The plates were incubated at 30°C for seven days to allow good-sized colonies to develop. Forty colonies (His<sup>+</sup>) grew, which were candidates to contain both pAS2-1 and pACT2 plasmids.

### β-galactosidase Assay

To eliminate false positives, the colonies that grew (His positive, His<sup>+</sup>) were subjected to β-galactosidase colony-lift filter assay, as per Clontech's *MATCHMAKER Yeast Protocols Handbook*. For each plate of transformants to be assayed, a Whatman #5 sterile filter was pre-soaked in 5 ml of Z buffer/X-gal solution. Z buffer consisted of 16.1 g/L Na<sub>2</sub>HPO<sub>4</sub>, 5.5 g/L NaH<sub>2</sub>PO<sub>4</sub>, 0.75 g/L KCl, 0.246 g/L MgSO<sub>4</sub>, pH adjusted to 7.0. X-gal stock solution contained 5-bromo-4-chloro-3-indolyl-β-D-galactopyranoside dissolved in N,N-cismethylformamide at a concentration of 20 mg/ml. Z buffer/X-gal solution comprised 100 ml Z buffer, 0.27 ml β-mercaptoethanol, 1.67 ml X-gal stock solution.

A clean dry filter was placed over the surface of each plate, and gently rubbed to help colonies cling to the filter. The filter was cut to allow for correct orientation. After the filter was evenly wetted, it was transferred (colonies facing up) to a pool of liquid nitrogen and completely submerged for 10 sec, after which it was removed and allowed to thaw at room temperature. The dried filter was placed, colony side up, on the pre-soaked filter, where it was incubated at 30°C until blue colonies developed in less than 8 hr. Eleven colonies (His<sup>+</sup> and LacZ<sup>+</sup>) turned blue within 3 hr. These should contain both the BD and ActD plasmids. The corresponding positive colonies were removed

from the original plates and spread grid-like fashion on fresh SD/-His/-Leu/-Trp/+ 45 mM 3-AT plates.

To put selection pressure on growth of colonies containing AD/brain cDNA constructs only (i.e. select for colonies that have spontaneously lost BD/APP<sub>770/2583</sub> constructs), some of the His<sup>+</sup>/LacZ<sup>+</sup> colonies were re-plated on SD/-Leu/+cycloheximide (cyh) medium. Y190 strain contains a genomic mutant recessive cyh resistant gene. The BD vector expresses the wild-type dominant cyh sensitive gene, while the ActD vector contains neither gene. Therefore, only pACT-2/brain cDNA-containing colonies which have no BD/APP<sub>770/2583</sub> constructs will grow on the cyh<sup>+</sup> medium. The pACT-2/brain cDNA clones were extracted from the yeast cells (by F. Amara) & stored at -20C for future sequencing & protein analysis.

### **3.2.2 Small-scale yeast two-hybrid assay**

#### **Verification of the APP<sub>770/2583</sub>-COX I interaction**

Following Clontech's protocol, to make competent yeast cells, 1 ml of YPD broth was inoculated with several colonies of previously prepared and frozen (-80°C) yeast strain Y190. After vortexing, it was transferred to 50 ml YPD liquid medium and incubated overnight at 30°C and 250 rpm. The overnight culture was transferred to 300 ml YPD and incubated for 3 hr at 30°C and 250 rpm. Fifty ml of the above culture were added to a centrifuge tube and the cells pelleted (centrifuged at 2500 rpm for 5 min). The supernatant was discarded and the cells re-suspended by vortexing in 25 ml water. The cells were pelleted again as before. The supernatant was decanted and the now competent

cells re-suspended in 1.5 ml 1X TE/LiAc.

To separate tubes were added 5 µg each of (i) pAS2-1/APP<sub>770/2583</sub>, (ii) pACT2/COX I, and (iii) pAS2-1/APP<sub>770/2583</sub> plus pACT2/COX I. To each tube were added 100 µl (1 mg) Herring testis carrier DNA and 300 µl competent yeast cells. The contents were mixed by vortexing. 600 µl PEG/LiAc were next added, the contents vortexed and then incubated for 30 min at 30°C and 250 rpm. Next, 175 µl DMSO were added and gently mixed in. The tubes were then heat shocked for 15 min in a 42°C water bath followed by cold shock on ice for 2 min. The cells were pelleted (centrifuged at 14,000 rpm for 5 sec), the supernatant discarded, and cells re-suspended in 200 µl TE buffer. The DNA-transformed Y190 suspension (200 µl) was spread onto SD/-Trp plates for pAS2-1/APP<sub>770</sub>-transformed cells, SD/-Leu for pACT2/COX1-transformed cells, and SD/-Leu/-Trp/-His/+45 mmol 3-AT plates for pAS2-1/APP<sub>770</sub> and pACT2-transformed cells. The plates were incubated at 30°C for 4 days to allow colonies to fully develop, after which, a β-galactosidase colony-lift filter assay was performed on the HIS<sup>+</sup> colonies.

#### Small scale yeast two-hybrid assay with the APP deletion constructs

The protocol was the same as that described above except that the transformation section involved adding to separate tubes 5 µg DNA constructs pAS2-1/APP<sub>770/N-T2020</sub>, pAS2-1/APP<sub>770/N-T1554</sub>, pAS2-1/APP<sub>770/N-T208</sub>, pAS2-1/APP<sub>770/2583</sub>, pAS2-1/APP<sub>C-TI-2020</sub>. The latter construct consisted of the APP<sub>770/2583</sub> construct with the NH<sub>2</sub>-terminal 2020 bps removed, and was prepared by B. Liang. To each tube were also added 5 µg pACT2/COX I. A β-galactosidase colony-lift filter assay was performed on the above

colonies that grew.

### **3.3.0 Assays of APP Stably-transfected Neuroblastoma Cell Line**

#### **3.3.1 Neuroblastoma cell culture**

The neuroblastoma SK-N-SH cells (ATCC) were grown in Neurobasal A medium (Gibco BRL), supplemented with 10% fetal bovine serum (Gibco BRL), 1% L-glutamine (Sigma), 1% gentamycin (Gibco BRL). Each 1 ml criovial of quickly thawed neuroblastoma SK-N-SH cells was added to a sterile 50 ml centrifuge tube, and to each tube was slowly mixed 47 ml of complete Neurobasal A medium. Next, 12 ml of this neuroblastoma/culture medium mixture was added to separate culture flasks, which were then incubated at 37°C in humidified atmosphere ( 5% CO<sub>2</sub>/95% air). The plasmids to be used expressed the geneticin-resistant gene G418, which was used as a selection agent to produce the stably transfected cell line. Cells were routinely passaged (trypsin/EDTA) at 70-80% confluence, and the medium changed as required.

#### **3.3.2 Transfection of neuroblastoma cell line**

The transfection reagent used to transfect the neuroblastoma cells was Boehringer-Mannheim's *FuGENE 6 Transfection Reagent*, a blend of lipids (non-liposomal formulation) and other components in 80% ethanol. The protocol followed was basically that recommended by the manufacturer, as follows: The neuroblastoma cells were subcultured 24 hr before transfection, which ensured they were 50-80% confluent in the culture flasks. To 970 µl of medium was added 30 µl FuGENE 6



Transfection reagent, and the mixture incubated at room temperature for 15 min. The DNA (12 µg) was added to a second centrifuge tube. Drop by drop, the diluted FuGENE 6 reagent was added to the DNA. The tube was gently tapped to mix the contents and incubated at room temperature for 30 min. This mixture was then added drop by drop to the neuroblastoma cells in 12 ml of medium in culture flasks, gently swirling the medium to mix. The cells were then returned to the incubator.

### **3.3.3 Isolation of mitochondria from the neuroblastoma cell line**

The protocol was based on Vander Heiden *et al.* (1997). The medium was vacuum aspirated from the culture flasks growing the neuroblastoma cells, and then 5 ml of 1X trypsin/EDTA added for 2-3 min. Next, 10 ml of complete medium was added, and the cells centrifuged at 2500 rpm for 5 min to pellet the cells. The neuroblastoma cells were re-suspended in 0.8 ml ice-cold Buffer A (250 mM sucrose, 20 mM HEPES, 10 mM KCl, 1.5 mM MgCl<sub>2</sub>, 1 mM EDTA, 1 mM EGTA, 1 mM DTT, 17 µg/ml PMSF, 8 µg/ml aprotinin, 2 µg/ml leupeptin, pH 7.4), followed by ultrasonic homogenization on ice. The homogenate was centrifuged at 750 x g for 10 min to pellet unlysed cells and nuclei. The supernatant was centrifuged at 10,000 x g for 25 min. The resultant mitochondrial pellet was re-suspended in buffer A. The supernatant was centrifuged at 100,000 x g for 1 hr, the resulting supernatant being the cytosolic fraction.

### **3.3.4 COX activity assay in APP-transfected neuroblastoma cell line**

A reduced, approximately 5 mM cytochrome c solution was prepared, excess

solid ascorbic acid was added and the mixture allowed to stand for 10 min. A Sepharose G50 column was prepared and equilibrated with 500 ml assay buffer (20 mM  $K_2PO_4$ , pH 7.0), any excess being allowed to drain. The reduced cytochrome c was pipetted into the column, which was allowed to drain. More assay buffer was added to the column, and the elution of cytochrome c followed visually, and collected in about 250  $\mu$ l aliquots.

Prior to the COX assay the absorbance reading was checked at 550 nm, and rechecked after the addition of sodium dithionate, to ensure cytochrome c was fully reduced. For this assay, 990  $\mu$ l of assay buffer was added to a cuvette and the  $A_{550}$  set to zero. To the buffer 10  $\mu$ l reduced cytochrome c was added and mixed by inversion. The assay mixture consisted of 50  $\mu$ g mitochondrial protein, 0.2 mg dodecyl-maltoside (20  $\mu$ l of a 10 mg/ml aqueous solution), 10  $\mu$ l of reduced cytochrome c, and assay buffer to make 1 ml. The buffer and dodecylmaltoside were added to a cuvette, and the  $A_{550}$  set to zero. Reduced cytochrome c was then added, and the cuvette equilibrated at 30°C for 3 min. Next, the mitochondrial protein was added, and mixed twice by gentle inversion. The absorbance was recorded over 90 sec.

### **3.3.5 Complex I activity assay in APP-transfected neuroblastoma cell line**

The mitochondrial protein solution was diluted to a concentration of about 2 mg/ml in sucrose-TRIS-ATP buffer, and 200  $\mu$ l of this was added to an eppendorf tube and ultrasonically homogenized in ice. The assay was performed on 50  $\mu$ g mitochondrial protein. The assay volume was 1 ml, which consisted of 97  $\mu$ l assay buffer (25 mM  $K_2PO_4$ , pH 8.0, 0.25 mM  $K^+$ EDTA, 1 mM KCN, 100  $\mu$ M NADH). The buffer-containing

cuvette was warmed to 30°C for 3 min., and the reaction initiated by adding 3 µl of 20 mM ubiquinone in ethanol. The NADH oxidation was followed for 3 min at 340 nm. The 1 min reading was taken as average.

### **3.3.6 Detection of apoptosis in APP-transfected neuroblastoma cell line**

The neuroblastoma cells were subcultured on coverslips in wells containing 2 ml Neuralbasal A medium. When the cells were 50-80% confluent, the culture medium was removed and the slips immersed in cold (2-8°C) 1X phosphate buffered saline (PBS) (Sigma). The incubation reagent was prepared and was composed of 10 µl of 10X binding buffer, 10 µl of propidium iodide (Genzyme) to check for cell necrosis, 1 µl of Annexin V conjugate (Genzyme), 79 µl ddwater, to make a total volume of 100 µl. The 1X PBS wash was removed from the slips, and excess liquid blotted away. 100 µl of the incubation reagent was added to each sample, and incubated for 15 min at room temperature in the dark. The cells were then washed twice for 2 min each wash with 50 ml 1X binding buffer, followed immediately by fluorescence microscopy.

### **3.3.7 Assay for ROS levels in APP-transfected neuroblastoma cell line**

Cultures were washed with Dulbecco's modified eagle's medium (DMEM) (Sigma) and allowed to take up 10 µg (dichlorofluoroscein diacetate (DCF-DA) (added as 10 nM stock in DMSO) for 1 hr. The cultures were washed twice with Hank's buffered saline solution (HBSS) (Sigma) and 5 µg/ml propidium iodide (Genzyme) was added to exclude debris and dead cells before data collection. The cultures were then

washed again with HBSS, and cellular fluorescence was viewed in HBSS using a Leitz microscope with fluorescence filters. In some cases, to provide standardized quantitation of cell numbers, the nucleus-specific fluorescent dye Hoechst 33342 (Molecular Probes) was added at 1 µg/ml at the time of addition of DCF-DA. Cultures were compared, with stable transfectants and control conditions blind to the investigators. Fluorescence was determined quantitatively by counting from first bright field micrographs, and then under fluorescence microscopy. Results were expressed as percent fluorescent cells.

### **3.3.8 Assay of glutathione peroxidase activity in APP-transfected neuroblastoma cell line**

The reaction mixture consisted of 0.25 mM *tert*-butyl hydroperoxide, 1 mM GSH, 1.4 units glutathione reductase, 1.43 mM NADPH, and 1.5 mM KCN in a 100 mM potassium phosphate buffer (pH 7.0) (Sigma). Volume = 1 ml - mitochondrial supernatant volume. *tert*-butyl hydroperoxide was used as substrate in order to measure selenium-dependent glutathione peroxidase, the only isoform found in brain. Blank values, obtained without addition of samples, were subtracted from assay values.

### **3.3.9 Assay of superoxide dismutase activity in APP-transfected neuroblastoma cell line**

Assay consisted of adding 25 µl of 24 mM pyrogallol in 10 mM HCl, 10 µl of 30 µM catalase (25,000 U/mg), 50 µg mitochondrial protein, and assay buffer (50 mM TRIS-HCl plus 1 mM diethylenetriamine pentaacetic acid (pH 8.2)) to make 3 ml

(Sigma). Absorbance was read at 420 nm. The blank contained 25  $\mu$ l pyrogallol, 10  $\mu$ l catalase, and 2.965 ml buffer.

### **3.4.0 Classic *In Vitro* Mitochondrial Import Assay**

#### **3.4.1 TnT *in vitro* transcription-translation system**

As supplied by Promega, the reaction mixture consisted of 25  $\mu$ l rabbit reticulocyte lysate, 2  $\mu$ l TnT reaction buffer, 1  $\mu$ l TnT SP6 RNA polymerase, 1  $\mu$ l of 1 mM amino acid mixture minus methionine, 40 microcurie ( $\mu$ Ci)  $^{35}$ S-methionine (1000 Ci/mmol at 10 mCi/ml), 1  $\mu$ l RNasin ribonuclease inhibitor (at 40 uCi/ml), 1  $\mu$ g pGEM5zf/APP<sub>770/2583</sub>, 15  $\mu$ l RNA-free ddwater. The ingredients were mixed on ice and the reaction mixture incubated for 2 hr at 30°C. At the end of the incubation, 10  $\mu$ l of TnT reaction was then added to 10  $\mu$ l of gel loading sample buffer (50 mM Tris.Cl (pH 6.8), 10% glycerol, 2% sodium dodecyl sulfate (SDS), 0.1% bromophenol blue, 100 mM DTT) (Sigma), and the remainder stored at -20°C. The sample was heated at 100°C for 2 min to denature the protein, and was then loaded on to a 10% SDS-polyacrylamide gel and subjected to electrophoresis (10% SDS-PAGE), protocol and material as per Sambrook *et al.*, (1989), with Gibco-BRL's *BenchMark Protein Ladder* as a marker (5  $\mu$ l in 15  $\mu$ l of sample buffer). After the samples had run the length of the gel, the gel removed from the apparatus. The portion containing the protein ladder segment was excised and fixed and stained with Coumassie blue, as per Sambrook *et al.*, (1989). The gel was then dried and photographed.

The rest of the gel was placed on dry Whatman 3MM paper, and then wrapped in plastic wrap, and dried in a heated, vacuum drier. The gel was subjected to autoradiography for 4 hr. A dominant main band of just under 100 kDa was seen, which approximates the expected size of APP. For the experiment, six TnT reactions were performed and pooled at the end.

### **3.4.2 Isolation of rat mitochondria**

Mitochondria were isolated from rat livers based on Giulivi *et al.*, (1998). Two rat livers (about 30 g total) were excised from anesthetized rats and washed in 0.25 M sucrose. Each liver was homogenized in about 50 ml MSHE buffer (0.25 M mannitol, 0.07 M sucrose, 0.5 mM EGTA, 0.1% fatty acid-free bovine serum albumin (BSA), 2 mM K<sup>+</sup>-HEPES, pH7.4) (Sigma) at 4°C. The homogenate was centrifuged for 10 min at 6000 x g, and the resulting supernatant centrifuged at 10,000 x g for 15 min to isolate the mitochondrial pellet. To further purify and isolate the mitochondria, the pellet was re-suspended in 5 ml MSHE plus 20 ml of 30% Percoll in 225 mM mannitol, 1 mM EGTA, 25 mM HEPES, 0.1% bovine serum albumin, and centrifuged for 30 min at 95,000 x g. The mitochondria were collected from the low dense yellow-brown band. The mitochondria were washed twice in MSHE at 6,300 x g for 10 min to remove the percoll. The purified mitochondria were then washed twice in 150 mM KCl at 12,000 x g for 5 min, followed by two washes in MSHE at 12,000 x g for 5 min. The mitochondria were finally re-suspended in 1 ml MSHE, and the concentration of mitochondrial protein determined by the Bradford assay.

### **3.4.3 *In vitro* mitochondrial import assay**

The protocol for the classic mitochondrial import assay was based on Glick (1992), Glick *et al.* (1992), and Casari *et al.* (1998). To remove ribosomes, the TnT reaction was centrifuged at 100,000 x g for 15 min. The import reaction was divided into three different conditions: (i)  $^{35}\text{S}$ -APP<sub>770</sub> plus mitochondria, (ii)  $^{35}\text{S}$ -APP<sub>770</sub> plus mitochondria plus trypsin, (iii)  $^{35}\text{S}$ -APP<sub>770</sub> plus mitochondria plus trypsin plus valinomycin.

**Reaction 1.** 50  $\mu\text{l}$  TnT reaction were added with 51.3  $\mu\text{g}$  mitochondrial protein to 200  $\mu\text{l}$  import buffer (0.6 M sorbitol, 50 nM  $\text{K}^+$ -HEPES, pH7.0, 50 mM KCl, 10 mM  $\text{MgCl}_2$ , 2.5 mM EDTA, 2 mM  $\text{KH}_2\text{PO}_4$ , 2 mM ATP, 1 mg/ml BSA, fatty acid free) (Sigma), and incubated for 1 hr at 12°C, after which the reaction was terminated on ice.

**Reaction 2.** Two import reactions were run. After the import reaction 0.25 mg/ml and 0.5 mg/ml trypsin (Sigma) were added to the two separate reactions and incubated on ice for 20 min. 1 mg/ml of trypsin inhibitor (Sigma) was then added and incubated on ice for 10 min.

**Reaction 3.** 1  $\mu\text{g}/\text{ml}$  valinomycin (dissolved in ethanol) plus 50 mM KCl (Sigma) was added to 51.3  $\mu\text{g}$  mitochondrial protein in 200  $\mu\text{l}$  import buffer and put on ice for 10 min. 20  $\mu\text{l}$  TnT reaction was then added, and the import reaction allowed to occur as above. This was followed by the trypsin and trypsin inhibitor treatments as above.

Samples from all four reactions were then centrifuged for 10 min at 12,000 x g at 4°C, followed by resuspension in 100  $\mu\text{l}$  import buffer and 1 mg/ml trypsin inhibitor. All reactions were then centrifuged at 12,000 x g for 10 min and re-suspended in 180  $\mu\text{l}$

import buffer. To this, 20  $\mu$ l of 50% trichloroacetic acid (TCA) (Sigma) was added and the mixtures heated at 60°C for 5 min. The samples were then put on ice for 5 min, followed by centrifugation at 12,000 x g for 5 min. The supernatant was removed and the pellets re-suspended in 40  $\mu$ l SDS-sample buffer. The samples, along with the TnT reaction as a standard and a Rainbow protein marker, were then subjected to 12% SDS-PAGE. To decrease background radioactivity, after electrophoresis, the gel was boiled for 5 min in 5% TCA, followed by a 5 min boil in water and then a 5 min soak in 1 M Tris base. The gel was then vacuum-dried and subjected to autoradiography.

### **3.5 Treatment of Neuroblastoma Cells with MitoTracker Probes**

The same protocol applies to MitoTracker Green FM and MitoTracker Red CMXRos (Molecular Probes). The powdered dyes were first dissolved in DMSO (Sigma) to make a final concentration of 1 mM. Several concentrations were tested for best resolution (20-500 mM) and it was found 20 mM or less to be most efficient.

The neuroblastoma cells were grown on coverslips in supplemented Neurobasal A medium (as described previously) until 50-80% confluent. At this stage, the medium was removed and replaced by pre-warmed (37°C) probe-containing medium, and incubated for 45 minutes in the cell culture incubator. During the testing experiments to determine the optimum probe concentration, the cells were now examined by fluorescence microscopy. For the experiment proper, the cells were next fixed. First, the cells were washed at 37°C with PBS. They were then fixed for 15 min at 37°C using



freshly prepared 3.7% paraformaldehyde in HBSS, following which, they were rinsed several times with PBS. The cells were then examined by fluorescence microscopy, using the appropriate filter sets for each probe.

### **3.6.0 Immunoelectron Microscopy**

#### **3.6.1 Immunoelectron microscopy to detect APP in mammalian tissue**

Ultrathin sections from human and rat brain cortex and human kidneys were cut from tissue embedded in epoxy resin that had been fixed in Karnovsky's fixative followed by post-fixation in 1% osmium tetroxide. Gold grid mounted sections were pre-treated with 11% sodium metaperiodate for 1 hr. After several washes with distilled water, the sections were blocked with a universal blocking buffer (DAKO) for 5 min. The sections were then incubated with mouse anti-human APP (NH<sub>2</sub> terminus) antibody (Zymed) (diluted 1:5 in antibody dilution buffer [DAKO]) for 90 mins. Control sections were incubated with anti-mouse immunoglobulin G (IgG) antibody, diluted 1:10. After several washes in PBS, sections were incubated with goat anti-mouse gold-conjugated IgG (diluted 1:5) for 5 hrs. Gold particle size was 10 nm (Cedar Lane Labs). All incubations and washes were conducted at room temperature. Following several washes, the sections were fixed in glutaraldehyde and treated with 3% uranyl acetate for 5 min. prior to visualization. Labelled sections were viewed with a Phillips 201 transmission electron microscope, and representative areas were photographed.

### **3.6.2 Immunoelectron microscopy to detect APP and $\beta$ AP in human brain**

Ultrathin sections from temporal cortex of AD (n = 4) and non-AD patients (n = 4) (National Neurological Research Specimen Bank, V.A. Medical Centre, LA) were cut from tissue embedded in epoxy resin that had been fixed in Karnovsky's fixative followed by post-fixation in 1% osmium tetroxide. Nickel grid mounted sections were pre-treated with 11% sodium metaperiodate for 1 hr. After several washes with distilled water, the sections were blocked with a universal blocking buffer (DAKO) for 5 min. The sections were then incubated with mouse anti-human APP (NH<sub>2</sub> terminus) antibody (Zymed) (1:5 dilution in antibody dilution buffer [DAKO]) for 90 mins. Control sections were incubated with anti-mouse IgG antibody, diluted 1:5. After several washes in PBS, sections were incubated with goat anti-mouse IgG gold-conjugated antibody (diluted 1:5) for 2 hrs. Gold particle size was 10 nm (Cedar Lane Labs). All incubations and washes were conducted at room temperature. Following several washes, the sections were fixed in glutaraldehyde and treated with 3% uranyl acetate for 5 min prior to visualization. Labeled sections were viewed with a Phillips 201 transmission electron microscope, and representative areas were photographed. Similarly,  $\beta$ AP was visualized using rabbit anti-human  $\beta$ AP antibody (Zymed, dilution 1:50), and gold conjugated (5 nm), goat anti-rabbit IgG (British Biocell, dilution 1:50).

## 4.0 RESULTS

The APP constructs that were used as bait proteins in the yeast two-hybrid assay were prepared as described. First, the pAS2-1/APP<sub>770/2583</sub> construct was prepared. To verify the originating pGEM9zf/APP<sub>770/3432</sub> construct, it was restricted with Bgl II. APP<sub>770/3432</sub> has one Bgl II site at bp 1994, while the plasmid pGEM9zf has no Bgl II sites. The one DNA band of about 6.5 Kb was seen on the agarose gel (data not shown).

To isolate the APP<sub>770/2583</sub> fragment for insert into the pGEM5zf plasmid, the pGEM9zf/APP<sub>770/3432</sub> construct was restricted with Spe I. APP<sub>770/3432</sub> has one Spe I site at bp 2583, while pGEM9zf has an Spe I site in the MCS NH<sub>2</sub>-terminal to the APP insert. Thus, there were two bands of about 3 Kb (pGEM9zf plasmid) and 2.58 Kb (APP<sub>770/2583</sub>) (data not shown)..

The pGEM5zf plasmid was then restricted with Spe I to prepare it to accept the Spe I-restricted APP<sub>770/3432</sub> fragment. The pGEM5zf plasmid has only one Spe I site in the MCS, and therefore there was only one band of 3 Kb seen on AGE (data not shown). To verify the correct orientation of the APP<sub>770/2583</sub> insert after ligation into the pGEM5zf plasmid, the pGEM5zf/APP<sub>770/2583</sub> construct was restricted separately with Sac I and Pst I. Sac I has one site in APP<sub>770/2583</sub> at bp 1813, and one site in the MCS of pGEM5zf. Therefore, for Sac I-restricted pGEM5zf/APP<sub>770/2583</sub>, correct orientation produced two bands of 0.8 Kb and 4.9 Kb, and the incorrect orientation produced two bands of 1.85 Kb and 3.86 Kb. Pst I has four sites in APP<sub>770/2583</sub>, at bps 208, 238, 1438, and 1655. It has one site in the MCS of pGEM5zf. Therefore, for Pst I-restricted pGEM5zf/APP<sub>770/2583</sub>,

the correct orientation produced four bands visible of 0.22 Kb, 0.95 Kb, 1.2 Kb and 3.32 Kb., while the incorrect orientation produced four bands visible of 0.22 Kb, 0.23 Kb, 1.2 Kb and 4.04 Kb (data not shown).

To prepare the APP<sub>770/2583</sub> insert and the GAL-4 binding domain (BD) plasmid, pAS2-1, to receive the insert, both the pGEM5zf/APP<sub>770/2583</sub> construct and pAS2-1, were simultaneously restricted with Nco I and Sal I. There is one Nco I and one Sal I site in the MCSs of each plasmid. In the pGEM5zf plasmid, the Nco I site is 5' to the Spe I site (and therefore the APP insert), while the Sal I site is 3' to the Spe I (and therefore APP insert) site. Therefore, for Nco I/Sal I-restricted pGEM5zf/APP<sub>770</sub>, there were two bands of 2.66 Kb (APP<sub>770/2583</sub>) and 3 Kb (pGEM5zf plasmid). For the Nco I/Sal I-restricted pAS2-1, there was one band of 8.4 Kb (linearized plasmid) (data not shown).

After ligation of APP<sub>770/2583</sub> into pAS2-1, the constructs were verified by restricting pAS2-1/APP<sub>770/2583</sub> in separate tubes with Pst I, Bgl II or Hind III. Pst I-restricted pAS2-1/APP<sub>770/2583</sub> showed six bands of 0.003 Kb, 0.018 Kb, 0.03 Kb, 0.22 Kb, 0.93 Kb and 1.2 Kb. Bgl II has one site in pAS2-1 at bp 3969, and one site in APP<sub>770/2583</sub> at bp 1994. Therefore, Bgl II-restricted pAS2-1/APP<sub>770/2583</sub> showed two bands of 4.56 Kb and 6.43 Kb. Hind III has four sites in pAS2-1 at bps 2397, 3284, 5477, 6224, and no sites in APP<sub>770/2583</sub>. Therefore, Hind III-restricted pAS2-1/APP<sub>770/2583</sub> demonstrated four bands of 0.89 Kb, 2.19 Kb, 3.36 Kb and 4.57 Kb (data not shown).

## 4.1 Yeast Two-Hybrid Technology

Eukaryotic transcription factors (TF) contain two physically and functionally separable domains - an NH<sub>2</sub>-terminal DNA-binding domain and a COOH-terminal, acidic activation domain. The BD specifically binds to a promoter or other *cis*-regulatory element. The ActD directs RNA Polymerase II to transcribe the gene downstream of the DNA binding site. The physically divided TF can function normally, as long as a bridge is provided that localizes the ActD to the BD bound to the promoter. The bridge is formed by the interaction of one protein expressed as protein X (e.g APP) fused to a BD with another protein expressed as protein Y (e.g brain cDNA) fused to an AD, where proteins X and Y normally interact in cells. (Figure 6). In the yeast assay, an interaction between two human proteins brings together the modular BD and ActD of the yeast GAL4 TF, which causes the activation of transcription of a reporter gene in the yeast host.

The yeast strain used in the assay, Y190, has two reporter genes, *LacZ* and *HIS3*, as separate constructs integrated into its genome. The *LacZ* gene encodes the bacterial enzyme beta-galactosidase, which causes colonies to turn blue when exposed to a specific substrate. The *HIS3* gene encodes an enzyme in the histidine biosynthetic pathway, and acts as a nutritional marker for yeast cells grown on histidine-deficient medium. As well, Y190 is auxotrophic for tryptophan and leucine, two amino acids encoded by the BD and ActD plasmids, respectively. This allows selective growth by the yeast cells on histidine-, tryptophan- and leucine-deficient medium by only those yeast

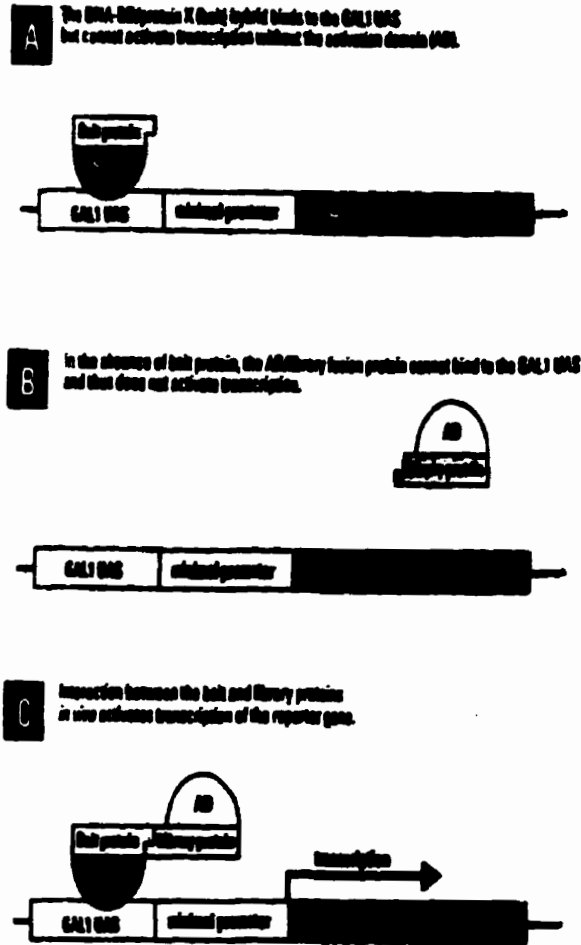


Figure 6 Schematic diagram of the MATCHMAKER GAL4-based two-hybrid systems. (Adapted from Clontech catalog).

cells transfected with both plasmids (Figure 7).

Figure 8 summarizes the findings of the screening of the human brain cDNA expression library. Screening of  $10^6$  double transformants resulted in 40 *HIS3* positive colonies, of which 11 were subsequently shown to be both *HIS3* and *LacZ* positive.

#### 4.2 Analysis of Positive Clones

Two clones (A-2 and A-14) that showed the strongest protein-protein interactions, based on the speed and intensity of the  $\beta$ -galactosidase blue color development, were selected for further analysis. They were sequenced at the fusion site and shown to be in-frame with the GAL4-pACT2 ActD. A-14 comprised 680 bases with an open reading frame ending at 606, encoding a protein of 202 amino acids. A-2 was of the same gene but longer by 938 bases.

To identify homologous proteins, the BLAST data base of the National Centre for Biotechnology Information was searched. Both cDNA clones shared over 99% identity with the family of cytochrome c oxidase enzymes of the mitochondrial ETC. Sequence analysis (Devereux *et al.*, 1984) of *Match* clones identified them as complete and partial COX subunit I gene sequences coupled to tRNA<sup>Ser</sup> (Anderson *et al.*, 1981). A-14 was found to be identical to the last 606 bps of COX I plus the adjacent (in the mitochondrial genome) tRNA<sup>Ser</sup>, while A-2 was composed of the whole COX I sequence attached to tRNA<sup>Ser</sup>. The A-2 COX I gene sequence comprised bps 5899-7444 of the mitochondrial genome, while A-14 consisted of bps 6837-7444 (see Figure 9).

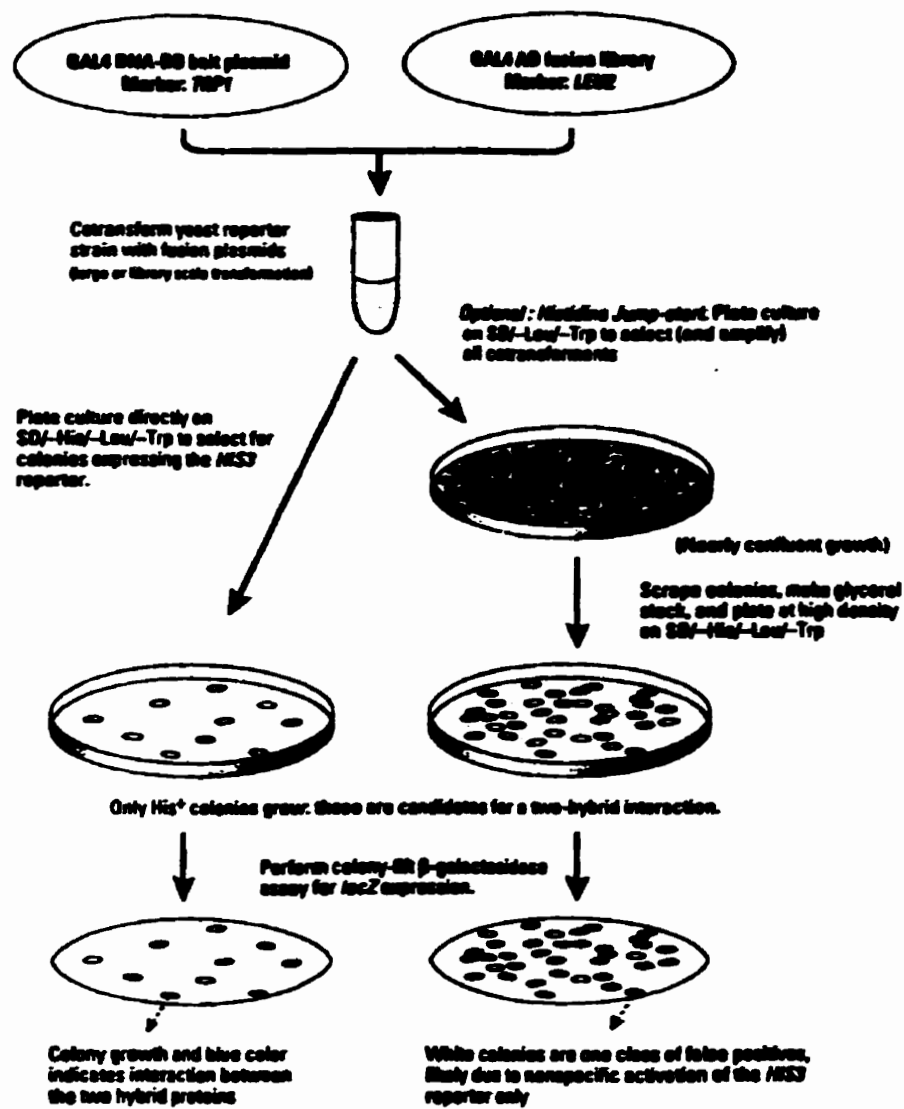


Figure 7 Screening an AD fusion library for proteins that interact with a bait protein. (Adapted from Clontech catalog).



**10<sup>6</sup> double transformants screened**

↓

**40 colonies, His<sup>+</sup>**

↓

**11 colonies, His<sup>+</sup> and *LacZ*<sup>+</sup>**

↓

**Two clones, A-2 and A-14 were independently isolated.  
These clones encode complete and partial cDNA sequences of human brain  
mitochondrial cytochrome *c* oxidase subunit 1 (COX I) coupled with the complete  
cDNA sequence of tRNA<sup>Serine</sup>**

**Figure 8 Matchmaker two-hybrid screen. pAS2-1/APP was used to screen a whole human brain cDNA library. Among the interacting clones, A-2 and A-14 encode sequences of COX I and tRNA<sup>Ser</sup> (Anderson *et al.*, 1981).**

Figure 9 Sequence of clone A-14; the partial COX I-tRNA<sup>Ser</sup> gene.

I P T G V K V F S W L A T L H G S N M K W S A A V L W A L G F I F L F T V G G L  
CATCGCTATCCACCGGGGTCAAAGTATTAGCTGACTCGCCACACTCCACGGAAGCAATATGAAATGATCTGCTGCAGTGCTCTGAGCCCTAGGATTTCATCTTTCTTTCCACGTAGGTGGCC  
1 (8836)

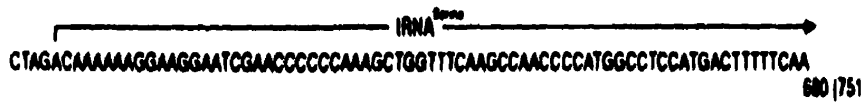
T G I V L A N S S L D I V L H D T Y Y V V A H F H Y V L S M G A V F A I M G G F  
TGACTGGCATTGTATTAGCAAACCTCCTACTAGACATCGTACTACAGCACGACTACGTTGTAGCICACTTCCACTATGTCCTATCAATAGGAGCTGTATTGCCATCATAGGAGGCT

I H W F P L F S G Y T L D Q T Y A K I H F T I M F I G V N L T F F P Q H T L G L  
TCATTCAGTGATTTCCCTATTCTCAGGCTACACCCTAGACCAAACCTACGCCAAAATCCATTTCACTATCATATTCATCGGCGTAAATCTAATTTCTCCACAAACACTTCTCGGCC

S G M P R R Y S D Y F D A Y T T W N I L S S V G S F I S L T A V M L M I F M I W  
TATCCGGAATGCCCGACGTTACTCGGACTACCCCGATGCATACCCACATGAACATCCTATCATCTGTAGGCTCATTCTTCTAACAGCAGTAATATTAATAATTTCATGATT

E A F A S K R K V L M V E E P S M N L E W L Y G C P P P Y H T F E E P V Y M K S  
GAGAGGCCCTTCGCTTCGAAGCGAAAGTCTAATAGTAGAAGAACCCTCCATAAACCTGGAGTGACTATATGGATGCCCCCACCCTACCACACATCGAAGAACCCTATACATAAAAT

CTAGACAAAAAGGAAGGAATCGAACCCTCAAGCTGGTTTCAAGCCAACCCATGGCCTCCATGACTTTTCAA  
680 (7516)



### **4.3 Verification of specificity of APP/COX I interaction**

To establish that the interaction of APP<sub>770/2583</sub> and COX I was specific, yeast Y190 cells were transformed in separate experiments with pAS2-1/APP<sub>770/2583</sub> alone, pACT2/COX I alone, and the two constructs together, using Clontech's *Matchmaker Gal4 Two-Hybrid User Manual* for small-scale transformation, followed by Clontech's  $\beta$ -galactosidase colony-lift filter assay. Neither pAS2-1/APP<sub>770</sub> nor pACT2/COX I by themselves activated  $\beta$ -galactosidase activity, indicating that neither APP<sub>770</sub> nor COX I contained a latent transcriptional activator. Only when the GAL4-BD/APP<sub>770/2583</sub> gene was co-transformed with the GAL4-ActD/COX I did activation of the *LacZ* reporter gene occur. Thus, it appears APP<sub>770/2583</sub> and COX I do not interact non-specifically with other proteins using the yeast *MATCHMAKER* system. The specificity of the APP-COX I interaction was also confirmed by Amara and Junaid (manuscript in revision) by the lack of  $\beta$ -galactosidase activity when the APP-related constructs or COX I were expressed alone, or when APP<sub>751</sub> was co-expressed with COX II and COX III, while the three major isoforms of APP interacted with COX I (Table 1).

#### **4.4.0 Preparation of APP Deletion Constructs**

To determine what general region of APP<sub>770</sub> is involved in the interaction with COX I, REs were used to delete portions of the APP<sub>770</sub> cDNA, as described. The resulting constructs were tested for interaction with COX I using the *MATCHMAKER*

Bait Construct	Activating	beta-galactosidase activity	Colour intensity (Filters)
—	A - 14	0.6 ± 0.2	white
pAS2-1	A - 14	0.4 ± 0.0	white
pAS2-1/APP <sub>695</sub>	A - 14	301 ± 2.5	blue
pAS2-1/APP <sub>751</sub>	A - 14	289 ± 1.1	blue
pAS2-1/APP <sub>770</sub>	A - 14	316 ± 3.3	blue
pAS2-1/APP <sub>751</sub>	Cox2	0.7 ± 0.1	white
pAS2-1/APP <sub>751</sub>	Cox3	0.4 ± 0.3	white

**Table 1** Interaction of APP and COX I in yeast. Amyloid precursor protein plasmids (pAS2-1/APPs) cloned into a GAL4 DNA binding domain fusion vector were tested for their ability to interact with COX I-GAL4 activation domain fusions. Positive results were measured as the development of blue color on X-gal filter lifts of colonies expressing both activator and DNA binding constructs relative to colonies expressing each construct alone. Filter results (column 4) were confirmed by quantitative liquid culture assay (column 3). Negative results (white colonies) were obtained for the interaction between GAL4-binding domain/APP<sub>751</sub> and GAL4-activation domain/COX II and COX III. (Courtesy Amara and Junaid [manuscript in revision]).

yeast two-hybrid assay and  $\beta$ -galactosidase colony-lift filter assay.

#### **4.4.1 pAS2-1/APP2020 construct**

The pAS2-1/APP<sub>770/N-T2583</sub> construct has EcoR 1 sites at bps -15 of the 5' UTR of APP and at bp 2020 of APP. Therefore, EcoR 1 restriction removed a segment of APP from pAS2-1/APP<sub>770/N-T2583</sub> that contained the first 2020 base pairs of APP plus 15 bps of the 5' UTR. Two bands of 9 Kb (pAS2-1 plus COOH-terminal APP) and 2.035 Kb (the APP<sub>770/N-T2020</sub> band, comprising APP<sub>770</sub>, bps 1-2020) were seen on the agarose gel (Figure 10). This NH<sub>2</sub>-terminal APP segment was inserted into the pAS2-1 plasmid to create the construct, pAS2-1/APP<sub>770/N-T2020</sub>.

To verify the correct ligation and orientation of the APP<sub>770/N-T2020</sub> fragment into pAS2-1, the pAS2-1/APP<sub>770/N-T2020</sub> constructs were restricted with Sac 1. The pAS2-1/APP<sub>770/N-T2020</sub> construct has two Sac 1 sites: one at bp 3298 of pAS2-1, and one at bp 1813 of APP<sub>770/N-T2020</sub>. Therefore, correctly oriented constructs produced two bands of 4.52 Kb and 5.92 Kb, and incorrectly oriented constructs showed two bands of 0.9 Kb and 7.75 Kb (data not shown). To re-verify the correct construct, the pAS2-1/APP<sub>770/N-T2020</sub> preparation after amplification was restricted with Sac 1. The 4.52 Kb and 5.2 Kb bands were seen (Figure 11).

#### **pAS2-1/APP<sub>770/N-T1554</sub> and pAS2-1/APP<sub>770/N-T208</sub> constructs**

To create smaller APP deletion constructs, pAS2-1/APP<sub>770/N-T2020</sub> was restricted separately with BamH I and Pst I. The pAS2-1/APP<sub>770/N-T2020</sub> construct has two BamH I

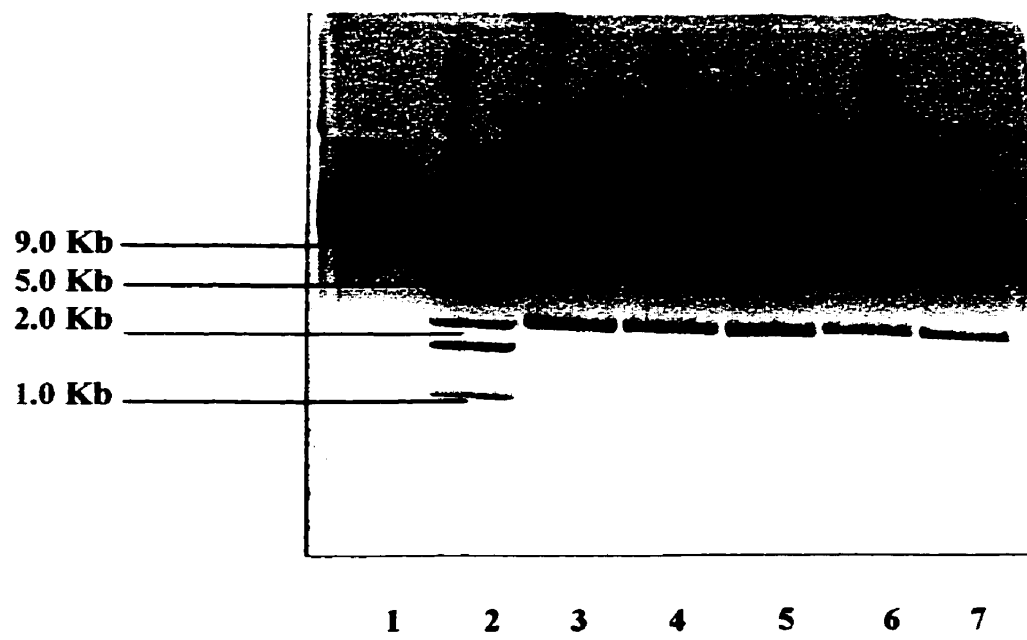


Figure 10 Restriction enzyme digestion of pAS2-1/APP<sub>770/2583</sub> with EcoR 1. Lane 1. Unrestricted pAS2-1/APP<sub>770/2583</sub>. Lane 2. 1 Kb DNA ladder (GibcoBRL). Lanes 3-7. EcoR 1-restricted pAS2-1/APP<sub>770/2583</sub>. DNA stained with ethidium bromide in 0.8% agarose gel.

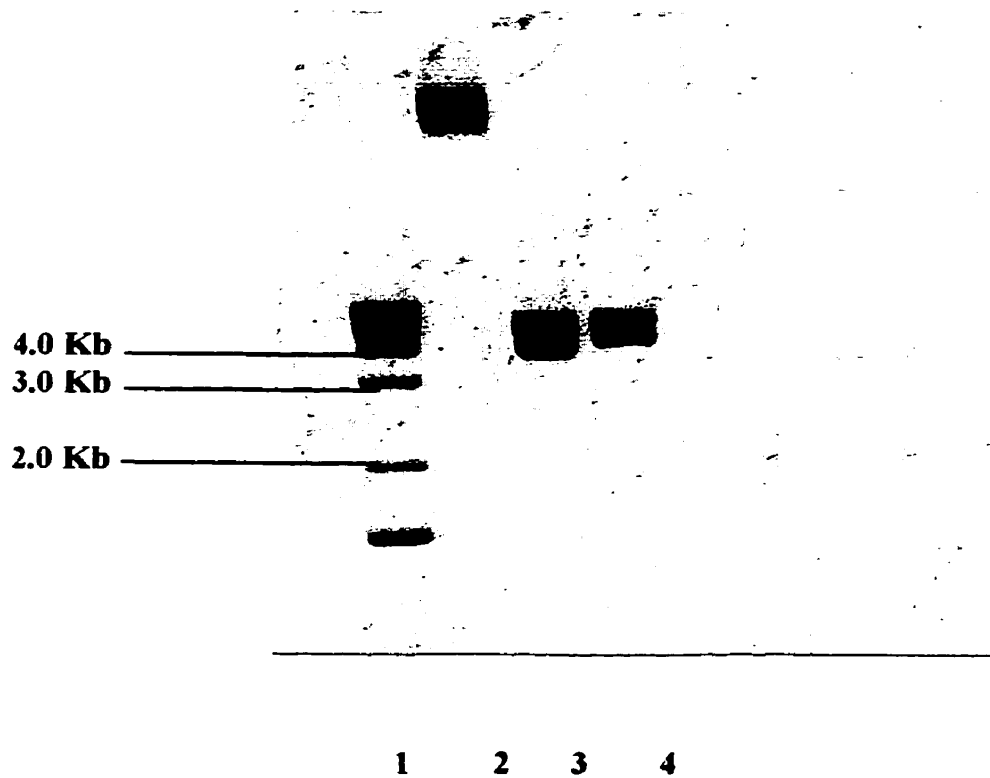


Figure 11 *Sac* I restriction enzyme digestion of pAS2-1/APP<sub>770N-T2020</sub> construct. Lane 1. 1 Kb DNA ladder (GibcoBRL). Lane 2. Unrestricted pAS2-1/APP<sub>770N-T2020</sub>. Lanes 3 & 4. *Sac* I-restricted pAS2-1/APP<sub>770N-T2020</sub>. Verification that construct was in correct orientation. DNA stained with ethidium bromide in 0.8% agarose gel.

sites: one in the MCS of pAS2-1, COOH-terminal to the APP insert, and one at bp 1554 of the APP insert. Therefore, the BamH 1-restricted pAS2-1/APP<sub>770N-T2020</sub> yielded two bands of 0.47 Kb and 9.97 Kb (data not shown). The pAS2-1/APP<sub>770N-T2020</sub> construct has five Pst 1 sites: one in the MCS of pAS2-1 COOH-terminal to the APP insert, and four sites in APP<sub>770N-T2020</sub> at bps 208, 238, 1438, and 1655. Therefore, the Pst 1-restricted pAS2-1/APP<sub>770N-T2020</sub> yielded five bands of 0.03 Kb, 0.2 Kb, 0.4 Kb, 1.2 Kb and 8.64 Kb (data not shown). BamH 1 produced pAS2-1/APP<sub>770N-T1554</sub> (APP<sub>770</sub> insert containing bps 1-1554), and Pst 1 produced pAS2-1/APP<sub>770N-T208</sub> (APP<sub>770</sub> insert containing bps 1-208).

After ligation of the pAS2-1/APP<sub>770N-T208</sub> and pAS2-1/APP<sub>770N-T1554</sub> constructs, they were verified using Hind III restriction. In both constructs, Hind III has no sites in the APP inserts, but has four sites in pAS2-1 at bps 2397, 3284, 5477 and 6224. Therefore, the Hind III-restricted pAS2-1/APP<sub>770N-T208</sub> construct yielded four bands of 0.89 Kb, 0.94 Kb, 2.19 Kb and 4.57 Kb. The Hind III-restricted pAS2-1/APP<sub>770N-T1554</sub> construct produced four bands of 0.89 Kb, 2.19 Kb, 2.31 Kb and 4.57 Kb (Figure 12).

#### **4.4 Yeast Two-hybrid Assay With APP Deletion Constructs**

To determine with which APP constructs COX I interacts, and thus determine what general region of APP<sub>770</sub> is involved in the interaction, a small scale yeast two-hybrid assay was performed, followed by a  $\beta$ -galactosidase colony-lift filter assay. All constructs were positive except for pAS2-1/APP<sub>C-T/N-T2020</sub>. This suggests the APP-COX I interaction involves the first 208 NH<sub>2</sub>-terminal nucleotides of APP<sub>770</sub>. These results



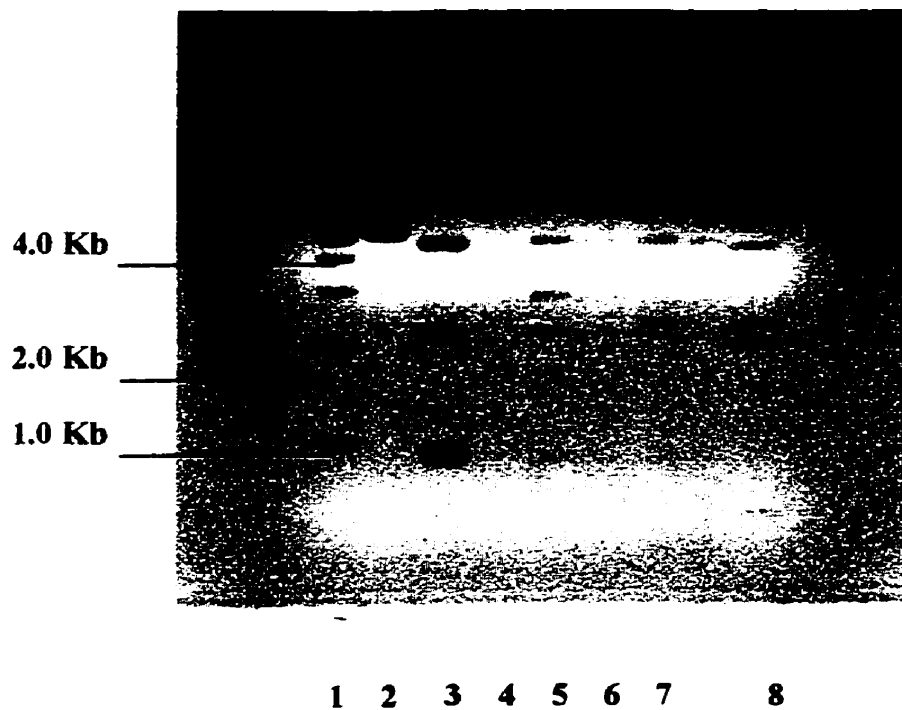


Figure 12 *Hind* III restriction of constructs pAS2-1/APP<sub>770N-T208</sub> & pAS2-1/APP<sub>770N-T1554</sub>. Lane 1. 1 Kb DNA ladder (Biorad). Lane 2. Unrestricted pAS2-1/APP<sub>770N-T208</sub>. Lane 3. *Hind* III-restricted pAS2-1/APP<sub>770N-T208</sub>. Lane 6. Unrestricted pAS2-1/APP<sub>770N-T1554</sub>. Lane 7. *Hind* III-restricted pAS2-1/APP<sub>770N-T1554</sub>. Lane 8. High molecular weight DNA marker (Biorad). The two constructs were verified. DNA stained with ethidium bromide in 0.8% agarose gel.

were supported by a repeat small scale yeast two-hybrid assay. Plasmids examined were pAS2-1/APP<sub>770/N-T2020</sub>, pAS2-1/APP<sub>770/2583</sub>, and pAS2-1/APP<sub>C-T1-2020</sub>, all with pACT2 added, plus pAS2-1/APP<sub>770/2583</sub> alone. Only pAS2-1/APP<sub>770/N-T2020</sub> and pAS2-1/APP<sub>770/2583</sub> showed significant values for  $\beta$ -galactosidase activity (data not shown). This confirmed that at least the NH<sub>2</sub>-terminal 2020 amino acids are involved in APP's interaction with COX I.

#### **4.5.0 APP and Mitochondria**

For APP to interact with a facultative mitochondrial protein, we postulate that the interaction must take place in the mitochondria, and that therefore, APP must be targeted to, and localized in, mitochondria.

##### **4.5.1 Mitochondrial targeting signal**

If APP is targeted to and localizes in mitochondria, it should contain a mitochondrial targeting sequence. Computer analysis of the APP leader peptide sequence using the PSORT II program (see <http://psort.nibb.ac.jp/cgi-bin/okumura>), suggested the first 17 amino acids are a possible mitochondrial targeting sequence (MITDISC), and that the cleavage site for the mitochondrial pre-sequence occurs between residues 17 and 18 in the sequence ARALEV (Gavel). These results were supported by the SignalP (see <http://genome.cbs.dtu.dk/htbin/nph-webface>) program which suggested APP has a signal sequence consisting of the first 17 amino acids. These findings are consistent with a high

probability of intra-mitochondrial sorting of APP (Gavel and von Heijne, 1990). Based on this analysis, we tested our hypothesis that APP resides in mitochondria and under certain conditions, impairs the activity of COX, enhances the production of ROS and its attendant lipid peroxidation, and induces apoptosis in mammalian cells, specifically, a neuroblastoma cell line.

#### **4.6.0 Assays on Neuroblastoma Cells Overexpressing APP**

To examine the role of APP overexpression in AD, SK-N-SH neuroblastoma cells were stably transfected with various APP constructs, and the following parameters were examined; (i) complex I and complex IV enzyme activities of the ETC, (ii) levels of ROS production and lipid peroxidation, (iii) anti-oxidant enzyme activities of superoxide dismutase and glutathione peroxidase, and (iv) the degree of apoptosis induced. The pShooter expression vector, pCMV/myc/mito, which expresses a mitochondrial targeting sequence, was used as the transfecting vector to successfully express APP in mitochondria. In addition, the expression vector pCI-neo (Promega), which allows generalized expression of APP, was also employed by Amara and Junaid.

The effects of targeting APP to mitochondria on the various parameters mentioned were determined by inserting APP<sub>770/2583</sub> cDNA into pCMV/myc/mito to create the construct pCMV/myc/mito/APP<sub>770/2583</sub>. To isolate the APP<sub>770/2583</sub> fragment, the pGEM5zf/APP<sub>770/2583</sub> construct was restricted with Spe I. The construct has two Spe I sites: one 39 bps 5' to the amino terminus of the APP insert, and one at bp 2583 of the

APP insert. Therefore, the Spe I-restricted pGEM5zf/APP<sub>770/2583</sub> produced two bands of 2.62 Kb (the APP<sub>770/2583</sub> insert) and 3 Kb (pGEM5zf plasmid) on an agarose gel (data not shown).

The pBluescript II SK was next restricted with Spe I to allow it to accept the Spe I-restricted APP<sub>770/2583</sub> fragment. There is only one Spe I site in pBluescript II SK in the MCS, which was seen on AGE (data not shown). After ligation of the APP<sub>770/2583</sub> fragment into the pBluescript II SK phagemid to create the pBluescript II SK/APP<sub>770/2583</sub> construct, the correct orientation of the insert was verified by RE analysis (data not shown).

To prepare the pCMV/myc/mito plasmid to accept the APP<sub>770/2583</sub> insert, it was simultaneously restricted with Sal I & Not I REs. There is one site each for Sal I and Not I in the MCS of pCMV/myc/mito. Therefore, two bands of 0.02 Kb (MCS segment) and 4.94 Kb (Sal I/Not I-restricted plasmid) were present on AGE (data not shown). The pBluescript II SK/APP<sub>770/2583</sub> construct was also restricted with Sal I and Not I to yield the APP<sub>770/2583</sub> fragment, which was ligated into the Sal I/Not I-restricted pCMV/myc/mito plasmid to create pCMV/myc/mito/APP<sub>770/2583</sub>. This construct was verified by RE analysis (data not shown).

#### **4.6.1 Assays of COX and Complex I enzymatic activities**

##### **COX activity assay**

The assay involved following the oxidation of cytochrome c, and the protocol was based on Parker *et al.* (1994 b). Activity was calculated as a first order rate constant,

calculations being based on the equation:

$$\text{Velocity} = k[\text{cyt c}] \mu\text{M}/\text{sec},$$

where  $k$  = first order rate constant =  $2.3 \log A_{550} (\text{at time } 0) / A_{550}$   
(at time 0 + time 1 min)  $\text{min}^{-1}$ .

The cytochrome c concentration was deduced by the equation:

$$[\text{cyt. c}] = A_{550} / 0.029.$$

(Extinction or absorbance coefficient for cytochrome c is  $29\text{mM}^{-1}$ ).

### **Complex 1 activity assay**

To compare the effects of APP on other enzymes of the ETC, the activity of Complex 1 was also assayed by following the oxidation of NADH. Calculations were based on the following:

- (i) The molar extinction coefficient of NADH is  $6.81 \text{ mM}^{-1}$ .
- (ii)  $[\text{NADH}] = A_{340} / \text{Ext. Coef.}$
- (iii) Rate = initial  $[\text{NADH}]$  added ( $100 \mu\text{M}$ ) -  $[\text{NADH}]$  at time 1 min ( $\mu\text{M}/\text{min}$ ).

The assay was then repeated in the presence of  $2.5 \mu\text{M}$  rotenone, which inhibits Complex 1 activity. Final rate was calculated as that without rotenone - that with rotenone.

### **Results of COX and complex I enzyme activity assays**

There was a markedly reduced level of total COX activity in the cells overexpressing mitochondria-targeted APP compared with other transfectants (Table 2).

Enzyme	untransfected cells	transfected cells			
	control	pc1neo	pc1neo/APP	pmyc/mito	pmyc/mito/APP
Complex I nmol min <sup>-1</sup> ±S.E.M.	0.52±0.02	0.48±0.03	0.50±0.01	0.49±0.01	0.54±0.02
Complex IV Sec <sup>-1</sup> /mg protein±S.E.M.	0.093±0.002	0.085±0.001	0.090±0.012	0.080±0.002	0.035±0.001

**Table 2** Complex I and complex IV enzyme activities in neuroblastoma cells overexpressing APP. The specified values represent the means of complex I and Complex IV activities +/- S.E.M. of ten replicates. Activity was measured by spectrophotometry. The human neuroblastoma cells were stably transfected with different plasmid constructs in contrast to untransfected cells.

In contrast, no significant change was observed for complex I activity between the SK-N-SH transfectants. It is noteworthy that nuclei-targeted APP or mitochondria-targeted  $\alpha$ -1 antichymotrypsin (a  $\beta$ AP plaque-associated protein) overexpression did not significantly affect COX activity in SK-N-SH stable transfectants (data not shown). This suggests that the accumulation of APP in mitochondria plays a crucial role in specifically mediating decreased COX activity.

#### **4.6.2 APP overexpression and apoptosis in neuroblastoma cell line**

Using Genzyme's *TACS Annexin V Apoptosis Detection Kit*, there was found to be a prominent rise in apoptosis in cells transfected with pCMV/myc/mito/APP (Mitochondrial expression of APP), compared with either vector alone (pCMV/myc/mito) or untransfected cells (Figure 13). In contrast, there was no significant difference in the extent of apoptosis in cells transfected with pCI-neo/APP (generalized cellular expression of APP), compared with vector alone (pCI-neo) or untransfected cells (data not shown) (Amara and Junaid [manuscript in revision]). These results suggest that overexpression of APP on its own, may not be sufficient to induce apoptosis in neurons without the accumulation of APP in mitochondria.

#### **4.6.3 APP overexpression and ROS production in neuroblastoma cell line**

To determine the role of ROS in APP-mediated neuronal apoptosis, it was examined whether neuroblastoma cells targeted with overexpression of APP would generate increased levels of ROS. To detect ROS, the non-fluorescent dye 2',7'-

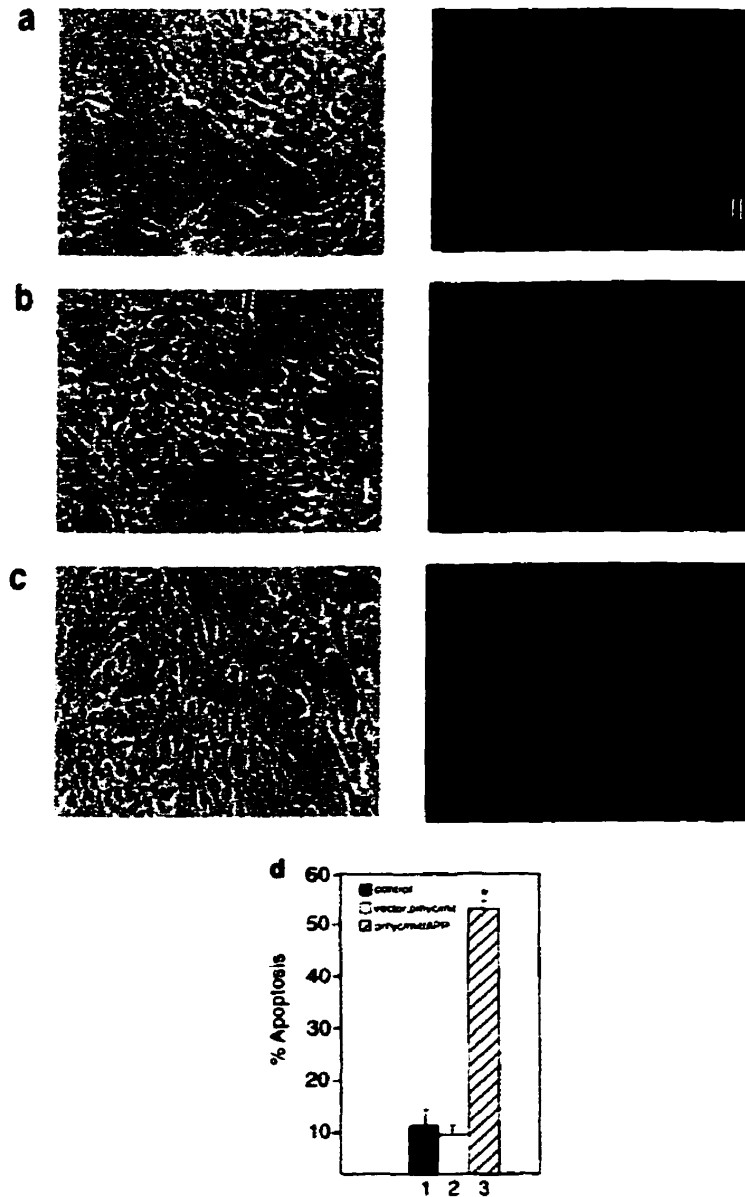


**Figure 13** Targeting APP into mitochondria potentiates apoptosis. SK-N-SH cells were **a.** untransfected, **b.** stably expressing pCMV/myc/mito, and **c.** stably expressing pCMV/myc/mito/APP. Plasmid constructs were assayed for induction of percentage apoptosis by Annexin conjugate according to the manufacturer's instructions (Zymed). In apoptotic assays the percentage of necrotic cells was negligible (<4%). Late apoptotic cells were stained red/green. Scale bar: 100  $\mu$ m. **d.** Percentage apoptosis index. The mean  $\pm$  S.E.M. of 10 replicates as calculated for >200 cells is shown. Asterisks: P, 0.01. The images were enhanced in size 2.0-4.0 fold. Cells were transfected using FuGENE 6, according to the manufacturer's instructions, and stably selected in 600  $\mu$ g/ml G418 (Invitrogen).



dichlorofluorescein diacetate (DCF-DA) was used, which interacts with intracellular ROS to generate the fluorescent 2',7'-dichlorofluorescein product (Rozenkranz *et al.*, 1992). Fluorescence microscopy demonstrated no significant difference between levels of DCF in control cells transfected with pCI-neo and pCI-neo/APP (Figure 14 a,c). In contrast, there was markedly increased ROS generation in pCMV/myc/mito/APP stably transfected cells compared with pCMV/myc/mito, and with untransfected cells (Figure 14 b,d).

#### **4.6.4 APP overexpression and the formation of lipid peroxidation**

To confirm that increased free radical generation resulted in cellular damage in pCMV/myc/mito/APP transfectants, lipid peroxidation based on loss of fluorescence from incorporated *cis*-parinaric acid (CPA) was determined. Lipid peroxidation in pCI-Neo/APP cells was not significantly different than that detected in normal control or SK-N-SH pCI-neo transfectants (Figure 14 e), but was significantly greater in pCMV/myc/mito/APP SK-N-SH transfectants compared with pCMV/myc/mito transfectants and untransfected SK-N-SH cells (Figure 14 f). These results suggest that a defect in metabolism of ROS in mitochondria-targeted APP overexpressed SK-N-SH cells leads to apoptosis.

#### **4.6.5 Anti-oxidant enzyme assays**

To assess the possibility that enhanced ROS production may be due to an APP-mediated effect on ROS scavenger enzymes, the activation of free radical scavenging

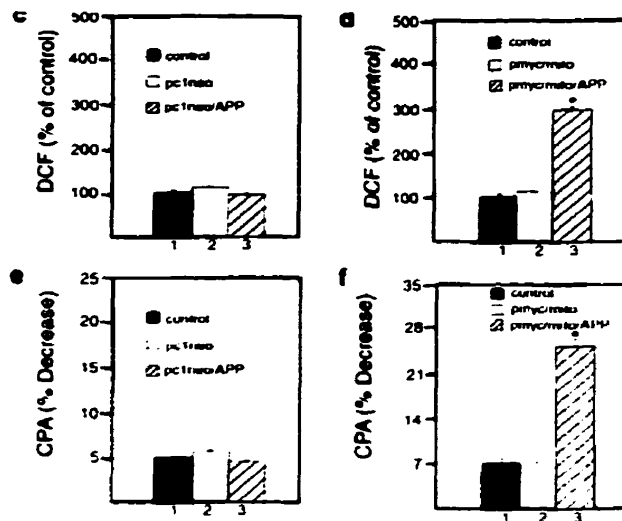
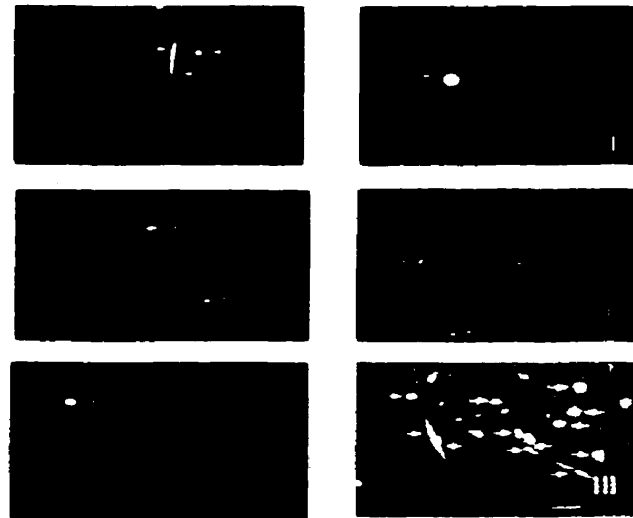


**Figure 14** Induction of ROS and lipid peroxidation in SK-N-SH cells. **a.** SK-N-SH cells (I) untransfected, stably expressing (II) pCI-neo and (III) pCI-neo/APP were exposed to 10  $\mu$ g 2',7'-dichlorofluorescein diacetate for 1 hr. The cells were washed with HBSS and viewed with a fluorescence microscope using fluorescein optics. Arrow heads indicate some of the intracellularly appearing fluorescence. Scale bar: 100  $\mu$ m. **b.** (I) SK-N-SH cells untransfected, and stably expressing (II) pCMV/myc/mito, and (III) pCMV/myc/mito/APP were treated with DCF-DA as described above. Scale bar: 100  $\mu$ m. Fields were chosen to illustrate representative fluorescence micrographs. **c/d.** Values are expressed as percent of the DCF level in normal cultures (100%) and represent the mean  $\pm$  S.E.M.,  $n > 400$  cells. **e/f.** Lipid peroxidation is indicated by the percent decrease in *cis*-parinaric acid (CPA) fluorescence. Values are the mean  $\pm$  S.E.M.,  $n > 400$  cells. Asterisks:  $P < 0.001$ . The images were enhanced in size 1.5-2.0 fold.

enzymes, glutathione peroxidase and superoxide dismutase, were examined in the neuroblastoma cells.

### **Glutathione peroxidase assay**

Glutathione peroxidases catalyze the reduction of hydroperoxides (ROOH) by glutathione (GSH):



GSSG is reduced by the reaction catalyzed by glutathione reductase:



Glutathione peroxidase activity was measured at 37°C by a coupled assay system in which the oxidation of reduced glutathione (GSH) was coupled to NADPH oxidation catalysed by glutathione reductase, following a protocol based on Carmagnol *et al.* (1983). Specific activity was determined as the amount of enzyme that catalyzed the transformation of 1 nmol of NADPH/min. Rate = nmol NADPH transformed /min.

### **Superoxide dismutase assay**

SOD activity is assayed by tracking the inhibition of pyrogallol autooxidation. The protocol used was based on Marklund (1985). Calculations were based on the equation:

$$\% \text{ inhibition} = (\Delta \dot{A} \text{ sample} - \Delta \dot{A} \text{ pyrogallol}) / \Delta \dot{A} \text{ pyrogallol}$$

where pyrogallol gives a  $\Delta \dot{A} = 0.02/\text{min}$ .

## **Results**

APP overexpression had no significant effect on the activity of glutathione peroxidase (Carmagnol *et al.*, 1983) in the stably transfected (Figure 15 a) cells compared to control cells, but there was a significant increase in SOD activity (Nagi *et al.*, 1995) in the pCMV/myc/mito cells compared to other transfectants and control cells (Figure 15 b). Thus, only mitochondria-targeted APP once again had an effect. This action may be a sign of a compensatory response by the enzyme to increased ROS production.

### **4.7.0 Evidence for the Physiological Location of APP in Mitochondria**

For APP to interact with a mitochondrial enzyme, APP must be targeted to and localized in mitochondria. To examine this, three experiments were performed: (i) a classic *in vitro* mitochondrial import assay, (ii) fluorescent microscopy of neuroblastoma cells transiently transfected with chimeric APP-GFP constructs, and (iii) immunoelectron microscopy of brain tissue from AD and control patients to visualize the location of endogenous APP and  $\beta$ AP.

#### **4.7.1 Classic *in vitro* mitochondrial import assay**

The aim was to show that <sup>35</sup>S-methionine-labelled APP is imported into mitochondria (isolated from rat livers) in an energy-dependent manner. It is known that proteins to be imported into mitochondria are synthesized in the cytoplasm in a

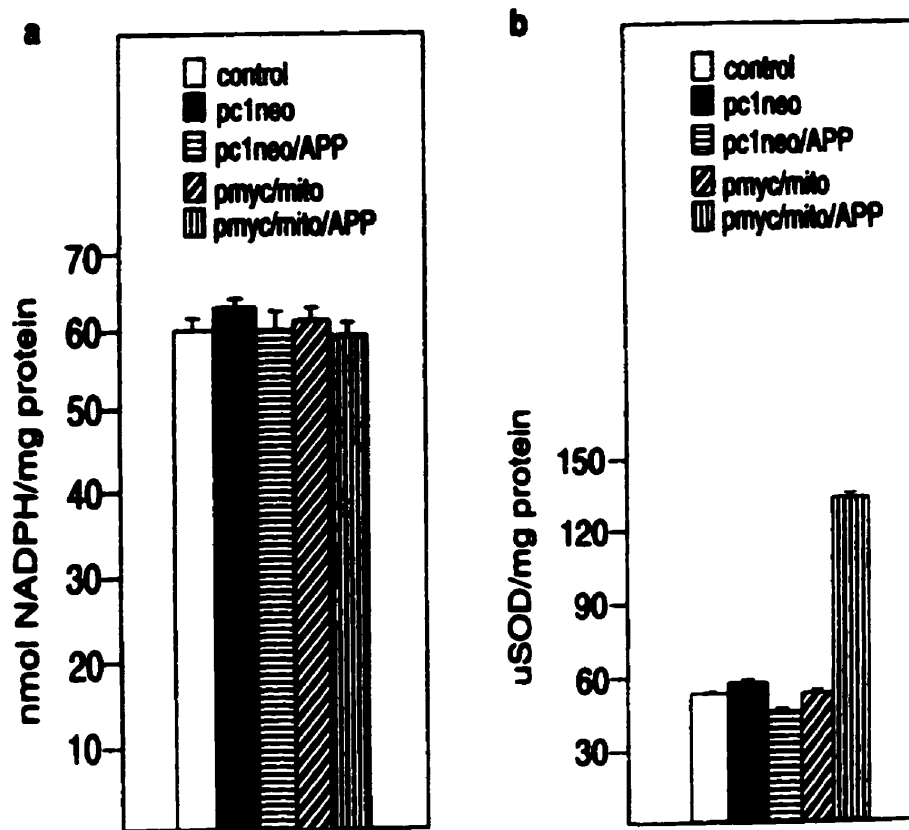


**Figure 15** Comparison of the free radical scavenging enzyme activities. **a.** Glutathione peroxidase, and **b.** Superoxide dismutase (SOD) in SK-N-SH neuroblastoma cells stably transfected with different plasmid constructs and control cells (untransfected).

precursor form, whose mitochondrial targeting sequence is cleaved after import, generating one or more shorter mature forms. The experimental conditions allow APP to be imported into mitochondria (if it has a mitochondrial targeting sequence). The mitochondrial preparations are then treated with trypsin to completely digest any unimported APP. This will determine if any APP was imported into mitochondria, and therefore spared from trypsin proteolysis. It will also allow determination of the approximate size of the imported fragment (s) and therefore, show whether a portion (e.g., targeting sequence) has been cleaved off within the mitochondria. In a separate experiment, the import reactions were also pre-treated with valinomycin, a potent inhibitor of COX. Because valinomycin destroys the ability of mitochondria to produce any energy, no APP should be imported into mitochondria, if such importation is energy-dependent.

Therefore, from the experimental setup, expected bands include: (i) TnT product (<sup>35</sup>S-APP) lane. One band representing the precursor APP<sub>770</sub>. (ii) Mitochondrial import reaction without trypsin treatment (APP<sub>770</sub> plus mitochondria lane). Two or more bands representing precursor APP<sub>770</sub> plus one or more mature shorter forms of APP<sub>770</sub>, with the mitochondrial targeting sequence cleaved off. (iii) Mitochondrial import reaction followed by trypsin treatment (APP<sub>770</sub> plus mitochondria plus trypsin lane). One or more mature bands, but no precursor APP<sub>770</sub> band. The APP within the mitochondria is inaccessible to the trypsin, whereas the precursor APP is accessible and fully cleaved. (iv) Pre-treatment of import reaction with valinomycin (APP<sub>770</sub> plus mitochondria plus trypsin plus valinomycin lane). No bands, as there is no energy to import APP. This

shows that the import of APP into mitochondria is energy-dependent.

In agreement with predictions, results showed (Figure 16) that there was one band present when the TnT reaction product was assayed (precursor APP), two main bands after mitochondrial import (precursor plus mature APP), one main band when trypsin was added to the import reaction (mature, mitochondrial APP), and no bands in the presence of valinomycin. The import reaction also showed evidence of much smaller bands. These may be proteolytic products of APP, suggesting that APP is processed within mitochondria. The results suggest that APP is targeted to and resides in mitochondria, where it may be further processed into smaller species.

#### **4.7.2 Dual color *in vivo* fluorescence microscopy of neuroblastoma cell line**

Chimeric APP-GFP products, expressed from the pEGFP-N1 plasmid (which contains no mitochondrial targeting sequence), were utilized to visualize whether APP transiently overexpressed in SK-N-SH neuroblastoma cells is located within mitochondria. Chimeric protein coding regions were created by in-framed fusion of APP with GFP in the vector, and five such constructs were designed as follows:

- i pEGFP-N1 alone
- ii pCMV/myc/mito/GFP (COX VIII mitochondrial cDNA, positive control encoding a mitochondrial targeting sequence) (Rizzuto *et al.*, 1992)
- iii pEGFP-N1/APP<sub>695/N-T1795</sub> (almost complete coding region)
- iv pEGFP-N1/APP<sub>695/N-T208</sub> (APP, NH<sub>2</sub>-terminal nucleotides 1-208)
- v mutant pEGFP-N1/APP<sub>ΔN-T</sub> (deletion mutant of APP<sub>695</sub> lacking nucleotides 1-

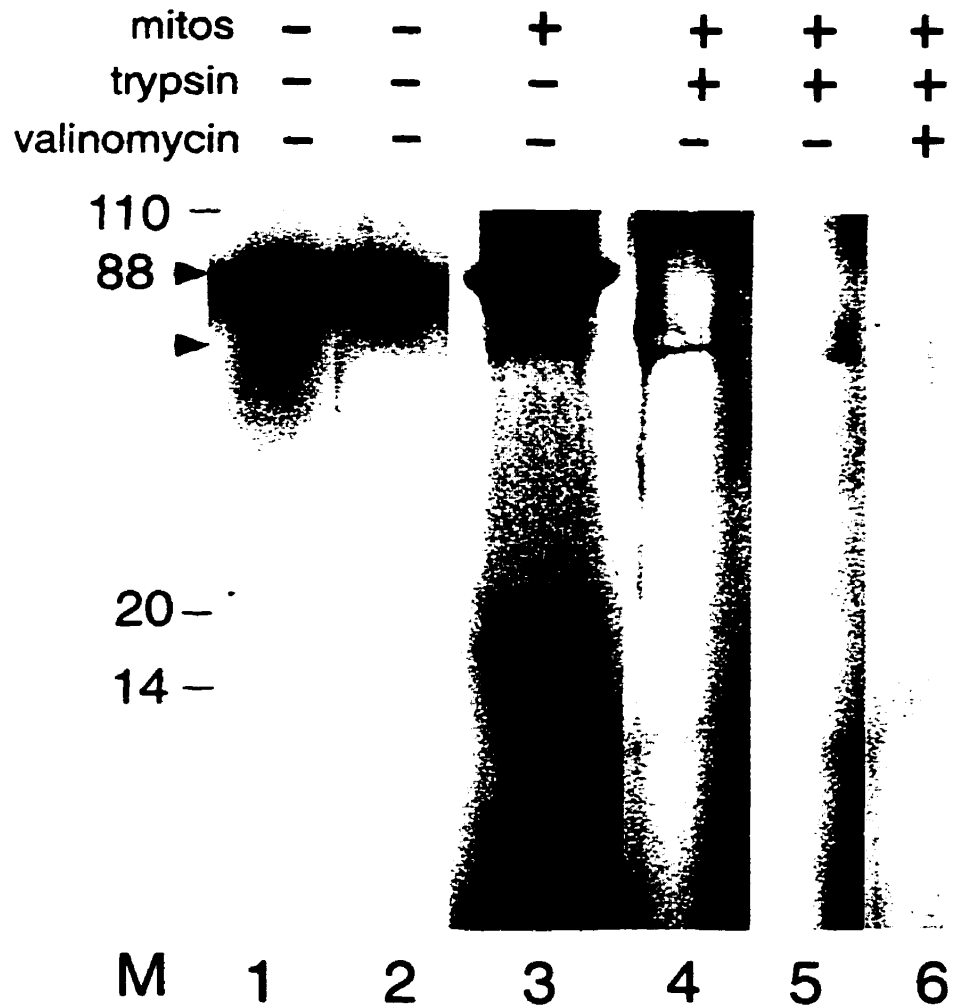


Figure 16 Mitochondrial import *in vitro*. Lane 1. Translation product of full-length APP<sub>770</sub> (i.e. <sup>35</sup>S-methionine-labelled APP). Lane 2. Same as Lane 1, loading 1/5. Lane 3 <sup>35</sup>S-APP in presence of mitochondria. Lane 4. <sup>35</sup>S-APP in presence of mitochondria and trypsin, 500 µg/ml. Lane 5. <sup>35</sup>S-APP in presence of mitochondria and trypsin, 250 µg/ml. Lane 6. <sup>35</sup>S-APP in presence of mitochondria and trypsin (400 µg/ml), preceded by valinomycin treatment.



111, i.e. the putative mitochondrial signal).

To isolate the APP<sub>695/N-T1795</sub> fragment, pGEM9zf/APP<sub>695/3207</sub> was restricted with EcoR 1. For pGEM9zf/APP<sub>695/3207</sub>, there are three EcoR 1 sites, at bps -15 of 5' UTR, plus 1795 and 2851 of the APP insert. Therefore, EcoR 1-restricted pGEM9zf/APP<sub>695/3207</sub> yielded three bands of 1.06 Kb, 1.81 Kb (= APP<sub>695/N-T1795</sub>), and 3.34 Kb (data not shown)

The pEGFP-N1 plasmid was amplified and verified by EcoR 1 restriction. There is one EcoR 1 site in the MCS of pEGFP-N1. Therefore, EcoR 1-restricted pEGFP-N1 yielded one band of 4.7 Kb (data not shown). Additional 2 Kb and 0.5 Kb supercoil bands were seen. The manufacturer stated that additional supercoil bands were a normal feature of the pEGFP-N1 plasmid. To re-verify pEGFP-N1, two more restrictions of pEGFP-N1 with EcoR 1 were carried out, the last restriction showing only the 4.7 Kb band (data not shown).

Following ligation of the APP<sub>695/N-T1795</sub> fragment into EcoR 1-restricted pEGFP-N1 to produce the pEGFP-N1/ APP<sub>695/N-T1795</sub> construct, an insert was verified by EcoR 1 restriction analysis. The pEGFP-N1/ APP<sub>695/N-T1795</sub> construct has two EcoR 1 sites, at each end of the APP insert. Therefore, EcoR 1-restricted pEGFP-N1/APP<sub>695/N-T1795</sub> yielded two bands of 1.8 Kb (APP<sub>695/N-T1795</sub>) and 4.7 Kb (pEGFP-N1) (data not shown).

To verify the correct orientation of the insert, the construct was restricted with BamH 1. There are two BamH 1 sites in the pEGFP-N1/APP<sub>N-T/1795</sub> construct, at bp 1329 of the APP insert, and in the MCS of pEGFP-N1, 3' to the APP insert. Therefore, BamH 1-restricted, correctly oriented pEGFP-N1/APP<sub>N-T/1795</sub> yielded two bands of 0.5 Kb and 6 Kb. BamH 1-restricted, incorrectly oriented pEGFP-N1/APP<sub>N-T/1795</sub> yielded two bands

of 1.4 Kb and 5.2 Kb. Once again supercoil bands were present that overlapped the expected bands, especially around the 0.4 Kb area (data not shown).

For further verification of the construct, the DNA was restricted separately with EcoR 1 and BamH 1. In order to get a better separation of the DNA bands, the small AGE was repeated with 1.6% agarose (Figure 17). The supercoil bands can now be differentiated from the expected bands.

The pEGFP-N1/APP<sub>695N-T208</sub> construct was prepared from pEGFP-N1/APP<sub>N-T/1795</sub> by restriction with Pst 1, followed by ligation of the linearized construct. EcoR 1 restriction analysis was used to verify the constructs, pEGFP-N1/APP<sub>695N-T208</sub> and pEGFP-N1. There is one EcoR 1 site in the MCS of each construct. Therefore, EcoR 1-restricted pEGFP-N1/APP<sub>695N-T208</sub> yielded one band of 4.9 Kb, and the EcoR 1-restricted pEGFP-N1 yielded one band of 4.7 Kb (Figure 18). Expected bands are seen, plus the 0.5 Kb supercoil artifact.

To compare the fluorescence pattern created by the chimeric proteins with that of the normal distribution of mitochondria, the neuroblastoma cells were also transfected with a plasmid that expresses GFP fused to a mitochondrial targeting sequence, pCMV/myc/mito/GFP. Following amplification of the pCMV/myc/mito/GFP plasmid, it was verified by Pst 1 restriction analysis. There is one Pst 1 site in the MCS of pCMV/myc/mito/GFP. Therefore, Pst 1-restricted pCMV/myc/mito/GFP yielded one band of 5.7 Kb (Figure 19).

SK-N-SH neuroblastoma cells were transiently transfected with the chimeric DNA constructs and pCMV/myc/mito/GFP. To determine the normal fluorescence

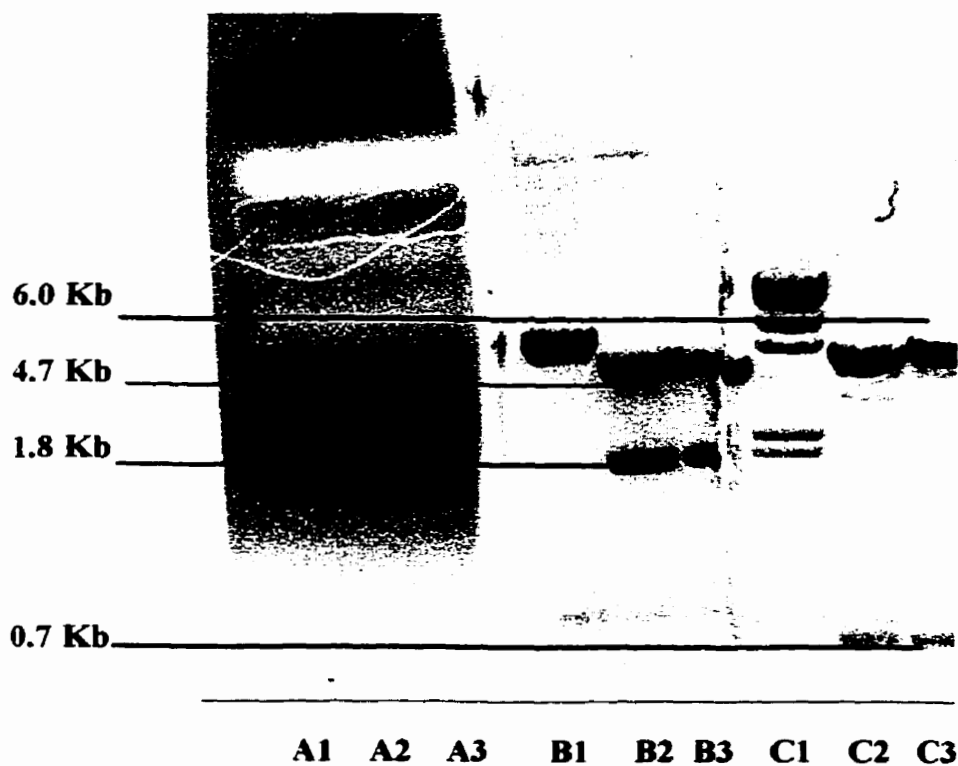


Figure 17 EcoR I & BamH I restriction of pEGFP-N1/APP<sub>695/N-T1795</sub> ligation constructs. Lanes A 1-3. Unrestricted pEGFP-N1. Lanes B 1-3. EcoR1-restricted pEGFP-N1/APP<sub>695/N-T1795</sub>. Lane C 1. High molecular weight DNA marker (Biorad). Lanes C 2-3. BamH I-restricted pEGFP-N1/APP<sub>695/N-T1795</sub>. DNA was stained with ethidium bromide in 1.6% agarose. Expected DNA bands can now be differentiated from supercoil artifacts.

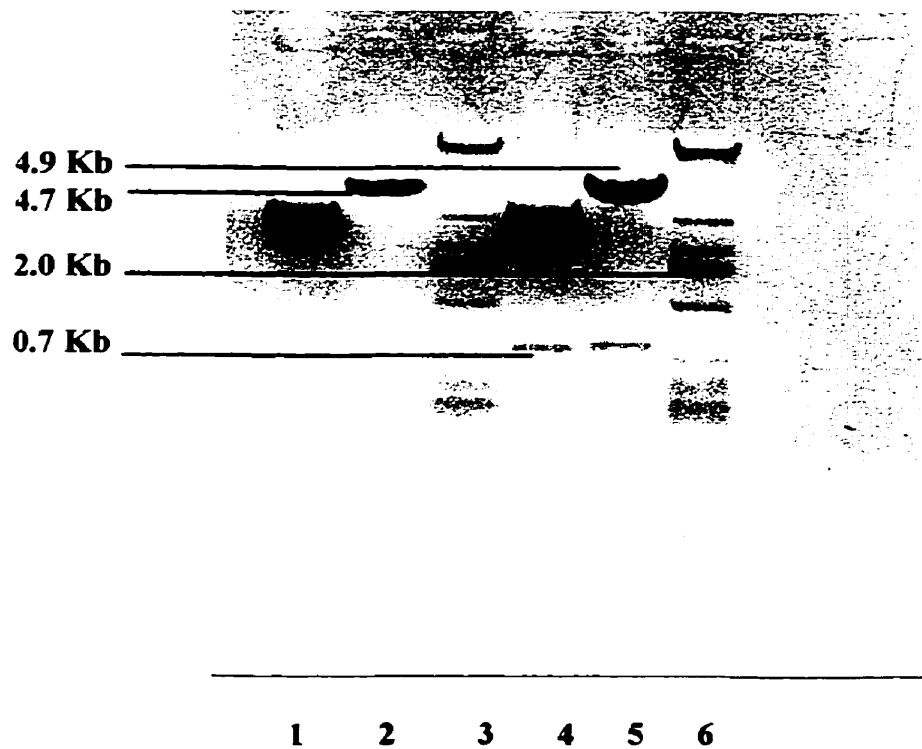


Figure 18 EcoR 1 restriction of pEGFP-N1 and pEGFP-N1/APP<sub>695/N-T208</sub>. Lane 1. Unrestricted pEGFP-N1. Lane 2. EcoR 1-restricted pEGFP-N1. Lanes 3 & 6. 1 Kb DNA ladder (Gibco BRL). Lane 4. Unrestricted pEGFP-N1/APP<sub>695/N-T208</sub>. Lane 5. EcoR 1-restricted pEGFP-N1/APP<sub>695/N-T208</sub>. The expected 4.7 Kb (pEGFP-N1) and 4.9 Kb (pEGFP-N1/APP<sub>695/N-T208</sub>) DNA bands are present. DNA stained with ethidium bromide in 0.8% agarose gel.

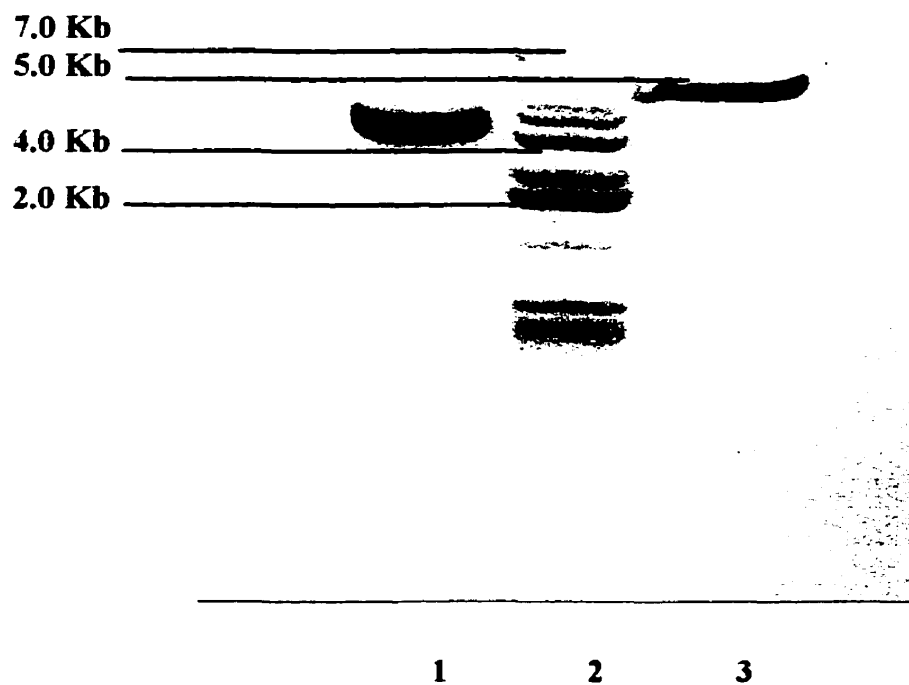


Figure 19 Pst I restriction of pCMV/myc/mito/GFP. Lane 1. Unrestricted pCMV/myc/mito/GFP. Lane 2. 1 Kb DNA ladder (Gibco BRL). Lane 3. Pst I-restricted pCMV/myc/mito/GFP. Stained with ethidium bromide in 0.8% agarose gel.

pattern of mitochondria in neuroblastoma cells, and to create the dual color overlay (green of GFP plus red of MitoTracker Red produces a yellow colour when overlaid), the cells were also treated with the with the mitochondrial probe, MitoTracker Red.

## **Results**

Uniform cytoplasmic and nuclear fluorescence was detected in pEGFP-N1 transfectants (Figure 20 a). pEGFP-N1/mito transfectants fluoresced in a punctated perinuclear pattern that co-localized with mitochondrial fluorescence within the same cell (Figure 20 b). Consistent with a mitochondrial location, pEGFP-N1/APP<sub>695/N-T1795</sub> localized to cytoplasmic areas of punctated fluorescence (Figure 20 c). pEGFP-N1/APP<sub>695/N-T208</sub> fluorescence was identical to that observed with pEGFP-N1/mito, strongly indicative of a mitochondrial location (Figure 20 d). Mutation of the NH<sub>2</sub>-terminal domain of APP (pEGFP-N1/APP<sub>ΔN-T</sub>) abolished mitochondrial fluorescence (Figure 20 e). These results indicate that the NH<sub>2</sub>-terminus of APP is capable of targeting this protein to mitochondria. These findings have also been verified in human teratocarcinoma-derived NT2 cells (Stratagene, data not shown). However, the resolution seen with this technique is not adequate to make a definitive claim, and therefore, future studies will involve the use of confocal microscopy.

### **4.7.3 Immunoelectron microscopy to detect endogenous APP and βAP in mammalian tissue**

To determine whether endogenous APP is found in mitochondria, mammalian

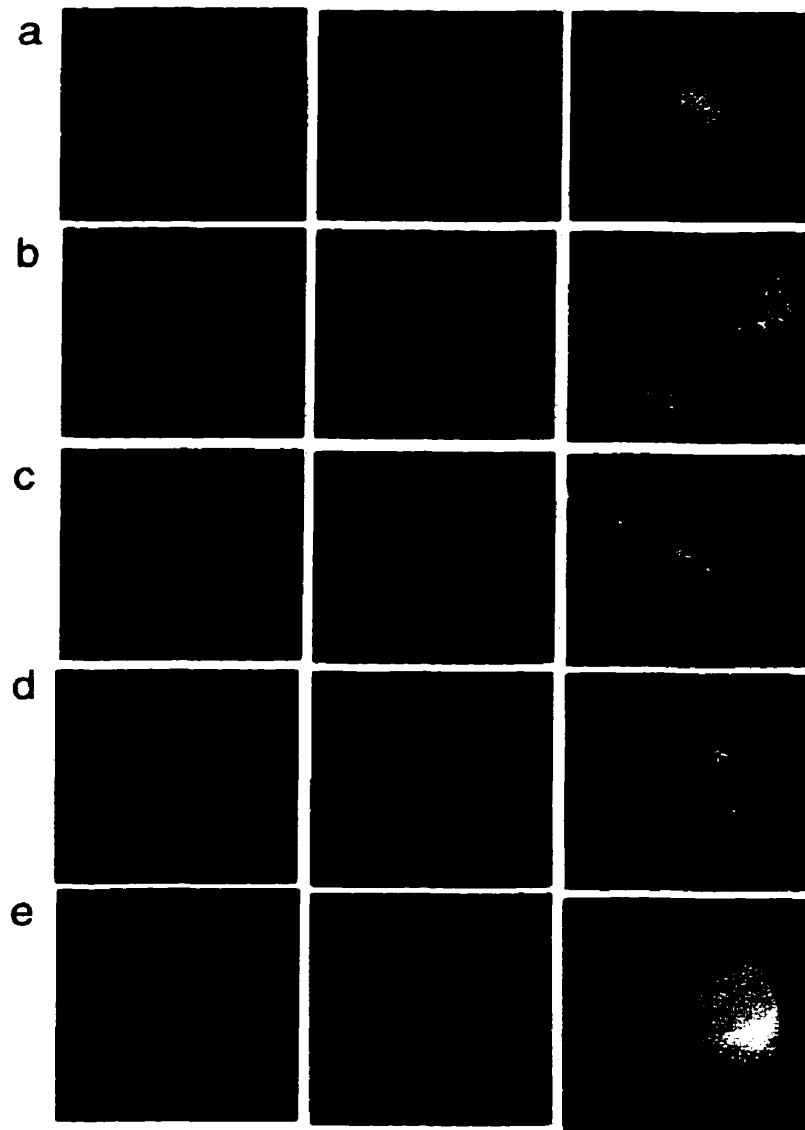


Figure 20 SK-N-SH neuroblastoma cell mitochondrial labelling. Cells were transiently transfected with pCMV/myc/mito/GFP or pEGFP-N1 or its APP fusion proteins, as well as being stained by MitoTracker Red. The first column indicates transient transfections with **a.** pEGFP-N1, **b.** pCMV/myc/mito/GFP, **c.** pEGFP-N1/APP<sub>695/N-T1795</sub>, **d.** pEGFP-N1/APP<sub>695/N-T208</sub>, **e.** pEGFP-N1/APP<sub>695/ΔN-T</sub>, in which pEGFP-N1 and its fusion proteins appear green. The second column represents the same neuroblastoma cells stained with MitoTracker Red, which appear red. The third column represents the above red and green superimposed images which, when green areas are directly superimposed on red images, produces a yellow colour, and indicates areas of the cell where pEGFP-N1 and its APP fusion proteins have localized.

tissue sections were examined by immunoelectron microscopy, using gold-conjugated antibodies to APP. Immunoelectron microscopy analysis confirmed the presence of APP associated with the mitochondrial cristae, the site of COX I localization in human, pig and rat brain tissues, plus human kidney tissues (Figure 21).

#### **4.7.4 Immunoelectron microscopy to detect endogenous APP and $\beta$ AP in AD and control brains**

Since AD is associated with a reduction in COX activity as well as over-accumulation of amyloidogenic fragments, it is possible that mitochondrial occupation by APP and  $\beta$ AP may be more marked in AD versus non-AD brains. To examine this, immunoelectron microscopy was performed to detect endogenous APP and  $\beta$ AP in brains of AD patients and non-AD controls. Results show that APP localized to mitochondria and other membrane-bound organelles in both AD (Figure 22 a) and non-AD sections (arrows indicate mitochondria). Forty to fifty percent of mitochondria retained at least three gold particles, and both membranous and luminal regions of mitochondria were seen to be labelled. However, there was no apparent difference in degree of APP labelling of mitochondria from AD and non-AD specimens.  $\beta$ AP had a similar distribution to that of APP, except that the frequency of  $\beta$ AP in mitochondria of AD sections (Figure 22 b) appeared to be higher than that of non-AD sections (Figure 22 c). This novel finding suggests, similar to the mitochondrial import assay results, that APP may be processed in mitochondria to release amyloidogenic peptides.



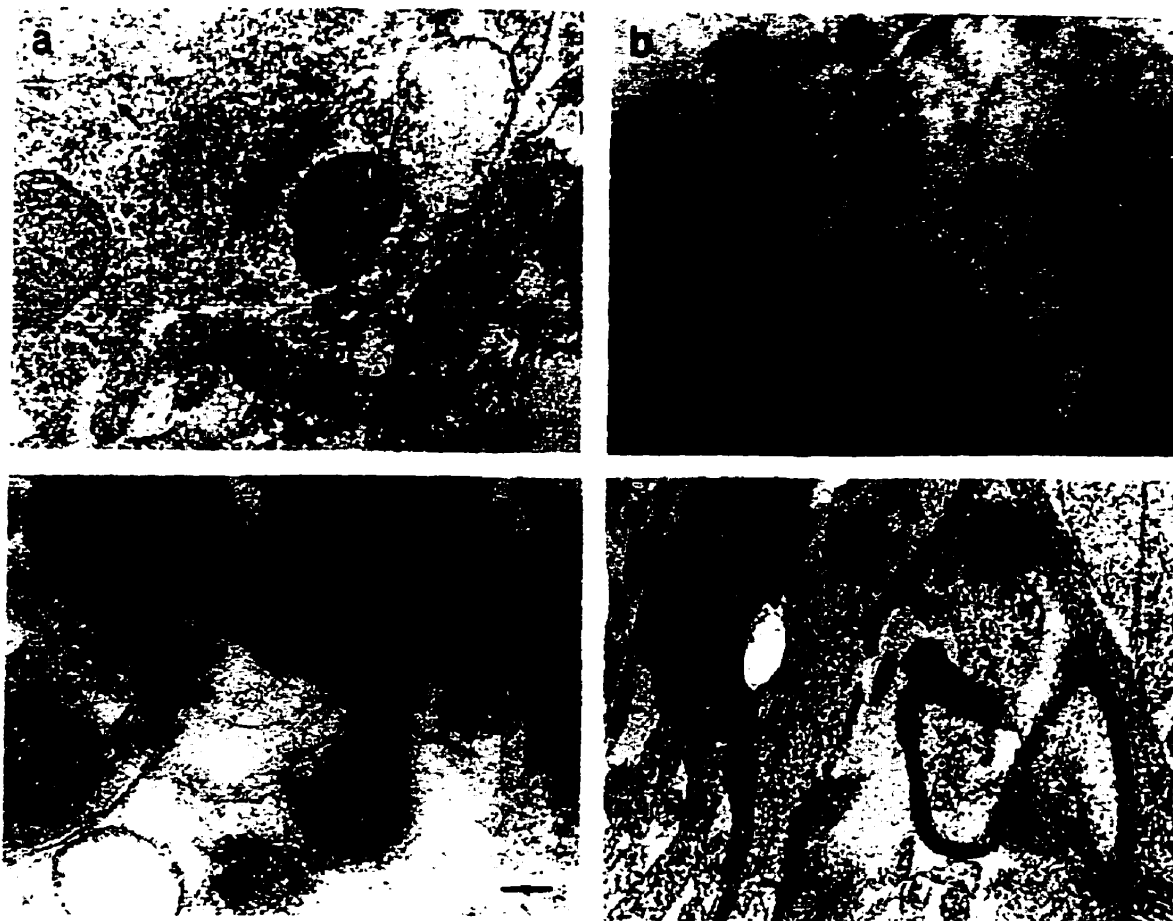


Figure 21 Localization of APP by immunoelectron microscopy in mammalian brain and kidney. **a.** Human brain, **b.** Human kidney, **c.** Pig brain, **d.** Rat brain. Visualization of APP was performed using mouse anti-human APP and goat, anti-mouse gold-conjugated IgG (gold particle size, 10 nm). Control sections were incubated with mouse anti-IgG. Labelling of APP is seen clearly by gold particles associated with the mitochondrial cristae (arrows). Scale bar: 1 cm = 5.0  $\mu\text{m}$  in (a), 0.16  $\mu\text{m}$  in (b), 0.24  $\mu\text{m}$  in (c), 3.4  $\mu\text{m}$  in (d). The images were enhanced in size 2.0-4.0 fold.

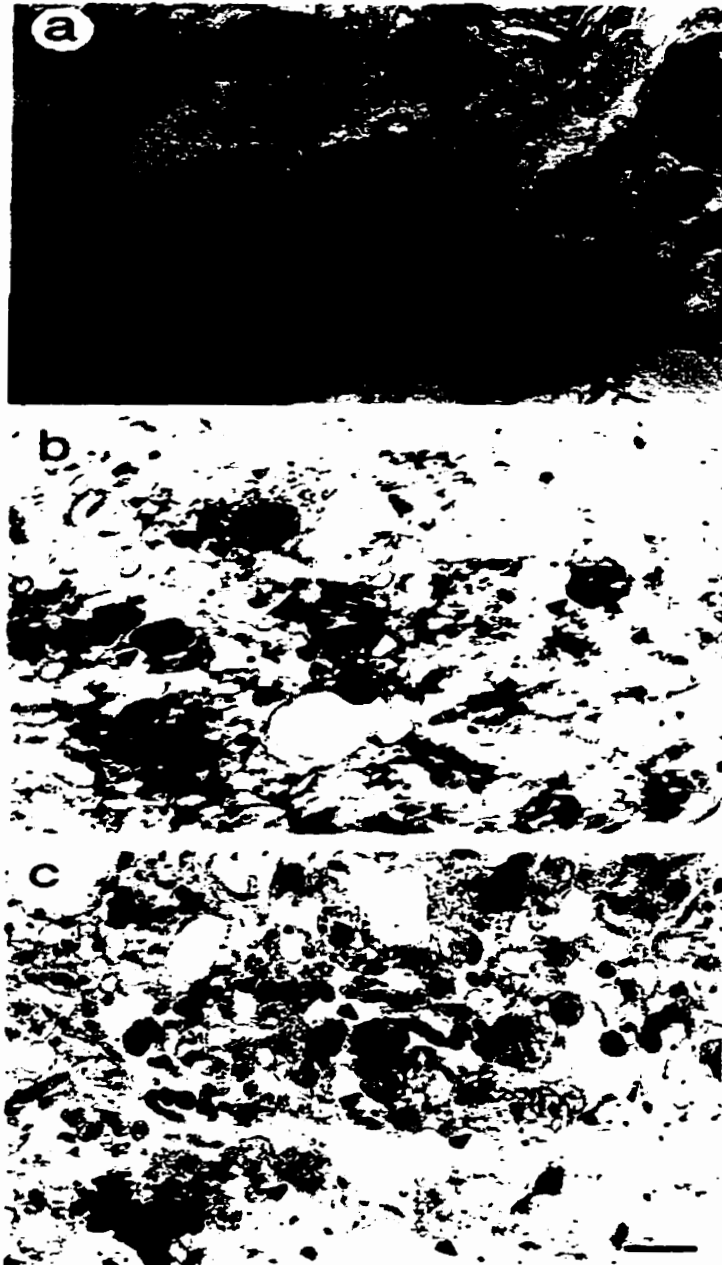


Figure 22 Localization of APP and  $\beta$ AP by immunoelectron microscopy in human AD and non-AD brain. **a.** Human brain, APP, **b.** AD brain,  $\beta$ AP, **c.** non-AD brain,  $\beta$ AP. Visualization of APP was performed using mouse anti-human APP and goat anti-mouse, gold-conjugated IgG (gold particle size, 10 nm). Control sections were incubated with mouse anti-IgG. Visualization of  $\beta$ AP was performed using rabbit anti- $\beta$ AP and goat anti-rabbit, gold conjugated IgG (gold particle size 5 nm). Labelling of APP is seen by gold particles associated with the mitochondria (arrows) and other membrane-bound organelles. Scale bar: the images were enhanced in size 2.0-4.0 fold.

## 5.0 DISCUSSION

The pathophysiology involved in AD is very complex, and incorporates an integration of developmental and late life events, encompassing genetic and environmental factors. It is clear several biochemical processes are involved in various converging pathways that lead to the histopathology of AD. Of these, deficits in energy metabolism appear to play a fundamental role.

Our results demonstrate, for the first time, that a protein of mitochondrial ETC-specific origin (COX I) (Davis *et al.*, 1994) interacts with a cytoplasmic membrane-bound protein (APP), and that APP and  $\beta$ AP may directly influence mitochondrial energy metabolism by their effects on COX. The ability of COX I to interact with APP appears to be distinct from this protein's life-sustaining role in oxidative respiration (Zhang *et al.*, 1990). Both APP and COX I are highly conserved and widely expressed in eukaryotes (Anderson *et al.*, 1981; Tanzi *et al.*, 1987; Yamada *et al.*, 1989). The fact that APP is expressed in most cells and that the APP gene promoter is similar to that of housekeeping genes (Salbaum *et al.*, 1988), suggests a fundamental role for this protein. For example, the presence of APP and  $\beta$ AP in mitochondria of non-AD brain suggests a role for these proteins in normal mitochondrial function. The APP-COX interaction may thus serve another conserved role, which could provide several links between energy metabolism with other aspects of AD, such as free radical and  $\beta$ AP generation that initiate neuronal apoptosis. The dysregulation of this mitochondrial-APP/ $\beta$ AP interaction may contribute to the pathogenesis of AD. If COX I binds specifically with APP, then overexpression

of APP may modulate the activity of COX I, thereby indirectly inhibiting COX, which will lead to deficits in energy metabolism. This is consistent with the findings that overexpression of APP in cultured human muscle fibres resulted in a specifically decreased COX activity and severe mitochondrial ultrastructural abnormalities (Askanas *et al.*, 1996). This mechanism may also be responsible for mitochondrial and COX abnormalities in the brains of AD patients. There is evidence that there are deficits in energy metabolism in the brains of patients with AD (Blass and Gibson, 1991).

Although proteolytic cleavage of APP generates the  $\beta$ AP species that are the main components of the NPs associated with neurotoxicity (LaFeria *et al.*, 1995), the detailed mechanism of the association between APP and neurodegeneration are not precisely defined. The present study was initiated to identify APP effector-binding proteins in the hope of deriving possible functions for APP. A yeast two-hybrid system assay showed cytochrome c oxidase subunit I, one of the catalytic subunits of Complex IV of the mitochondrial ETC, interacted with various APP isoforms (APP<sub>695</sub>, APP<sub>751</sub>, APP<sub>770</sub>), and that this interaction involved the extracellular domain of APP. The observed interaction between APP and COX I could have been non-specific, because COX causes frequent false positives in yeast two-hybrid systems (See [www.fccc.edu/research/labs.golemis/main.false.html](http://www.fccc.edu/research/labs.golemis/main.false.html)). As well, APP and COX I may not be in their native conformation, or be correctly post-translationally modified in yeast, and hence do not mimic metabolism in mammalian cells. In addition, there are no known examples of mitochondrial-specific enzymes interacting with membrane-bound receptor/proteins. However, due to the connection of APP and COX to AD, it was

**important to investigate this interaction further.**

**Due to the documented cases of deficits in energy metabolism and COX activity in AD, the determination of mechanisms by which a COX deficiency might develop in humans is of considerable clinical significance. This involves trying to define how APP could affect mitochondrial structure and function in AD. We propose that increased levels of APP in mitochondria of AD brain may have a causal relationship to the corresponding decreased COX activity (i.e. overexpression of APP causes a selective deficit of COX activity in AD brains). Therefore, it was important to investigate the relationship between APP accumulation and COX deficiency in mitochondria.**

**For APP to interact with a facultative mitochondrial protein, we postulate that the interaction takes place in the mitochondria, and that therefore, APP must be targeted to, and localized in, this organelle. In support of this theory, computer data base analysis of the APP leader peptide sequence suggested APP contains a possible mitochondrial targeting sequence. Based on this analysis, we tested our hypothesis that APP may also reside in mitochondria and under certain conditions, impair the activity of COX, and subsequently, the ETC.**

**A markedly reduced level of total COX activity in the cells overexpressing mitochondria-targeted APP was found when compared with other transfected constructs, including those transfected by a plasmid that caused generalized APP expression. In contrast, no significant change was observed for complex I activity between the SK-N-SH transfectants. It is noteworthy that nuclei-targeted APP or mitochondria-targeted  $\alpha$ -1 antichymotrypsin (a  $\beta$ AP plaque-associated protein) overexpression did not significantly**

affect COX activity in SK-N-SH stable transfectants. This suggests that the accumulation of APP in mitochondria plays a crucial role in specifically mediating decreased COX activity.

Because mechanisms of apoptosis that apply to neurodegeneration in general may also apply to AD (Smale *et al.*, 1995), and have been tied to defects in energy metabolism (Beal, 1995; Greenlund *et al.*, 1995), it was assessed whether APP-mediated decreased COX activity potentiates apoptosis in SK-N-SH neuroblastoma cell transfectants. There was a prominent and significant rise in apoptosis only in those neuroblastoma cells transfected with mitochondria-targeted APP, suggesting that overexpression of APP on its own may not be sufficient to induce apoptosis in neurons without the accumulation of APP in mitochondria.

The excessive production of ROS that ultimately leads to initiation of apoptosis has been suggested as the link between a generalized defect in bioenergetics and the pathogenesis of AD (Coyle and Puttfarcken, 1993). To determine the role of ROS in APP-mediated neuronal apoptosis, the levels of ROS were measured in neuroblastoma cells targeted with overexpression of APP. There was markedly increased ROS generation only in those cells stably transfected with mitochondria-targeted APP. Thus, it appears the generation of ROS by APP overexpression depends on an APP-mitochondrial association. Measuring lipid peroxidation, it was found that the increased free radical generation resulted in cellular damage in the neuroblastoma cell transfectants. However, the lipid peroxidation was only significantly elevated in the APP-mitochondria-targeted SK-N-SH transfectants. These results suggest that a defect in metabolism of ROS in

mitochondria-targeted APP overexpressing SK-N-SH cells leads to apoptosis, and that mitochondria are intimately involved in the process.

To assess the possibility that enhanced ROS production may be due to an APP-mediated effect on ROS scavenger enzymes, the activation of free radical scavenging enzymes, glutathione peroxidase and superoxide dismutase, was assessed. APP had no significant effect on the activity of glutathione peroxidase (Carmagnol *et al.*, 1983) in the stably transfected cells compared with control cells, but there was a significant increase in SOD activity (Nagi *et al.*, 1995) in the APP-targeted transfectants compared with other transfectants and control cells. Thus, only mitochondria-targeted APP once again had an effect. This action may be a sign of a compensatory response by the enzyme to increased ROS production.

For APP to interact with a mitochondrial enzyme, APP must be targeted to and localized in mitochondria. A classic *in vitro* mitochondrial import assay showed that an apparent precursor, <sup>35</sup>S-methionine-labeled APP, was imported into rat liver mitochondria in an energy-dependent manner, and that once in mitochondria it is cleaved into a shorter mature form. This assay seemed to also demonstrate the important finding that APP may be further processed in the mitochondria into shorter products.

Two APP constructs containing, respectively, the NH<sub>2</sub>-terminal 1795 and 208 base pairs, when transiently overexpressed in SK-N-SH neuroblastoma cells, created fluorescence patterns consistent with a mitochondrial location, while a mutant APP construct with the first 111 NH<sub>2</sub>-terminal base pairs deleted, showed a pattern of generalized localization. These results indicate, for the first time, that APP is targeted to

mitochondria, and that the NH<sub>2</sub> terminus of APP is capable of, and necessary for, this targeting (i.e. the NH<sub>2</sub> terminus of APP contains a mitochondrial targeting sequence). However, if this is the case, it is puzzling to me why in the previous experiments on stably transfected cells, the APP expressed from the pCI-neo/APP constructs did not also adversely affect the parameters measured (at least, not significantly). Although speculative, perhaps this is due to the different parameters being examined in the two experimental settings.

Because the resolution of the previous experiment was not sufficient to conclusively confirm the presence of APP in mitochondria, electron microscopy was next employed, and confocal microscopy will be employed in the future. Immunoelectron microscopy analysis, utilizing gold-conjugated antibodies, confirmed the presence of APP associated with the mitochondrial cristae, the site of COX localization, in human, pig, and rat brain and in human kidney. As AD is associated with a reduction in COX activity as well as over accumulation of amyloidogenic fragments, it is possible that mitochondrial occupation by APP and  $\beta$ AP may be more marked in AD versus non-AD brains. To examine this, immunoelectron microscopy in both AD and non-AD sections were performed. Forty to fifty percent of mitochondria retained at least three gold particles, and both membranous and luminal regions of mitochondria were seen to be labelled. However, there was no apparent difference in degree of APP labelling of mitochondria from AD and non-AD specimens.  $\beta$ AP had a similar distribution to that of APP, except that the frequency of  $\beta$ AP in mitochondria of AD sections appeared to be higher than that of non-AD sections, suggesting that, in AD, there may be enhanced



**amyloidogenic processing of APP inside mitochondria.**

**Our studies thus support the hypothesis that APP is targeted to mitochondria, probably the inner mitochondrial membrane, where its NH<sub>2</sub>-terminal domain interacts with COX I. We have also provided evidence for the link between APP metabolism and different features of AD, such as mitochondrial dysfunction (deficit in COX activity), oxidative stress (enhanced ROS levels and lipid peroxidation), and neuronal degeneration (lipid peroxidation and apoptosis). The results are consistent with the hypothesis that accumulation of APP in mitochondria could lead to aberrant APP-COX I interaction and, consequently, decreased COX activity. This, in turn, causes the enhanced generation of ROS levels and lipid peroxidation, leading to neuronal apoptosis. The alteration in energy metabolism may also alter the processing of APP and induce potentially amyloidogenic peptides (Gabuzda *et al.*, 1994), which cause and perpetuate a cycle of mitochondrial and cellular neuronal degeneration and apoptosis.**

**The mechanisms by which incomplete oxidation affects APP metabolism have remained unresolved. As suggested by our results, the direct interaction of COX I with APP and hence the close proximity of this interaction to the terminal ETC (Hill, 1994), may provide an immediate environment for the reaction of ROS with APP. This reaction may lead to abnormal processing of APP or, alternatively, the radical-induced formation of  $\beta$ AP. The interaction between COX I and APP could provide evidence of the direct involvement of COX I activity specifically in the metabolism of APP.**

**Alternatively, it could be argued that the accumulation of APP and  $\beta$ AP species in the brains of AD patients may only reflect a generalized accumulation of amyloid**

proteins in this condition. However, there was seen to be an apparent increase in mitochondrial  $\beta$ AP in sections from AD compared to non-AD brains. This suggests that there is enhanced amyloidogenic processing of APP in the mitochondria of AD patients.

Other unresolved features of AD, such as neuronal apoptosis, may also be related to the interaction between COX I and APP. This interaction may affect the release of cytochrome c, which is also coupled to COX, and thought to be critical in the cascade of events leading to apoptosis (Liu *et al.*, 1996; Kluck *et al.*, 1997; Yang *et al.*, 1997). It is known that caspases cleave APP to release an apoptosis-related, amyloidogenic peptide (Gervais *et al.*, 1999; Weidemann *et al.*, 1999), and that caspases are found in the mitochondria (Susin *et al.*, 1999; Krajewski *et al.*, 1999). The inner mitochondrial membrane may act as a site where the intra-membrane cleavage of APP occurs. Therefore, accumulation of APP in mitochondria could lead to abnormal processing of APP and increased generation of amyloidogenic peptides.

Although the function of APP in the brain is as yet unknown, an attractive hypothesis for the biological role for the APP-COX interaction may be that APP is involved in the translocation of COX I. Alternatively, because both APP<sub>751</sub> and APP<sub>770</sub> contain a 56 amino acid segment encoding a Kunitz protease inhibitor domain (KPI) (Kitaguchi *et al.*, 1990; Van Nostrand *et al.*, 1989) in addition to the APP<sub>695</sub> primary sequence, APP may be involved in the processing of non-assembled inner mitochondrial membrane proteins.

The localization of APP and  $\beta$ AP to mitochondria is novel and warrants further investigation into the function of these proteins in mitochondria. Several parameters

remain unresolved. For example, whether the pathophysiology is altered by the interaction of the different isoforms of APP and mutant APPs with COX I, and assessment of the functional importance of this interaction in AD. Nevertheless, our results have generated a molecular model that will be useful in studying the regulation of this interaction by neurological factors, and therapeutic drugs that interfere with the early stages of the disease.

In conclusion, we suggest that the events involved in the pathophysiology of AD can be tightly associated with deficits in energy metabolism through the interaction between APP and COX I.

## 6.0 REFERENCES

- Anderson S, Bankier AT, Barrell BG, de Bruijn MH, Coulson AR, Drouin J, Eperon IC, Nierlich DP, Roe BA, Sanger F, Schreier PH, Smith AJ, Staden R, Young IG. (1981) Sequence and organization of the human mitochondrial genome. *Nature*; 290(5806): 457-65.
- Anderson JP, Esch FJ, Keim PS, Sambamurti K, Lieberburg I, and Robakis NK. (1991) Exact cleavage site of Alzheimer amyloid precursor in neuronal PC-12 cells. *Neurosci. Lett.*; 128: 126-128.
- Anderson AJ, Pike CJ, and Cotman CW. (1995) Differential induction of immediate early gene proteins in cultured neurons by beta-amyloid (A beta): association of c-Jun with A beta-induced apoptosis. *J. Neurochem.*; 65: 1487-1498.
- Araujo D and Cotman C. (1992) Beta-amyloid stimulates glial cells in vitro to produce growth factors that accumulate in senile plaques in Alzheimer's disease. *Brain Res.*; 569: 141-145.
- Arispe N, Rojas J, and Pollard HB. (1993) Alzheimer disease amyloid  $\beta$  protein forms calcium channels in bilayer membranes: blockade by tromethamine and aluminium. *Proc. Nat. Acad. Sci.*; 90: 567-571.
- Askanas V, McFerrin J, Baque S, Alvarez RB, Sarkozi E, and Engel WK. (1996) transfer of  $\beta$ -amyloid precursor proetain gene using adenovirus vector causes mitochondrial abnormalities in cultured normal human muscle. *Proc. Nat. Acad. Sci.*; 93: 1314-1319.
- Barnes NY, Li L, Yoshikawa K, Schwartz LM, Oppenheim RW, and Milligan CE. (1998) Increased production of amyloid precursor protein provides a substrate for caspase-3 in dying motoneurons. *J. Neurosci.*; 18: 5869-5880.
- Beal MF. (1992) Does impairment of energy metabolism result in excitotoxic neuronal death in neurodegenerative illnesses? *Ann. Neurol.*; 31: 119-130.
- Beal MF. (1995) Aging, energy, and oxidative stress in neurodegenerative diseases. *Ann. Neurol.*; 38: 357-366.
- Beal MF. (1997) New techniques for investigating mitochondrial DNA in neurodegenerative diseases. *Neurology*; 49: 907-908.
- Behl C, Davis J, Cole GM, and Schubert D. (1992) Vitamin E protects nerve cells from amyloid  $\beta$  protein toxicity. *Biochem. Biophys. Res. Commun.*; 186: 944-952.

- Behl C, Davis JB, Lesley R, and Schubert D. (1994 a) Hydrogen peroxide mediates amyloid  $\beta$ -protein toxicity. *Cell*; 77: 817-827.
- Behl C, Davis JB, Klier FG, and Schubert D. (1994 b) Amyloid  $\beta$  protein induces necrosis rather than apoptosis. *Brain Res.*; 645: 253-264.
- Bennett MC, Diamond DM, Stryker SC, Parks JK, and Parker WD. (1992) Cytochrome oxidase inhibition: a novel animal model of Alzheimer's disease. *J. Geriatr. Psychiatry Neurol.*; 5; 93-101.
- Benveniste H, Dreyer J, Schousboe A, and Diemer NH. (1984) Elevation of the extracellular concentrations of glutamate and aspartate in rat hippocampus during transient cerebral ischemia monitored by intracerebral microdialysis. *J. Neurochem.*; 43: 1369-1374.
- Benzi G and Moretti A.(1995) Are reactive oxygen species involved in Alzheimer's disease? *Neurobiol. Aging*; 16: 661-674.
- Blass JP, Sheu RK-F, and Cedarbaum JM. (1988) Energy metabolism in disorders of the nervous system. *Rev. Neurol.*; 144: 534-563.
- Blass JP and Gibson GE. (1991) The role of oxidative abnormalities in the pathophysiology of Alzheimer's disease. *Rev. Neurol.*; 147: 513-525.
- Breen KC, Bruce M, and Anderton BH. (1991) Beta amyloid precursor protein mediates neuronal cell-cell and cell-surface adhesion. *Neurosci. Res.*; 28(1): 90-100.
- Brustovetsky N and Klingenberg M. (1996) Mitochondrial ADP/ATP carrier can be reversibly converted into a large channel by  $Ca^{2+}$ . *Biochemistry*; 35(26): 8483-8488.
- Busciglio J, Gabuzda DH, Matsudaira P, and Yankner BA. (1993) Generation of beta-amyloid in the secretory pathway in neuronal and nonneuronal cells. *Proc. Nat. Acad. Sci.*; 90(5): 2092-2096.
- Busciglio J and Yanker B (1995) Apoptosis and increased generation of reactive oxygen species in Down's syndrome neurons *in vitro*. *Nature*; 378:776-779.
- Caporaso GL, Gandy SE, Buxbaum JD, and Greengard P. (1992) Chloroquine inhibits intracellular degradation but not secretion of Alzheimer beta/A4 amyloid precursor protein. *Proc. Nat. Acad. Sci.*; 89(6): 2252-2256.
- Carmagnol F, Sinet PM, and Jerome H. (1983) Selenium-dependent and non-selenium-dependent glutathione peroxidases in human tissue extracts. *Biochimica et Biophysica Acta*; 759: 49-57.

- Casari G, De Fusco M, Ciamatori S, Zeviani M, Mora M, Fernandez P, De Michele G, Filla A, Coccozza S, Marconi R, Durr A, Fontaine B, and Ballabio A. (1998) Spastic paraplegia and OXPHOS impairment caused by mutations in paraplegin, a nuclear-encoded mitochondrial metalloprotease. *Cell*; 93(6): 973-983.
- Chandrasekaran K, Giordano T, Brady DR, Stoll J, Martin LJ, and Rapoport SI. (1994) Impairment in mitochondrial cytochrome oxidase gene expression in Alzheimer disease. *Brain Res. Mol. Brain Res.*; 24(1-4): 336-40 .
- Chandrasekaran K, Hatanpaa K, Brady DR, Stoll J, and Rapoport SI. (1998) Downregulation of oxidative phosphorylation in Alzheimer disease: loss of cytochrome c oxidase subunit mRNA in the hippocampus and entorhinal cortex. *Brain Res.*; 796(1-2): 13-19.
- Chandrasekaran K, Hatanpaa K, Brady DR, and Rapoport SI. (1996) Evidence for physiological down-regulation of brain oxidative phosphorylation in Alzheimer's disease. *Exp. Neurol.*; 142(1): 80-88.
- Chandrasekaran K, Hatanpaa K, Rapoport SI, and Brady DR. (1997) Decreased expression of nuclear and mitochondrial DNA-encoded genes of oxidative phosphorylation in association neocortex in Alzheimer disease. *Brain Res. Mol. Brain Res.*; 44(1): 99-104.
- Chartier-Harlin MC, Crawford F, Houlden H, Warren A, Hughs D, Fidani L, Goate A, Rossor M, Roques P, Hardy J, and Mullan M. (1991) Early-onset Alzheimer's disease caused by mutations at codon 717 of the  $\beta$ -amyloid precursor protein gene. *Nature*; 353: 844-846.
- Chow N, Korenberg JR, Chen XN, and Neve RL. (1996) APP-BP1, a novel protein that binds to the carboxy-terminal region of the amyloid precursor protein. *J. Biol. Chem.*; 271(19): 11339-11346.
- Christie RH, Freeman M, and Hyman BT. (1996) Expression of the macrophage scavenger receptor, a multifunctional lipoprotein receptor, in microglia associated with senile plaques in Alzheimer's disease. *Am. J. Pathol.*; 148(2): 399-403
- Cohen ML, Golde TE, Usiak MF, Younkin LH, and Younkin SG. (1988) In situ hybridization of nucleus basalis neurons shows increased beta-amyloid mRNA in Alzheimer disease. *Proc. Nat. Acad. Sci.*; 85(4):1227-1231.
- Cordell B. (1994) beta-Amyloid formation as a potential therapeutic target for Alzheimer's disease. *Annu. Rev. Pharmacol. Toxicol.*; 34:69-89.

- Corder EH, Saunders AM, Strittmatter WJ, et al. (1993) Gene dose of apolipoprotein E type 4 allele and the increased risk of Alzheimer's disease in late-onset families. *Science*; 261: 921-923.
- Cotman CW and Su JH. (1996) Mechanisms of neuronal death in Alzheimer's disease. *Brain Pathol.*; 6: 493-506.
- Cotman C and Anderson A. (1995) A potential role for apoptosis in neurodegeneration and Alzheimer's disease. *Mol. Neurobiol.*; 10: 19-45.
- Coyle JT and Puttfarcken P. (1993) Oxidative stress, glutamate, and neurodegenerative disorders. *Science*; 262: 689-695.
- Cummings JL, Vinters HV, Cole GM, and Khachaturian ZS. (1998) Alzheimer's disease: Etiologies, pathophysiology, cognitive reserve, and treatment opportunities. *Neurology*; 51: S2-S17.
- Curti D, Rognoni F, Gasparini L, Cattaneo A, Paolillo M, Racchi M, Zani L, Bianchetti A, Trabucchi M, Bergamaschi S, and Govoni S. (1997) Oxidative metabolism in cultured fibroblasts derived from sporadic Alzheimer's disease (AD) patients. *Neurosci. Lett.*; 236(1):13-6.
- Danks D. (1983) Hereditary disorders of copper metabolism in Wilson's disease and Menke's disease, in *The Metabolic Basis of Inherited Disease*, edition 5, Stanbury JB, Wyngaarden JB, Fredricksen DS, Golstein JL, Brown MS, eds. (McGraw-Hill New York), pp. 1261-1266.
- Davis PW Jr., Parks J, Filley CM, and Kleinschmidt-De Masters BK. (1994) Electron transport chain defects in Alzheimer's disease brain. *Neurol.*; 44: 1090-1096.
- Davis J, McMurray H, and Schubert D. (1992) The amyloid beta-protein of Alzheimer's disease is chemotactic for mononuclear phagocytes. *Biochem. Biophys. Res. Commun.*; 189(2): 1096-1100.
- De Strooper B, Umans L, Van Leuven F, and Van Den Berghe H. (1993) Study of the synthesis and secretion of normal and artificial mutants of murine amyloid precursor protein (APP): cleavage of APP occurs in a late compartment of the default secretion pathway. *J. Cell Biol.*; 121(2): 295-304.
- Devereux J, Haerberli P, and Smithines O. (1984) A comprehensive set of sequence analysis programs for VAX. *Nucleic Acid Res.*; 12: 387-395.

- Dewji NN and Singer SJ. (1996) Specific transcellular binding between membrane proteins crucial to Alzheimer's disease. *Proc. Nat. Acad. Sci.*; 93: 12575-12580.
- Dewji NN and Singer SJ. (1997) The seven-transmembrane-spanning topography of the Alzheimer disease-related presenilin proteins in the plasma membranes of cultured cells. *Proc. Nat. Acad. Sci.*; 94: 14025-14030.
- Dumuis A, Sebben M, Haynes H, Pin JP, and Bockaert J. (1988) NMDA receptors activate the arachidonic acid cascade system in striatal neurons. *Nature*; 336: 68-78.
- Dyrks T, Dyrks E, Hartmann T, Masters C, and Beyreuther K. (1992) Amyloidogenicity of  $\beta$ A4 and  $\beta$ A4-bearing amyloid protein precursor fragments by metal-catalysed oxidation. *J. Biol. Chem.*; 267: 18210-18217.
- Dyrks T, Weidemann A, Multhaup G, Salbaum JM, Lemaire HG, Kang J, Muller-Hill B, Masters CL, and Beyreuther K. (1988) Identification, transmembrane orientation and biogenesis of the amyloid A4 precursor of Alzheimer's disease. *EMBO J.*; 7(4): 949-957.
- Earnshaw WC. (1999) Apoptosis. A cellular poison cupboard. *Nature*; 397: 387-389.
- Edland SD, Silverman JM, Peskind ER, Tsuang D, Wijsman E, and Morris JC. (1996) Increased risk of dementia in mothers of Alzheimer's disease cases. *Neurology*; 47: 254-256.
- El Khoury J, Hickman SE, Thomas CA, Cao L, Silverstein SC, and Loike JD. (1996) Scavenger receptor-mediated adhesion of microglia to  $\beta$ -amyloid fibrils. *Nature*; 382: 716-719.
- Esch FS, Keim PL, Beattie EC, Blacher RW, Culwell AR, Oltersdorf T, McClure D, and Ward PJ. (1990) Cleavage of amyloid beta peptide during constitutive processing of its precursor. *Science*; 248: 1122-1124.
- Estus S, Golde TE, Kunishita T, Blades D, Lowery D, Eisen M, Usiak M, Qu X, Tabira T, Greenberg BD, and Younkin SG. (1992) Potentially amyloidogenic, carboxyl-terminal derivatives of the amyloid protein precursor. *Science*; 255: 726-728.
- Forloni G, Bugiani O, Tagliavini F, and Salmona M. (1996) Apoptosis-mediated neurotoxicity induced by beta-amyloid and PrP fragments. *Mol. Chem. Neuropathol.*; 28: 163-171.
- Forloni G, Chiesa R, Smioldo S, Verga L, Salmona M, Tagliavini F, and Angeretti N. (1993) Apoptosis mediated neurotoxicity induced by chronic application of beta



amyloid fragment 25-35. *Neuro Report*; 4: 523-526.

Fuller SJ, Storey E, Li QX, Smith AI, Beyreuther K, and Masters CL. (1995) Intracellular production of  $\beta$ A4 amyloid of Alzheimer's disease: modulation by phosphoramidon and lack of coupling to the secretion of the amyloid precursor protein. *Biochem.*; 34: 8091-8098.

Furukawa K, Barger SW, Blalock EM, and Mattson MP. (1996) Activation of K<sup>+</sup> channels and suppression of neuronal activity by secreted  $\beta$ -amyloid precursorprotein. *Nature*; 379: 74-78.

Gabuzda D, Busciglio J, Chen LB, Matsudaira P, and Yankner BA. (1994) Inhibition of energy metabolism alters the processing of amyloid precursor protein and induces a potentially amyloidogenic derivative. *J. Biol. Chem.*; 269(18): 13623-13628.

Gabuzda D, Busciglio J, and Yankner BA. (1993) Generation of a potential precursor of beta amyloid from immature APP in the secretory pathway. *Soc. Neurosci. Abstr.*; 19: 19.

Games D, Adams D, Alessandrini R, Barbour R, Berthelette P, Blackwell C, Carr T, Clemens J, Donaldson T, Gillespie F, *et al.* (1995) Alzheimer-type neuropathology in transgenic mice overexpressing V717F beta-amyloid precursor protein. *Nature*; 373: 523-527.

Gasparini L, Racchi M, Benussi L, Curti D, Binetti G, Bianchetti A, Trabucchi M, and Govoni S. (1997) Effect of energy shortage and oxidative stress on amyloid precursor protein metabolism in COS cells. *Neurosci. Lett.*; 231(2):113-117.

Gavel Y and von Heijne G. (1990) Cleavage-site motifs in mitochondrial targeting peptides. *Protein Eng.*; 4(1): 33-37.

Gervais FG, Xu D, Robertson GS, Vaillancourt JP, Zhu Y, et al. (1999) Involvement of caspases in proteolytic cleavage of Alzheimer's amyloid- $\beta$  precursor protein and amyloidogenic A $\beta$  peptide formation. *Cell*; 97: 395-406.

Gibson GE, Sheu KF, and Blass JP. (1998) Abnormalities of mitochondrial enzymes in Alzheimer disease. *J. Neural. Transm.*; 105(8-9): 855-70.

Giulivi C, Poderoso JJ, and Boveris A. (1998) Production of nitric oxide by mitochondria. *J. Biol. Chem.*; 273(18): 11038-11043.

Glenner GG and Wong CW. (1984 a) Alzheimer's disease and Down's syndrome: sharing of a unique cerebrovascular amyloid fibril protein. *Biochem. Biophys. Res. Commun.*; 122(3): 1131-1135.

- Glennner GG and Wong CW. (1984 b) Alzheimer's disease: initial report of the purification and characterization of a novel cerebrovascular amyloid protein. *Biochem. Biophys. Res. Commun.*; 120(3): 885-890.**
- Glick BS. (1992) Protein import into isolated yeast mitochondria. *Methods in Cell Biol.*; 34: 389-399.**
- Glick BS, Brandt A, Cunningham K, Muller S, Hallberg RL, and Schatz G. (1992) Cytochromes c<sub>1</sub> and b<sub>2</sub> are sorted to the intermembrane space of yeast mitochondria by a stop-transfer mechanism. *Cell*; 69: 809-822.**
- Goate A, Chartier-Harlin MC, Mullan M, Brown J, Crawford F, Fidani L, Giuffra L, Haynes A, Irving N, James L, Mant R, Newton P, Rooke K, Roques P, Talbot C, Pericak-Vance M, Roses A, Williamson R, Rossor M, Owen M, and Hardy J, (1991) Segregation of a missense mutation in the amyloid precursor protein with familial Alzheimer's disease. *Nature*; 349: 704-706.**
- Goedert M. (1993) Tau protein and the neurofibrillary pathology of Alzheimer's disease. *Trends Neurosci.*; 16(11): 460-465.**
- Golde TE, Estus S, Younkin LH, Selkoe DJ, and Younkin SG. (1992) Processing of the amyloid protein precursor to potentially amyloidogenic derivatives. *Science*; 255: 728-730.**
- Gomez-Isla T, Hollister R, West H, et al. (1997) Neuronal loss correlates with but exceeds neurofibrillary tangles in Alzheimer's disease. *Ann. Neurol.*; 41: 17-24.**
- Gomez-Isla T, West HL, Rebeck GW, et al. (1996) Clinical and pathological correlates of apolipoprotein E  $\epsilon$ -4 in Alzheimer's disease. *Ann. Neurol.*; 39: 62-70.**
- Good PF, Werner P, Hsu A, Olanow CW, and Perl DP. (1996) Evidence of neuronal oxidative damage in Alzheimer's disease. *Am. J. Pathol.*; 149(1): 21-28.**
- Govoni S, Bergamaschi S, Gasparini L, et al. (1996) Fibroblasts of patients affected by Down's syndrome oversecrete amyloid precursor protein and are hyporesponsive to protein kinase c stimulation. *Neurology*; 47: 1069-1075.**
- Green DR and Reed JC. (1998) Mitochondria and apoptosis. *Science*; 281: 1309-1312.**
- Greenlund LJS, Deckwerth TL, and Johnson EM. (1995) Superoxide dismutase delays neuronal apoptosis: a role for reactive oxygen species in programmed cell death. *Neuron*; 14: 303-331.**

- Guo Q, Fu W, Luo H, Sells SF, Geddes JW, Bondada V, Rangnekar VM, and Mattson MP. (1998) Par-4 is a mediator of neuronal degeneration associated with the pathogenesis of Alzheimer disease. *Nat. Med.*; 4(8): 957-962.
- Haass C and Selkoe DJ. (1993) Cellular processing of beta-amyloid precursor protein and the genesis of amyloid beta-peptide. *Cell*; 75: 1039-1042.
- Haass C, Hung AY, Schlossmacher MG, Teplow DB, and Selkoe DJ. (1993) beta-Amyloid peptide and a 3-kDa fragment are derived by distinct cellular mechanisms. *J. Biol. Chem.*; 268(5): 3021-3024.
- Halliwell B and Gutteridge JMC, (1989) in *Free Radicals in Biology and Medicine* (Clarendon press, Oxford), edition 2, pp 1-81.
- Hardy J. (1997) Amyloid, the presenilins, and Alzheimer's disease. *Trends neurosci.*; 20: 154-159.
- Hardy JA and Higgins GA. (1992) Alzheimer's disease: The amyloid cascade hypothesis. *Science*; 256: 184-185.
- Harman D. (1995) Free radical theory of aging: Alzheimer's disease pathogenesis. *Age*; 18: 97-119.
- Hartmann T, Bieger SC, Bruhl B, Tienari PJ, Ida N, Allsop D, Roberts GW, Masters CL, Dotti CG, Unsicker K, and Beyreuther K. (1997) Distinct sites of intracellular production for Alzheimer's disease A beta40/42 amyloid peptides. *Nature Med.*; 3: 1016-1020.
- Hartung HP, Kladetzky RG, Melnik B, Hennerici M, *et al.* (1986) Stimulation of the scavenger receptor on monocytes-macrophages evokes release of arachidonic acid metabolites and reduced oxygen species. *Lab. Invest.*; 55: 209-216.
- Hensley K, Carney JM, Mattson MP, Aksenova M, Harris M, Wu JF, Floyd RA, and Butterfield DA. (1994) A model for  $\beta$ -amyloid aggregation and neurotoxicity based on free radical generation by the peptide: relevance to Alzheimer disease. *Proc. Nat. Acad. Sci.*; 91: 3270-3274.
- Higgins GA, Lewis DA, Bahmanyar S, Goldgaber D, Gajdusek DC, Young WG, Morrison JH, and Wilson MC. (1988) Differential regulation of amyloid- $\beta$ -protein mRNA expression within hippocampal neuronal subpopulations in Alzheimer disease. *Proc. Nat. Acad. Sci.*; 85: 1297-1301.
- Hill BC. (1994) Modeling the sequence of electron transfer reactions in the single turnover of reduced mammalian cytochrome c oxidase with oxygen. *J. Biol.*

*Chem.*; 269: 2419-2425.

Hockenbery DM, Oltval ZN, Yin X, Milliman CL, and Korsmeyer SJ. (1993) Bcl-2 functions in an antioxidant pathway to prevent apoptosis. *Cell*; 75: 241-251.

Howell N, Kubacka I, Xu M, and McCullough DA. (1991) Leber's hereditary optic neuropathy: involvement of the mitochondrial ND1 gene and evidence for an intragenic suppressor mutation. *Am. J. Hum Genet.*; 48: 935-942.

Hoyer S. (1993) Brain oxidative energy and related metabolism, neuronal stress, and Alzheimer's disease: A speculative hypothesis. *J. Geriatric Psychiatry. Neurol.*; 6: 3-13.

Huber S, Martin JR, Loffler J, and Moreau JL. (1993) Involvement of amyloid precursor protein in memory formation in the rat: an indirect antibody approach. *Brain Res.*; 603: 348-352.

Hurtley SM. (1998) Neurodegeneration. *Science*; 282: 1071.

Hyman BT. (1992) Down syndrome and Alzheimer disease. *Prog. Clin. Biol. Res.*; 379: 123-142.

Ikezu T, Trapp BD, Song KS, Schlegal A, Lisanti MP, and Okamoto T. (1998) Caveolae, plasma membrane microdomains for alpha-secretase-mediated processing of the amyloid precursor protein. *J. Biol. Chem.*; 273: 10485-10495.

Ishii K, Sasaki M, Kitagaki H, Yamaji S, Sakamoto S, Matsuda K, and Mori E. (1997) Reduction of cerebellar glucose metabolism in advanced Alzheimer's disease. *J. Nucl. Med.*; 38(6): 925-928.

Itagaki T, Itoh Y, Sugai Y, Suematsu N, Ohtomo E, and Yamada M. (1996) Glucose metabolism and Alzheimer's dementia. *Nippon Ronen Igakkai Zasshi, Abstr.*; 33(8): 569-72.

Iverfeldt K, Walaas SI, and Greengard P. (1993) Altered processing of Alzheimer amyloid precursor protein in response to neuronal degeneration. *Proc. Nat. Acad. Sci.*; 90: 4146-4150.

Iwatsubo T, Odaka A, Suzuki N, Mizusawa H, Nukina N, and Ihara Y. (1994) Visualization of A beta 42(43) and A beta 40 in senile plaques with end-specific A beta monoclonals: evidence that an initially deposited species is A beta 42(43). *Neuron*; 13: 45-53.

- Jarrett JT, Berger EP, and Lansbury PT (1993) The carboxy terminus of the beta amyloid protein is critical for the seeding of amyloid formation: implications for the pathogenesis of Alzheimer's disease. *Biochemistry*; 32(18): 4693-4697.
- Jarrett JT and Lansbury PT. (1993) Seeding "one-dimensional crystallization" of amyloid: a pathogenic mechanism in Alzheimer's disease and scrapie? *Cell*; 73:1055-1058.
- Jin LW, Ninomia H, Roch JM, Schubert D, Masliah E, Otero DAC, and Saito T. (1994) Peptides containing the RERMS sequence of amyloid beta/A4 protein precursor bind cell surface and promote neurite extension. *J. Neurosci.*; 14(9): 5461-5470.
- Johnson SA, McNeill T, Cordell B, and Finch CE. (1990) Relation of neuronal APP-751/APP-695 mRNA ratio and neuritic plaque density in Alzheimer's disease. *Science*; 248: 854-856.
- Kang J, Lemaire HG, Unterbeck A, Salbaum JM, Masters CL, Grzeschik KH, Multhaup G, Beyreuther K, and Muller-Hill B. (1987) The precursor of Alzheimer's disease amyloid A4 protein resembles a cell-surface receptor. *Nature*; 325: 733-736.
- Katchman A and Hershkowitz N. (1993) Early anoxia-induced vesicular glutamate release results from mobilization of calcium from intracellular stores. *J. Neurophysiol.*; 70(1): 1-7.
- Katzman R. (1986) Alzheimer's disease. *N. Eng. J. Med.*; 314: 964-973.
- Keller JN, Pang Z, Geddes JW, Begley JG, Germeyer A, Waeg G, and Mattson MP. (1997) Impairment of glucose and glutamate transport and induction of mitochondrial oxidative stress and dysfunction in synaptosomes by amyloid beta-peptide: role of lipid peroxidation product 4-hydroxynonenal. *J. Neurochem.*; 69(1): 273-284.
- Keller JN, Pang Z, Geddes JW, Begley JG, Germeyer A, Waeg G, and Mattson MP. (1997) Impairment of glucose and glutamate transport and induction of mitochondrial oxidative stress and dysfunction in synaptosomes by amyloid beta-peptide: role of lipid peroxidation product 4-hydroxynonenal. *J. Neurochem.*; 69(1): 273-284.
- Khachaturian ZS. (1994) Calcium hypothesis of Alzheimer's disease and brain aging. *Ann. N. Y. Acad. Sci.*; 747: 1-11.
- Kish SJ, Bergeron C, Rajput A, Dozic S, Mastrogiacono F, Chang LHJ, Wilson JM, DiStefano LM, and Nobrega JN. (1992) Brain cytochrome oxidase in Alzheimer's disease. *J. Neurochem.*; 59: 113-114.

- Kish SJ, Bergeron C, Rajput A, Dozic S, Mastrogiacomo F, Chang LJ, Wilson JM, DiStefano LM, and Nobrega JN. (1995) Brain cytochrome oxidase in Alzheimer's disease. *Neurochem.*; 59(2): 776-9.
- Kitaguchi N, Takahashi Y, Tokushima Y, Shiojiri S, and Ito H. (1988) Novel precursor of Alzheimer's disease amyloid protein shows protease inhibitory activity. *Nature*; 331: 530-532.
- Kitaguchi N, Takahashi Y, Oishi K, Shiojiri S, Tokushima Y, Utsunomiya T, and Ito H. (1990) Enzyme specificity of proteinase inhibitor region in amyloid precursor protein of Alzheimer's disease: Different properties compared with protease nexin I. *Biochem. Biophys. Acta.*; 1038: 105-113.
- Klegeris A, Walker D, and McGeer P. (1994) Activation of macrophages by Alzheimer beta amyloid peptide. *Biochem. Biophys. Res. Commun.*; 199(2): 984-991.
- Kluck RM, Bossy-Wetzel E, Green DR, and Newmeyer DD. (1997) The release of cytochrome c from mitochondria: a primary site for Bcl-2 regulation of apoptosis. *Science*; 275: 1132-1136.
- Knauer MF, Soreghan B, Burdick D, Kosmoski J, and Glabe CG. (1992) Intracellular accumulation and resistance to degradation of the Alzheimer amyloid A4/  $\beta$  protein. *Proc. Nat. Acad. Sci.*; 89: 7437-7441.
- Knops J, Lieberburg I, and Sinha S. (1992) Evidence for a nonsecretory, acidic degradation pathway for amyloid precursor protein in 293 cells. Identification of a novel, 22-kDa, beta-peptide-containing intermediate. *J. Biol. Chem.*; 267: 16022-16024.
- Koh J, Yang LL, and Cotman CW. (1990) Beta-amyloid protein increases the vulnerability of cultured cortical neurons to excitotoxic damage. *Brain Res.*; 533: 315-320.
- Koo EH, Park L, and Selkoe DJ. (1993) Amyloid beta-protein as a substrate interacts with extracellular matrix to promote neurite outgrowth. *Proc. Nat. Acad. Sci.*; 90: 4748-4752.
- Kosik K. (1994) The Alzheimer's disease sphinx: a riddle with plaques and tangles. *J. Cell Biol.*; 127: 1501-1504.
- Kosik KS. (1999) A notable cleavage: Winding up with  $\beta$ -amyloid. *Proc. Nat. Acad. Sci.*; 96: 2574-2576.

- Krajewski S, Krajewska M, Ellerby LM, Welsh K, Xie Z, Deveraux QL, Salvesen GS, Bredesen DE, Rosenthal RE, Fiskum G, and Reed JC. (1999) Release of caspase-9 from mitochondria during neuronal apoptosis and cerebral ischemia. *Proc. Natl. Acad. Sci.*; 96(10): 5752-5757.
- Kuentzel SL, Ali SM, Altman RA, Greenberg BD, and Raub TJ. (1993) The Alzheimer beta-amyloid protein precursor/protease nexin-II is cleaved by secretase in a trans-Golgi secretory compartment in human neuroglioma cells. *Biochem. J.*; 295 (Pt. 2): 367-378.
- LaFerla FM, Troncoso JC, Strickland DK, Kawas CH, and Jay G. (1997) Neuronal cell death in Alzheimer's disease correlates with apoE uptake and intracellular A  $\beta$  stabilization. *J. Clin. Invest.*; 100(2): 310-320.
- La Fera FM, Tinkle BT, Bieberich CJ, Haudenschild CC, and Gilbert J. (1995) The Alzheimer's A beta-peptide induces neurodegeneration and apoptotic cell death in transgenic mice. *Nature Genet.*; 9: 21-30.
- Lafon-Cazal M, Pietri S, Cuicasi M, and Bockaert J. (1993) NMDA-dependent superoxide production and neurotoxicity. *Nature*; 364: 535-537.
- Lakis J, Glasco S, Miller SW, Thal LJ, and Davis RE. (1995) Production of reactive oxygen species correlates with decreased cytochrome oxidase activity in Alzheimer's disease cybrids. *Soc. Neurosci. Abst*; 21: 979.
- Lamb BT. (1997) Presenilins, amyloid- $\beta$  and Alzheimer's disease. *Nature Medicine*; 3(1): 28-29.
- Lansbury PT. (1997) Structural neurology: are seeds at the root of neuronal degeneration? *Neuron*; 19(6): 1151-1154.
- Lassmann H, Bancher C, Breitschopf H, Wegiel J, Bobinski M, Jellinger K, and Wisniewski HM. (1995) Cell death in Alzheimer's disease evaluated by DNA fragmentation in situ. *Acta Neuropathol.*; 89(1): 35-41.
- Lazararewicz JW, Wroblewski JT, Palmer ME, and Costa E. (1988) *Neuropharmacology*; 27: 765.
- LeBlanc A. (1995) Increased production of a 4 kDa amyloid beta-peptide in serum deprived human primary neuron cultures: possible involvement of apoptosis. *J. Neurosci.*; 15: 7837-7846.
- LeBlanc AC, Kovacs DM, Chen HY, Villare F, Tykocinski M, Autilio-Gambetti L, and Gambetti P. (1992). Role of amyloid precursor protein (APP): study with antisense

- transfection of human neuroblastoma cells. *J. Neurosci. Res.*; 31: 635-645.
- Ledesma M, Bonay P, Colaco C, and Avila J. (1994) Analysis of microtubule-associated protein tau glycation in paired helical filaments. *J. Biol. Chem.*; 269: 21614-21619.
- Lemere CA, Lopera F, Kosik KS, Lendon CL, Ossa J, Saido TC, Yamaguchi H, Ruiz A, Martinez A, Madrigal L, Hincapie L, Arango JC, Anthony DC, Koo EH, Goate AM, Selkoe DJ, and Arango JC. (1996) The E280A presenilin 1 Alzheimer mutation produces increased A beta 42 deposition and severe cerebellar pathology. *Nature Med.*; 2(10): 1146-1150.
- Lendon CL, Ashall F, and Goate AM. (1997) Exploring the etiology of Alzheimer's disease using molecular genetics. *JAMA*; 277: 825-836.
- Levy-Lahard E, Wasco W, Poorkaj P, Romano DM, Oshima J, Pettingell WH, Yu CE, Jondro PD, Schmidt SD, Wang K, *et al.* (1995 a) Candidate gene for the chromosome 1 familial Alzheimer's disease locus. *Science*; 269: 973-977.
- Levy-Lahard E, Wijsman EM, Nemens E, Andertson L, Goddard KA, Weber JL, Bird TD, and Schellenberg GD. (1995 b) A familial Alzheimer's disease locus on chromosome 1. *Science*; 269: 970-973.
- Li WP, Chan WY, Lai HW, and Yew DT. (1997) Terminal dUTP nick and labelling (TUNEL) positive cells in the different regions of the brain in normal aging and Alzheimer patients. *J. Mol. Neurosci.*; 8: 75-82.
- Liu X, Kim CN, Yang J, Jemmerson R, and Wang X. (1996) Induction of apoptotic program in cell free extracts: requirements for dATP and cytochrome c. *Cell*; 86: 147-157.
- Loo DT, Copani A, Pike CJ, Whitemore ER, Walencewicz AJ, and Cotman CW. (1993) Apoptosis is induced by beta-amyloid in cultured central nervous system neurons. *Proc. Nat. Acad. Sci.*; 90: 7951-7955.
- Lorenzo A and Yankner BA. (1994) Beta-amyloid neurotoxicity requires fibril formation and is inhibited by Congo red. *Proc. Nat. Acad. Sci.*; 91: 12243-12247.
- Mann DMA, Iwatsubo T, Cairns NJ, *et al.* (1996) Amyloid ss protein (Ass) deposition in chromosome 14-linked Alzheimer's disease: predominance of Ass42(43). *Ann. Neurol.*; 40: 149-156.
- Mann DMA, Mann DM, Iwatsubo T, Cairns NJ, Lantos PL, Nochlin D, Sumi SM, Bird TD, Poorkaj P, Hardy J, Hutton M, Prihar G, Crook R, Rossor MN, Haltia M, *et al.* (1996) Amyloid beta protein (Abeta) deposition in chromosome 14-linked



- Alzheimer's disease: predominance of Abeta42(43). *Ann. Neurol.*; 40(2): 149-156.
- Mann DMA, Iwatsubo T, Nochlin D, Sumi SM, Levy-Lahard E, and Bird TD. (1997) Amyloid (Ass) deposition in chromosome 1-linked Alzheimer's disease: the Volga German families. *Ann. Neurol.*; 41: 52-57.
- Mark RJ, Blane EM, and Mattson MP. (1996) Amyloid beta-peptide and oxidative cellular injury in Alzheimer's disease. *Mol. Neurobiol.*; 12(3): 211-224.
- Mark RJ, Hensley K, Butterfield DA, and Mattson MP. (1995) Amyloid beta-peptide impairs ion-motive ATPase activities: evidence for a role in loss of neuronal Ca<sup>2+</sup> homeostasis and cell death. *J. Neurosci.*; 15(9): 6239-6249.
- Markesbery WR. (1997) Oxidative stress hypothesis in Alzheimer's disease. *Free Rad. Biol. Med.*; 23(1): 134-147.
- Marklund SL. (1985) Pyrogallol autoxidation, in *Handbook of Methods for oxygen Radical Research*, Greenwald, RA (ed). (CRC Press, Boca Raton, Florida), pp. 283-284.
- Marx J. (1998) New gene tied to common form of Alzheimer's. *Science*; 281: 507-509.
- Marzo I, Brenner C, Zamzami N, Jurgensmeier JM, Susin SA, Vieira HL, Prevost MC, Xie Z, Matsuyama S, Reed JC, and Kroemer G. (1998) Bax and adenine nucleotide translocator cooperate in the mitochondrial control of apoptosis. *Science*; 281: 2027-2031.
- Masters CL, Simms G, Weinman N, Multhaup NA, McDonald G, and Bayreuther K. (1985 a) Amyloid plaque core protein in Alzheimer disease and Down syndrome. *Proc. Nat. Acad. Sci.*; 82(12): 4245-4249.
- Masters CL and Bayreuther K. (1988) in *Aging of the Brain*, RD Terry, ed, (Raven Press, New York), pp. 183-204.
- Masters CL, Multhaup NA, Simms G, Pottgiesser J, Martins RN, and Bayreuther K. (1985 b) Neuronal origin of a cerebral amyloid: neurofibrillary tangles of Alzheimer's disease contain the same protein as the amyloid of plaque cores and blood vessels. *EMBO J.*; 4: 2757-2763.
- Mattson MP. (1994 a) Calcium and neuronal injury in Alzheimer's disease. Contributions of beta-amyloid precursor protein mismetabolism, free radicals, and metabolic compromise. *Ann. N. Y. Acad. Sci.*; 747: 50-76.

- Mattson MP. (1994 b) Secreted forms of beta-amyloid precursor protein modulate dendrite outgrowth and calcium responses to glutamate in cultured embryonic hippocampal neurons. *J. Neurobiol.*; 25(4): 439-450.
- Mattson MP. (1997) Cellular actions of beta-amyloid precursor protein and its soluble and fibrillogenic derivatives. *Physiol. Rev.*; 77(4): 1081-1132.
- Mattson MP, Barger SW, Cheng B, Lieberburg I, Smith-Swintosky VL, and Rydel RE. (1993[b]) Beta-amyloid precursor protein metabolites and loss of neuronal Ca<sup>2+</sup> homeostasis in Alzheimer's disease. *Trends Neurosci.*; 16: 409-414.
- Mattson MP, Cheng B, Culwell AR, Esch FS, Lieberburg I, and Rydel R. (1993 a) Evidence for excitoprotective and interneuronal calcium-regulating roles for secreted forms of the  $\beta$ -amyloid precursor protein. *Neuron*; 10: 243-254.
- Mattson MP, Cheng B, Davis D, Bryant K, Lieberburg I, and Rydel R. (1992)  $\beta$ -amyloid peptides destabilize calcium homeostasis and render human cortical neurons vulnerable to excitotoxicity. *J. Neurosci.*; 12: 376-389.
- McGeer PI, Rogers J, and McGeer EG. (1994) Neuroimmune mechanisms in Alzheimer disease patients. *Alzheimer Dis. Assoc. Disord.*; 8: 149-158.
- Mecocci P, MacGarvey U, and Beal MF. (1994) Oxidative damage to mitochondrial DNA is increased in Alzheimer's disease. *Ann. Neurol.*; 36: 747-751.
- Mecocci P, Polidori MC, Ingegneri T, Cherubini A, Chionne F, Cecchetti R, and Senin U. (1998) Oxidative damage to DNA in lymphocytes from AD patients. *Neurol.*; 51: 1014-1017.
- Meda L, Cassatella MA, Szendrei GI, et al. (1995) Activation of microglia cells by beta-amyloid protein and interleukin-1. *Nature*; 374: 647-650.
- Meier-Ruge WA and Bertoni-Freddari C. (1997) Pathogenesis of decreased glucose turnover and oxidative phosphorylation in ischemic and trauma-induced dementia of the Alzheimer type. *Ann. N. Y. Acad. Sci.*; 826: 229-241.
- Muller U, Cristina N, Li ZW, Wolfer DP, Lipp HP, Rulicke T, Brandner S,
- Milward EA, Papadopoulos R, Fuller SJ, Moir RD, Small D, Beyreuther K, and Masters CL. (1992) The amyloid protein precursor of Alzheimer's disease is a mediator of the effects of nerve growth factor on neurite outgrowth. *Neuron*; 9(1): 129-137.
- Morris JC. (1995) Relationships of plaques and tangles to Alzheimer's disease phenotype, in *Pathobiology of Alzheimer's disease*, Eds. Goate AM and Ashall F.

(Academic press, New York), pp. 191-223.

- Mucke L, Masliah E, Johnson WB, Ruppe MD, Alford M, Rockenstein EM, Fross-Petter S, Pietropaolo M, Mallory M, and Abraham CR. (1994) Synaptotrophic effects of human amyloid beta protein precursors in the cortex of transgenic mice. *Brain Res.*; 666(2): 151-167.
- Mullan M, Crawford F, Axelman K, Houlden H, Lilius L, Winblad B, and Lannfelt L. (1992) A pathogenic mutation for probable Alzheimer's disease in the APP gene at the N-terminus of beta-amyloid. *Nat. Genet.*; 1(5): 345-347.
- Murphy MP, Hickman LJ, Eckman CB, Ulfon SN, Wang R, and Golde TE. (1999)  $\gamma$ -secretase, evidence for multiple proteolytic activities and influence of membrane positioning of substrate on generation of amyloid  $\beta$  peptides of varying length. *J. Biol. Chem.*; 274(17): 11914-11923.
- Murrell J, Farlow M, Ghetti B, and Benson MD. (1991) A mutation in the amyloid precursor protein associated with hereditary Alzheimer' disease. *Science*; 254: 97-99.
- Mutisya DM, Bowling AC, and Beal MF. (1994) Cortical cytochrome oxidase activity is reduced in Alzheimer's disease. *J. Neurochem.*; 63: 2179-2184.
- Mutisya DM, Bowling AC, Walker LC et al. (1993) Impaired energy metabolism in aging and Alzheimer's disease. *Neurosci. Abstr.*; 19:1474.
- Nagi MN, Al-Beeckairi AM, and Al Sawaf HA. (1995) Spectrophotometric assay for superoxide dismutase based on the nitroblue tetrazolium reduction by glucose-glucose oxidase. *Biochem. Molec. Bio. Int.*; 36: 633-638.
- Nalbantoglu J, Tirado-Santiago G, Lahsaini A, Poirier J, Goncalves O, Verge G, Momoli F, Welner SA, Massicte G, Julien J-P, and Shapiro ML. (1997) Impaired learning and LTP in mice expressing the carboxy terminus of the Alzheimer amyloid precursor protein. *Nature*; 387: 500-505.
- Neve RL, Finch EA, and Dawes LR. (1988) Expression of the Alzheimer amyloid precursor gene transcripts in the human brain. *Neuron.*; 1(8): 669-677.
- Oda T, Pasinetti GM, Osterberg HH, Anderson C, Johnson SA, and Finch CE. (1994) Purification and characterization of brain clusterin. *Biochem. Biophys. Res. Commun.*; 204: 1131-1136.
- Olanow CW and Arendash GW. (1994) Metals and free radicals in neurodegeneration. *Curr. Opin. Neurol.*; 7(6): 548-558.

- Olichney JM, Hansen LA, Hofstetter R, Grundman M, Katzman R, and Thal LJ. (1995) Cerebral infarction in Alzheimer's disease is associated with severe amyloid angiopathy and hypertension. *Arch. Neurol.*; 52: 702-708.
- Olichney JM, Hansen LA, Galasko D, et al. (1996) The apolipoprotein E e-4 allele is associated with increased neuritic plaques and cerebral amyloid angiopathy in Alzheimer's disease and the Lewy body variant. *Neurology*; 47: 190-196.
- Oltersdorf T, Fritz L, Schenk DB, Lieberburg I, Johnson-Wood KL, Beattie EC, Ward PJ, Blacker RW, Dovey HF, and Sinha S. (1989) The secreted form of the Alzheimer's amyloid precursor protein with the Kunitz domain is protease nexin-II. *Nature*; 341: 144-147.
- Parker WD, Oley CA, and Parks JK. (1989[a]) Deficient NADH:coenzyme Q oxidoreductase in Leber's hereditary optic neuropathy. *N. Eng. J. Med.*; 320: 1331-1333.
- Parker WD Jr. (1991) Cytochrome oxidase deficiency in Alzheimer's disease. *Ann. N. Y. Acad. Sci.*; 640: 59-64.
- Parker WD and Parks JK. (1995) Cytochrome c oxidase in Alzheimer's disease brain: purification and characterization. *Neurol.*; 45: 482-486.
- Parker WD, Boyson SJ, and Parks JK. (1989 b) Abnormalities of the electron transport chain in idiopathic Parkinson's disease. *Ann. Neurol.*; 26: 719-723.
- Parker WD, Boyson SJ, Luder AS, and Parks JK. (1990 b) Evidence for a defect in NADHG;ubiquinone oxidoreductase (complex I) in Huntington's disease. *Neurol.*; 40: 1231-1234.
- Parker WD, Filley CM, and Parks JK. (1990) Cytochrome oxidase deficiency in Alzheimer's disease. *Neurology*; 40: 1302-1303.
- Parker WD, Mahr NJ, Filley CM, Parks JK, Hughes D, Young DA, and Cullum CM. (1994 a) Reduced platelet cytochrome c oxidase deficiency in Alzheimer's disease. *Neurology*; 44: 1086-1090.
- Parker WD, Parks JK, Filley CM, and Kleinschmidt-DeMasters BK. (1994 b) Electron transport chain defects in Alzheimer's disease. *Neurology*; 44: 1090-1096.
- Partridge RS, Munroe SM, Parks JK, et al. (1994) Spin trapping of azidyl and hydroxyl radicals in azide-inhibited rat brain submitochondrial particles. *Arch. Biochem. Biophys.*; 310: 210-217.

- Pellegrini-Giampietro D, Cherici G, Alesiani M, Carla V, and Moroni F. (1988) Excitatory amino acid release from rat hippocampal slices as a consequence of free-radical formation. *J. Neurochem.*; 51(6): 1960-1963.
- Perez RG, Squazzo SL, and Koo EH. (1996) Enhanced release of amyloid beta-protein from codon 670/671 "Swedish" mutant beta-amyloid precursor protein occurs in both secretory and endocytic pathways. *J. Biol. Chem.*; 271(15): 9100-9107.
- Petit PX, Susin SA, Zamzami N, Mignotte B, and Kroemer G. (1996) Mitochondria and programmed cell death: back to the future. *FEBS Lett.*; 396(1): 7-13.
- Pike CJ, Burdick D, Walencewicz AJ, Glabe CG, and Cotman CW. (1993) Neurodegeneration induced by  $\beta$ -amyloid peptides *in vitro*: The role of peptide assembly state. *J. Neurosci.*; 13: 1676-1687.
- Pike CJ, Walencewicz AJ, Glabe CG, and Cotman CW. (1991) In vitro aging of beta-amyloid protein causes peptide aggregation and neurotoxicity. *Brain Res.*; 563(1-2): 313-314.
- Ponte P, Gonzalez-DeWhitt P, Schilling J, Miller J, Hsu D, Greenberg B, Davis K, Wallace W, Lieberburg I, and Fuller F, (1988) A new A4 amyloid mRNA contains a domain homologous to serine proteinase inhibitors. *Nature*; 331: 525-527.
- Price DL, Sisodia SS, and Borchelt DR. (1998) Genetic neurodegenerative diseases: The human illness and transgenic models. *Science*; 282: 1079-1083.
- Price DL and Sisodia SS. (1998) Mutant genes in familial Alzheimer's disease and transgenic models. *Ann. Rev. Neurosci.*; 21: 479-505.
- Prick MJJ, Gabreels FJM, Trijbels JMF, et al. (1983) Progressive poliodystrophy (Alper's disease) with a defect in cytochrome  $\alpha\alpha_3$  in muscle; a report of two unrelated patients. *Clin. Neurol. Neurosurg.*; 85: 57-70.
- Qiu WQ, Ferreira A, Miller C, Koo EH, and Selkoe DJ. (1995) Cell-surface beta-amyloid precursor protein stimulates neurite outgrowth of hippocampal neurons in an isoform-dependent manner. *J. Neurosci.* 15(3 Pt 2): 2157-2167.
- Reichmann H, Florke S, Hebenstrein G, Schrubar H, and Riederer P. (1993) Analysis of energy metabolism and mitochondrial genome in post-mortem brain from patients with Alzheimer's disease. *J. Neurol.*; 240: 377-380.
- Retz KC and Coyle JT. (1982) Effects of kainic acid on high-energy metabolites in the mouse striatum. *J. Neurochem.*; 38(1): 196-203.

- Riviere S, Birlouez-Aragon I, and Vellas B. (1998) Plasma protein glycation in Alzheimer's disease. *Glycoconj. J.*; 15(10): 1039-1042.
- Rizzuto R, Simpson AW, Brini M, and Pozzan T. (1992) Rapid changes of mitochondrial Ca<sup>2+</sup> revealed by specifically targeted recombinant aequorin. *Nature*; 358: 325-327.
- Roberts GW, Gentleman SM, Lynch A, and Graham DI. (1991) beta A4 amyloid protein deposition in brain after head trauma. *Lancet*; 338: 1422-1423.
- Roch JM, Masliah E, Roch-Levecq AC, Sundsmo MP, Otero DA, Veinbergs I, and Saitoh T. (1994) Increase of synaptic density and memory retention by a peptide representing the trophic domain of the amyloid beta/A4 protein precursor. *Proc. Nat. Acad. Sci.*; 91(16): 7450-7454.
- Rogaev EI, Sherrington R, Rogaeva EA, Levesque G, Ikeda M, *et al.* (1995) Familial Alzheimer's disease in kindreds with missense mutations in a gene on chromosome 1 related to Alzheimer's disease type 3 gene. *Nature*; 376: 775-778.
- Roher A, Wolfe D, Palutke M, and KuKurga D. (1986) Purification, ultrastructure, and chemical analysis of Alzheimer disease amyloid plaque core protein. *Proc. Nat. Acad. Sci.*; 83(8): 2662-2666.
- Roth M, Tomlinson BE, and Blessed G. (1966) Correlation between scores for dementia and counts of 'senile plaques' in cerebral grey matter of elderly subjects. *Nature*; 209: 109-110.
- Saido TC, Iwatsubo T, Mann DMA, Shimada H, Ihara Y, and Kawashima S. (1995) Dominant and differential deposition of distinct beta-amyloid peptide species, A beta N3(pE), in senile plaques. *Neuron*; 14(2): 457-466.
- Salbaum JM, Weidemann A, Lemaire HG, Masters CL, and Beyreuther K. (1988) The promoter of Alzheimer's disease amyloid A4 precursor gene. *EMBO J.*; 7(9): 2807-2813.
- Sambamurti K, Shioi J, Anderson JP, Papolla MA, and Robakis NK. (1992) Evidence for intracellular cleavage of the Alzheimer's amyloid precursor in PC12 cells. *J. Neurosci. Res.*; 33(2): 319-329.
- Sambrook J, Fritsch EF, and Maniatis T, (1989) in *Molecular Cloning: A Laboratory Manual*, 2<sup>nd</sup> Edn. Eds: Ford N, Nolan C, and Ferguson M. (Cold Springs Harbor Laboratory Press, Mass).

- Scheuner D, Eckman C, Jensen M, Song X, Citron M, *et al.* (1996) Secreted amyloid  $\beta$ -protein similar to that in the senile plaques of Alzheimer's disease is increased *in vivo* by the presenilin 1 and 2 and APP mutations linked to familial Alzheimer's disease. *Nat. Med.*; 2: 864-870.
- Schweers O, Mandelkow EM, Biernat J, and Mandelkow E. (1995) Oxidation of cysteine-322 in the repeat domain of microtubule-associated protein  $\tau$  controls the *in vitro* assembly of paired helical filaments. *Proc. Nat. Acad. Sci.*; 92: 8463-8467.
- Selkoe DJ. (1994 a) Alzheimer's disease: a central role for amyloid. *J. Neuropathol. Exp. Neurol.*; 53(5): 438-447.
- Selkoe DJ. (1994 b) Normal and abnormal biology of the beta-amyloid precursor protein. *Annu. Rev. Neurosci.*; 17: 489-517.
- Selkoe DJ. (1994 c) Amyloid beta-protein precursor: new clues to the genesis of Alzheimer's disease. *Curr. Opin. Neurobiol.*; 4(5): 708-716.
- Selkoe DJ. (1994 d) Cell biology of the amyloid beta-protein precursor and the mechanism of Alzheimer's disease. *Ann. Rev. Cell Biol.*; 10: 373-403.
- Seubert P, Oltsdorf T, Lee MG, Barbour R, Blomquist C, Davis DL, Bryant K, Fritz LC, Galasko D, Thal LJ, Lieberburg I, and Schenk D. (1993) Secretion of beta-amyloid precursor protein cleaved at the amino terminus of the beta-amyloid peptide. *Nature*; 361: 260-262.
- Shapira AHV, Cooper JM, Dexter D, Clark JB, Jenner P, and Marsden CD. (1990) Mitochondrial complex 1 deficiency in Parkinson's disease. *J. Neurochem.*; 54: 823-827.
- Sheehan JP, Swerdlow RH, Miller SW, Davis RE, Parks JK, Parker WD, and Tuttle JB. (1997) Calcium homeostasis and reactive oxygen species production in cells transformed by mitochondria from individuals with sporadic Alzheimer's disease. *J. Neurosci.*; 17(12): 4612-4622.
- Sherrington R, Rogaev EI, Liang Y, Rogaeva EA, Levesque G, *et al.* (1995) Cloning of a gene bearing missense mutations in early-onset familial Alzheimer's disease. *Nature*; 375: 754-760.
- Shigenaga MK, Hagen TM, and Ames BM. (1994) Oxidative damage and mitochondrial decay in aging. *Proc. Nat. Acad. Sci.*; 91(23): 10771-10778.

- Shimohama S, Tanino H, and Fujimoto S. (1999) Changes in caspase expression in Alzheimer's disease: comparison with development and aging. *Biochem. Biophys. Res. Commun.*; 16;256(2): 381-384.
- Shoffner JM, Watts RL, Juncos JL, Torroni A, and Wallace DC. (1991) Mitochondrial oxidative phosphorylation defects in Parkinson's disease. *Ann. Neurol.*; 30: 332-339.
- Shoffner JM, Lott MT, Lezza AMS, Seibel P, Ballinger SW, and Wallace DC. (1990) Myoclonic epilepsy and ragged-red fiber disease (MERRF) is associated with a mitochondrial DNA tRNA<sup>lys</sup> mutation. *Cell*; 61: 931-937.
- Shoji M, Golde TE, Ghiso J, Cheung TT, Estus S, Shaffer LM, Cai XD, McKay DM, Tintner R, Frangione B, and Younkin SG. (1992) Production of the Alzheimer amyloid beta protein by normal proteolytic processing. *Science*; 258: 126-129.
- Shoulson I. (1998) Experimental therapeutics of neurodegenerative disorders: Unmet needs. *Science*; 282: 1072-1074.
- Simmons MA and Schneider CR. (1993) Amyloid beta peptides act directly on single neurons. *Neurosci. Lett.*; 150(2): 133-136.
- Simonian NA and Hyman BT. (1994) Functional alterations in Alzheimer's disease: selective loss of mitochondrial-encoded cytochrome oxidase mRNA in the hippocampal formation. *Neuropathol. Exp. Neurol.*; 53(5): 508-12.
- Simonian NA and Coyle JT. (1996) Oxidative stress in neurodegenerative diseases. *Ann. Rev. Pharmacol. Toxicol.*; 36: 83-106.
- Sisodia SS. (1992) Beta-amyloid precursor protein cleavage by a membrane-bound protease. *Proc. Nat. Acad. Sci.*; 89(13): 6075-6079.
- Sisodia SS, Koo EH, Beyreuther K, Unterbeck A, and Price DL. (1990) Evidence that beta-amyloid protein in Alzheimer's disease is not derived by normal processing. *Science*; 248: 492-495.
- Smale G, Nichols NR, Brady DR, Finch CE, and Horton WE. (1995) Evidence for apoptotic cell death in Alzheimer's disease. *Exp. Neurol.*; 133: 225-230.
- Small DH, Nurcombe V, Moir R, Michaelson S, Monard D, Beyreuther K, and Masters CL. (1992) Association and release of the amyloid protein precursor of Alzheimer's disease from chick brain extracellular matrix. *J. Neurosci.*; 12(11): 4143-4150.



- Small DH, Nurcombe V, Reed G, Clarris H, Moi R, Beyreuther K, and Masters CL. (1994) A heparin-binding domain in the amyloid protein precursor of Alzheimer's disease is involved in the regulation of neurite outgrowth. *J. Neurosci.*; 14(4): 2117-2127.
- Smith CD, Carney JM, Starke-Reed PE, Oliver CN, Stadtman ER, Floyd RA, and Marksbery WR. (1991) Excess brain protein oxidation and enzyme dysfunction in normal aging and in Alzheimer disease. *Proc. Nat. Acad. Sci.*; 88: 10540-10543.
- Smith RP, Higuchi DA, and Broze GJ. (1990) Platelet coagulation factor XIa-inhibitor, a form of Alzheimer amyloid precursor protein. *Science*; 248: 1126-1128.
- Smith MA, Taneda S, Richey PL, Miyata S, Yan SD, Stern D, Sayre LM, Monnier VM, and Perry G. (1994) Advanced Maillard reaction end products are associated with Alzheimer disease pathology. *Proc. Nat. Acad. Sci.*; 91(12): 5710-5714.
- Snyder SW, Lador US, Wade WS, Wang GT, Barrett LW, Matayoshi ED, Krafft GA, and Holtzman TF. (1994) Amyloid-beta aggregation: selective inhibition of aggregation in mixtures of amyloid with different chain lengths. *Biophys. J.*; 67(3): 1216-1228.
- Su JH, Deng G, and Cotman CW. (1997) Bax protein expression is increased in Alzheimer's brain: correlations with DNA damage, Bcl-2 expression, and brain pathology. *J. Neuropathol. Exp. Neurol.*; 56:86-93.
- Su JH, Cummings BJ, and Cotman CW. (1994) Immunohistochemical evidence for apoptosis in Alzheimer's disease. *Neuroreport*; 5(18): 2529-2533.
- Susin SA, Lorenzo HK, Zamzami N, Marzo I, Snow BE, Brothers GM, Mangion J, Jacotot E, Costantini P, Loeffler M, Larochette N, Goodlett DR, Aebersold R, Siderovski DP, Penninger JM, and Kroemer G. (1999) Molecular characterization of mitochondrial apoptosis-inducing factor. *Nature*; 397: 441-446.
- Susin SA, Lorenzo HK, Zamzami N, Marzo I, Brenner C, Larochette N, Prevost MC, Alzari PM, and Kroemer G. (1999) Mitochondrial release of caspase-2 and -9 during the apoptotic process. *J. Exp. Med.*; 189(2): 381-394.
- Swerdlow R, Parks J, Cassarino D, Maguire D, Maguire R, Bennett Jr. J, Davis R, and Parker Jr. W. (1997) Cybrids in Alzheimer's Disease: A cellular model of the disease? *Neurology*; 49: 918-925.
- Swerdlow R, Marcus DL, Frey W, and Friedman ML. (1994) Comparative brain glucose and ketone body metabolism in Alzheimer's disease. *Am. J. Med. Sci.*; 308: 141-144.

- Tanzi RE, Gusella JF, Watkins PC, Bruns GA, St George-Hyslop P, Van Keuren ML, Patterson D, Pagan S, Kurnit DM, and Neve RL. (1987) Amyloid beta protein gene: cDNA, mRNA distribution, and genetic linkage near the Alzheimer locus. *Science*; 235: 880-884.
- Tanzi RE, McClatchey AI, Lamperti ED, Villa-Komaroff L, Gusella JF, and Neve RL. (1988) Protease inhibitor domain encoded by an amyloid protein precursor mRNA associated with Alzheimer's disease. *Nature*; 331: 528-30.
- Tatton WG and Chalmers-Redman RM. (1998) Mitochondria in neurodegenerative apoptosis: an opportunity for therapy? *Ann. Neurol.*; 44(3 suppl 1): S134-S141.
- Terry RD. (1997) The pathology of Alzheimer's disease: numbers count [letter]. *Ann. Neurol.*; 41: 7.
- Terry RD, Masliah E, Salmon DP, Butters N, DeTeresa R, Hill R, Hansen LA, and Katzman R. (1991) Physical basis of cognitive alterations in Alzheimer's disease: synapse loss is the major correlate of cognitive impairment. *Ann. Neurol.*; 30: 572-580.
- Thinakaran G, Teplow DB, Siman R, Greenberg B, and Sisodia SS. (1996) Metabolism of the "Swedish" amyloid precursor protein variant in neuro2a (N2a) cells. Evidence that cleavage at the "beta-secretase" site occurs in the golgi apparatus. *J. Biol. Chem.*; 271: 9390-9397.
- Thome J, Kornhuber J, Munch G, Schinzel R, Taneli Y, Zielke B, Rosler M, and Riederer P. (1996) New hypothesis on etiopathogenesis of Alzheimer syndrome. Advanced glycation end products. *Nervenarzt [Abstract]*; 67(11): 924-929.
- Tienari PJ, Ida N, Ikonen E, Simons M, Weidemann A, Multhaup G, Masters CL, Dotti CG, and Beyreuther K. Tienari P, et al. (1997) Intracellular and secreted Alzheimer  $\beta$ -amyloid species are generated by distinct mechanisms in cultured hippocampal neurons. *Proc. Nat. Acad. Sci.*; 94: 4125-4130.
- Trojanowski J and Lee V. (1994) Paired helical filament tau in Alzheimer's disease. The kinase connection. *Am. J. Path.*; 144(3): 449-453.
- Turner RS, Suzuki N, Chyung AS, Younkin SG, and Lee VM. (1996) Amyloid  $\beta_{40}$  and  $\beta_{42}$  are generated intracellularly in cultured human neurons and their secretion increases with maturation. *J. Biol. Chem.*; 271: 8966-8970.
- Urmoneit B, Prikulis I, Wihl G, D'Urso D, Frank R, Heeren J, Beisiegel U, and Prior R. (1997) Cerebrovascular smooth muscle cells internalize Alzheimer amyloid beta protein via a protein pathway: implications for cerebral amyloid

angiopathy. *Lab. Invest.*; 77: 157-166.

- Vander Heiden MG, Chandel NS, Williamson EK, Schumacker PT, and Thompson CB. (1997) Bcl-X<sub>L</sub> regulates the membrane potential and volume homeostasis of mitochondria. *Cell*; 91: 627-637.
- Van Nostrand WE, Wagner SL, Suzuki M, Choi BH, Farrow JS, Geddes JW, Cotman CW, and Cunningham DD. (1989) Protease nexin-II, a potent antichymotrypsin, shows identity to amyloid beta-protein precursor. *Nature*; 341: 546-549.
- Vinters HV, Wang ZZ, and Secor DL. (1996) Brain parenchymal and microvascular amyloid in Alzheimer's disease. *Brain Pathol.*; 6: 179-195.
- Vitek MP, Bhattacharya K, Glendening JM, Stopa E, Vlassara H, Bucala R, Manogue K, and Cerami A. (1994) Advanced glycation end products contribute to amyloidosis in Alzheimer disease. *Proc. Nat. Acad. Sci.*; 91(11): 4766-4770.
- Volicer L and Crino PB. (1990) Involvement of free radicals in dementia of the Alzheimer type: a hypothesis. *Neurobiol. Aging*; 11: 567-571.
- Wallace DC (1997), in *The Molecular and Genetic Basis of Neurological Disease*, Rosenberg RN, Prusiner SB, DiMauro S, Barchi RL, Eds. (Butterworth-Heinemann, Boston), pp. 237-269.
- Wallace DC. (1999) Mitochondrial diseases in man and mouse. *Science*; 283: 1482-1488.
- Wallace DC, Singh G, Lott MT, et al. (1988) Mitochondrial DNA mutation associated with Leber's hereditary optic neuropathy. *N. Eng. J. Med.*; 242: 1427-1430.
- Watt AJ, Pike CJ, Walencewicz-Wasserman AJ, and Cotman CW. (1994) Ultrastructural analysis of beta-amyloid-induced apoptosis in cultured hippocampal neurons. *Brain Res.*; 661(1-2): 147-156.
- Weidemann A, Konig G, Bunke D, Fischer P, Salbaum JM, Masters CL, and Beyreuther K. (1989) Identification, biogenesis, and localization of precursors of Alzheimer's disease A4 amyloid protein. *Cell*; 57(1): 115-126.
- Weidemann A, Paliga K, Durrwang U, Reinhard FBM, Schukert O, Evin G, and Masters C. (1999) Proteolytic processing of the Alzheimer's disease amyloid precursor protein within its cytoplasmic domain by caspase-like proteases. *J. Biol. Chem.*; 274(9): 5823-5829.

- Whittemore ER, Loo DT, and Cotman CW. (1994) Exposure to hydrogen peroxide induces cell death via apoptosis in cultured rat cortical neurons. *Neuro Report*; 5(12): 1485-1488.
- Wild-Bode C, Yamazaki T, Capell A, Leimer U, Steiner H, Ihara Y, and Haass C. (1997) Intracellular generation and accumulation of A $\beta$  terminating at amino acid 42. *J. Biol. Chem.*; 272: 16085-16088.
- Williams JH, Errington ML, Lynch MA, and Bliss TV. (1989) Arachidonic acid induces a long-term activity-dependent enhancement of synaptic transmission in the hippocampus. *Nature*; 341: 739-742.
- Wisniewski HM, Robe A, Zigman W, and Silverman W. (1989) Neuropathological diagnosis of Alzheimer disease. *J. Neuropath. Exp. Neurol.*; 48(6): 606-609.
- Wisniewski KE, Wisniewski HM, and Wen GL. (1985) Occurrence of neuropathological changes and dementia in Alzheimer's disease in Down's syndrome. *Ann. Neurol.*; 17: 278-282.
- Wong-Riley M, Antuono P, Ho KC, Egan R, Hevner R, Liebl W, Huang Z, Rachel R, and Jones J. (1997) Cytochrome oxidase in Alzheimer's disease: biochemical, histochemical, and immunohistochemical analyses of the visual and other systems. *Vision Res.*; 37(24): 3593-3608.
- Xia D and Samols D. (1997) Enhanced production and oligomerization of the 42-residue amyloid  $\beta$ -protein by chinese hamster ovary cells stably expressing mutant presenilins. *J. Biol. Chem.*; 272: 7977-7982.
- Xu H, Sweeney D, Wang R, Thinakaran G, Lo AC, Sisodia SS, Greengard P, and Gandy S. (1997) Generation of Alzheimer  $\beta$ -amyloid protein in the trans-Golgi network in the apparent absence of vesicle formation. *Proc. Nat. Acad. Sci.*; 94: 3748-3752.
- Yamada T, Sasaki H, Dohura K, Goto I, and Sakaki Y. (1989) Structure and expression of the alternatively-spliced forms of mRNA for the mouse homolog of Alzheimer's disease amyloid beta protein precursor. *Biochem. Biophys. Res. Commun.*; 158(3): 906-12.
- Yamatsuji T, Matsui T, Okamoto T, Komatsuzaki K, Takeda S, Fukumoto H, Iwatsubo T, Suzuki N, Asamiodaka A, Ireland S, Kinane TB, Giambarella U, and Nishimoto I. (1996 b) G protein-mediated neuronal DNA fragmentation induced by familial Alzheimer's disease-associated mutants of APP. *Science*; 272: 1349-1352.
- Yamatsuji T, Okamoto T, Takeda S, Murayama Y, Tanaka N, and Nishimoto I. (1996 a) Expression of V642 APP mutant causes cellular apoptosis as Alzheimer

- trait-linked phenotype. *EMBO J.*; 15(3): 498-509.
- Yan SD, Chen X, Fu J, Chen M, Zhu H, Roher A, Slattery T, Zhao L, Nagashima M, Morser J, Migheli A, Nawroth P, Stern D, and Schmidt AM. (1996) RAGE and amyloid-beta peptide neurotoxicity in Alzheimer's disease. *Nature*; 382: 685-691.
- Yan SD, Chen X, Schmidt AM, Brett J, Godman G, Zou YS, Scott CW, Caputo C, Frappier T, Smith MA, *et al.* (1994) Glycated tau protein in Alzheimer disease: a mechanism for induction of oxidant stress. *Proc. Nat. Acad. Sci.*; 91:7787-7791.
- Yan SD, Fu J, Soto C, Chen X, Zhu H, Al-Mohanna F, Collison K, Zhu A, Stern E, Saido T, Tohyama M, Ogawa S, Roher A, and Stern D. (1997) An intracellular protein that binds amyloid  $\beta$ -peptide and mediates neurotoxicity in Alzheimer's disease. *Nature*; 389: 689-695.
- Yang A, Knauer M, Burdick D, and Glabe C. (1995) Intracellular A  $\beta$ 1-42 aggregates stimulate the stable, insoluble amyloidogenic fragments of the amyloid precursor protein in transfected cells. *J. Biol. Chem.*; 270: 14786-14792.
- Yang X, Khosravi-Far R, Chang YH, and Baltimore D. (1997) Daxx, a novel fas-binding protein that activates JNK and apoptosis. *Cell*; 89: 1067-1076.
- Yankner BA. (1996) Mechanisms of neuronal degeneration in Alzheimer's disease. *Neuron*; 16(5): 921-932.
- Yankner BA, Dawes LR, Fisher S, Villa-Komaroff L, Oster-Granite ML, and Neve RL. (1989) Neurotoxicity of a fragment of the amyloid precursor associated with Alzheimer's disease. *Science*; 245: 417-420.
- Yankner BA, Duffy LK, and Kirschner DA. (1990) Neurotrophic and neurotoxic effects of amyloid  $\beta$  protein: reversal by tachykinin neuropeptides. *Science*; 250: 279-282.
- Yoshikawa K, Aizawa T, and Hayashi Y. (1992) Degeneration in vitro of post-mitotic neurons overexpressing the Alzheimer amyloid protein precursor. *Nature*; 359: 64-67.
- Zhang L, Zhao B, Yew DT, Kusiak JW, and Roth GS. (1997) Processing of Alzheimer's amyloid precursor protein during H<sub>2</sub>O<sub>2</sub>-induced apoptosis in human neuronal cells. *Biochem. Biophys. Res. Commun.*; 235: 845-848.
- Zhang Y, Marcillat O, Giulivi C, Ernster L, and Davis KJ. (1990) The oxidative inactivation of mitochondrial electron transport chain components and ATPase. *J. Biol. Chem.*; 265: 16330-16336.

**Zhao B, Chrest FJ, Horton WE, Jr., Sisodia SS, and Kusiak JW. (1997) Expression of mutant amyloid precursor proteins induces apoptosis in PC12 cells. *J. Neurosci. Res.*; 47(3): 253-263.**

**Zoratti M and Szabo I. (1995) The mitochondrial permeability transition. *Biochim. Biophys. Acta.*; 1241(2): 139-176.**